Technical Report Documentation Page

1. Report No. FHWA/TX-16/5-6719-01-1	2. Government Accession No.	3. Recipient's Catalog No.
4. Title and Subtitle Implementation Project: Strengthening a Continuous Steel Girder Bridge in Lakeport, Texas with Post-Installed Shear Connectors: Phase 1 – Bridge Strengthening Design and Load Testing		5. Report Date August 2016; Published March 2017 6. Performing Organization Code
7. Author(s) Kerry L. Kreitman, Amir R. Ghiami Azad, Michael D. Engelhardt, Todd A. Helwig, Eric B. Williamson		8. Performing Organization Report No. 5-6719-01-1
9. Performing Organization Name and Address Center for Transportation Research The University of Texas at Austin 1616 Guadalupe Street, Suite 4.202 Austin, TX 78701		10. Work Unit No. (TRAIS) 11. Contract or Grant No. 5-6719-01
12. Sponsoring Agency Name and Address Texas Department of Transportation Research and Technology Implementation Office P.O. Box 5080 Austin, TX 78763-5080		13. Type of Report and Period Covered Technical Report (12/15-8/16) 14. Sponsoring Agency Code
15. Supplementary Notes Project performed in cooperation with the Texas Department of Transportation and the Federal Highway Administration.		
16. Abstract In Implementation Project 5-6719, a non-composite continuous steel girder bridge located in Lakeport, Texas will be strengthened using techniques developed in TxDOT Research Project 0-6719. This strengthening technique involves the use of post-installed shear connectors in positive moment regions and the allowance of limited flexural yielding in negative moment regions. This Implementation Project is intended to demonstrate the strengthening technique, evaluate potential difficulties in design and construction and suggest solutions, and evaluate structural effectiveness and cost effectiveness of this bridge strengthening technique. Phase I of the Implementation Project includes selection of a non-composite continuous girder bridge in Texas for strengthening, detailed design of the strengthening system, detailed finite element analysis of the un-strengthened and strengthened bridge designs, and field load testing of the un-strengthened bridge to obtain baseline data on the behavior of the existing bridge for later comparison with field load testing data for the strengthened bridge. Phase II will include monitoring construction operations during the installation of post-installed shear connectors, collecting information on construction costs and difficulties, and field load testing of the bridge after strengthening is completed, to verify the effectiveness of the strengthening system.		
17. Key Words Continuous steel bridges, composite action, shear connectors, strengthening, shakedown, moment redistribution, fatigue	18. Distribution Statement No restrictions. This document is available to the public through the National Technical Information Service, Springfield, Virginia 22161; www.ntis.gov.	

19. Security Classif. (of report) Unclassified	20. Security Classif. (of this page) Unclassified	21. No. of pages 128	22. Price

Form DOT F 1700.7 (8-72) Reproduction of completed page authorized

THE UNIVERSITY OF TEXAS AT AUSTIN
CENTER FOR TRANSPORTATION RESEARCH

Implementation Project: Strengthening a Continuous Steel Girder Bridge in Lakeport, Texas with Post-Installed Shear Connectors: Phase 1 – Bridge Strengthening Design and Load Testing

Kerry L. Kreitman
Amir R. Ghiami Azad
Michael D. Engelhardt
Todd A. Helwig
Eric B. Williamson

CTR Technical Report:	5-6719-01-1
Report Date:	August 2016; Published March 2017
Project:	5-6719-01
Project Title:	Bridge Strengthening Design and Load Testing for a Continuous Steel Girder Bridge with Post-Installed Shear Connectors
Sponsoring Agency:	Texas Department of Transportation
Performing Agency:	Center for Transportation Research at The University of Texas at Austin

Project performed in cooperation with the Texas Department of Transportation and the Federal Highway Administration.

Center for Transportation Research
The University of Texas at Austin
1616 Guadalupe, Suite 4.202
Austin, TX 78701

http://ctr.utexas.edu/

Disclaimers

Author's Disclaimer: The contents of this report reflect the views of the authors, who are responsible for the facts and the accuracy of the data presented herein. The contents do not necessarily reflect the official view or policies of the Federal Highway Administration or the Texas Department of Transportation (TxDOT). This report does not constitute a standard, specification, or regulation.

Patent Disclaimer: There was no invention or discovery conceived or first actually reduced to practice in the course of or under this contract, including any art, method, process, machine manufacture, design or composition of matter, or any new useful improvement thereof, or any variety of plant, which is or may be patentable under the patent laws of the United States of America or any foreign country.

Notice: The United States Government and the State of Texas do not endorse products or manufacturers. If trade or manufacturers' names appear herein, it is solely because they are considered essential to the object of this report.

Engineering Disclaimer

NOT INTENDED FOR CONSTRUCTION, BIDDING, OR PERMIT PURPOSES.

Project Engineer: Michael D. Engelhardt
Professional Engineer License State and Number: Texas No. 88934
P. E. Designation: Research Supervisor

Acknowledgments

The authors extend appreciation to the Texas Department of Transportation for providing funding for this project. The authors also thank Darrin Jensen and Leon Flournoy of TxDOT for their support, encouragement and assistance with this project.

Table of Contents

CHAPTER 1. INTRODUCTION **1**

1.1 Overview 1

1.2 Project Objectives and Report Outline 1

CHAPTER 2. BACKGROUND 3

2.1 Overview 3

2.2 Composite Design 3

2.2.1 Fully and Partially Composite Behavior 3

2.2.2 Strength of Composite Girders 4

2.2.3 Stiffness of Composite Girders 5

2.3 Post-Installed Adhesive Anchor Shear Connectors 5

2.4 Inelastic Moment Redistribution 5

2.5 Load Factor Rating of Bridges 8

2.5.1 Rating Levels and Limit States 8

2.5.2 Rating Procedures 8

2.6 Summary 10

CHAPTER 3. STRENGTHENING DESIGN AND CONSTRUCTION RECOMMENDATIONS 11

3.1 Recommended Strengthening Design Procedure 11

3.1.1 Live Load Analysis 11

3.1.2 Evaluation of Existing Bridge 12

3.1.3 Targets for Strengthened Bridge 12

3.1.4 Check Negative Moment Regions and Redistribute Moments 12

3.1.5 Design Connectors for Positive Moment Regions 13

3.1.6 Locate Connectors along Bridge 13

3.1.7 Check Fatigue Strength of Connectors 14

3.2 Recommended Connector Installation Procedure 16

CHAPTER 4. LAKEPORT BRIDGE 18

4.1 Overview 18

4.2 Bridge Geometry and Properties 18

4.3 Evaluation of Existing Bridge and Strengthening Targets 20

4.4 Summary 22

CHAPTER 5. DESIGN OF STRENGTHENING SYSTEM 23

5.1 Overview 23

5.2 Design Considerations 23

5.3 Design Results 24

5.4 Summary 28
CHAPTER 6. LIVE LOAD TESTING OF THE NON-COMPOSITE LAKEPORT BRIDGE 29
6.1 Overview 29
6.2 Instrumentation of the Lakeport Bridge 29
6.3 Load Test Program 34
6.4 Finite Element Modeling 42
6.5 Load Test Results 44
6.5.1 Deflection Results 44
6.5.2 Slip Results 47
6.5.3 Stress Results 50
6.6 Summary 53
CHAPTER 7. SUMMARY AND CONCLUSIONS 54
7.1 Summary 54
7.2 Conclusions 54
7.3 Recommendations for Future Research 55
REFERENCES 56
APPENDIX. STRENGTHENING DESIGN CALCULATIONS 58

List of Figures

Figure 1.1 Post-Installed Adhesive Anchor Shear Connectors (Kwon et al. 2007) 1
Figure 2.1 Plastic Stress Distributions in Composite Girders..... 4
Figure 2.2 AASHTO Moment Redistribution Procedure 7
Figure 2.3 HS 20 Live Load (AASHTO 2002)..... 9
Figure 3.1 Design Procedure..... 11
Figure 3.2 Recommended Connector Layout 14
Figure 3.3 Connector Installation 17
Figure 4.1 Photograph of the Lakeport Bridge 18
Figure 4.2 Cross Section View of Half of the Bridge..... 19
Figure 4.3 Elevation View of Half of the Girders 19
Figure 4.4 Results from Load Rating of Existing Non-Composite Girders at Locations of Maximum Moment and Section Transitions..... 21
Figure 5.1 Cross-Sectional Layout of Connectors..... 24
Figure 5.2 Summary of Design Results 26
Figure 5.3 Results from Load Rating of Strengthened Girders at Locations of Maximum Moment and Section Transitions 27
Figure 5.4 Suggested Locations of New Cross Frames and Bearing Stiffeners Required for Moment Redistribution – (a) Elevation View and (b) Plan View of Girders 28
Figure 6.1 Scaffolding Towers Erected for Instrumentation – (a) South Span and (b) Middle Span..... 29
Figure 6.2 Photographs of the Bridge Prior To Instrumentation – (a) Jan 6, 2016 (b) Jun 6, 2016 (c) Aug 5, 2016 30
Figure 6.3 Installing Instrumentation on Girders B and C..... 31
Figure 6.4 Installing Strain Gages on the Bridge – (a) Grinding the Bottom Flange, (b) Grinding the Top Flange, (c) Strain Gage on the Mid-Height of the Bottom Flange, and (d) Strain Gage on the Mid-Height of the Top Flange..... 32
Figure 6.5 Bridge Instrumentation – (a) String Potentiometers Used to Measure Deflection (b) Longitudinal View of a Typical Slip Transducer (c) Transverse View of a Typical Slip Transducer..... 33
Figure 6.6 Data Acquisition System – (a) Datalogger and (b) Laptop Computer 34
Figure 6.7 Photograph of Typical Truck used in Load Test..... 34
Figure 6.8 Dimensions and Axle Weights of Trucks Used in Load Test 35
Figure 6.9 Test 70-B Setup 36

Figure 6.10 Test 70-C Setup 37
Figure 6.11 Test 70-BC Setup 38
Figure 6.12 Test 90-B Setup 39
Figure 6.13 Test 90-C Setup 40
Figure 6.14 Test 90-BC Setup 41
Figure 6.15 Photographs of (a) Back-to-Back Loading Configurations and (b) Side-by-Side Loading Configurations 42
Figure 6.16 Plan View of Half of the Bridge Showing Locations of Different Types of Cross Frames 43
Figure 6.17 Typical Cross Section View of Half of the Bridge in SAP2000 43
Figure 6.18 Typical Elevation View of the Bridge 43
Figure 6.19 3D Model of the Bridge 44
Figure 6.20 Deflection Results for Loading Configurations in the South Span 45
Figure 6.21 Deflection Results for Loading Configurations in the Middle Span 46
Figure 6.22 Slip Results for Loading Configurations in the South Span 48
Figure 6.23 Slip Results for Loading Configurations in the Middle Span 49
Figure 6.24 Stress Results for Loading Configurations in the South Span 51
Figure 6.25 Stress Results for Loading Configurations in the Middle Span 52
Figure 6.26 Estimated Neutral Axis Location for All Loading Configurations 53

Chapter 1. Introduction

1.1 Overview

Many older bridges in the state of Texas were constructed with floor systems consisting of a non-composite concrete deck over steel girders. While the individual elements in these bridges tend to still be in good condition, the structures often do not satisfy current load requirements and thus may need to be strengthened or replaced. A potentially economical method for strengthening these bridges is to develop composite action by attaching the existing concrete deck to the steel beams using post-installed shear connectors. This provides an increase in strength and stiffness to primarily regions of the bridge dominated by positive flexural demands, where the concrete deck is in compression and the steel beams are primarily in tension. To address any strength deficiencies near the interior supports of continuous bridges, which are dominated by negative flexural demands, inelastic moment redistribution can be considered.

These strengthening concepts were developed by TxDOT Project 0-6719, which investigated the structural behavior of strengthened continuous girders in the laboratory (Kreitman et al. 2015). Adhesive anchors, as shown in Figure 1.1, were used as post-installed shear connectors. These connectors have significantly improved fatigue strength over conventional welded shear studs, allowing for partially composite design in the strengthening process. Through this research, design recommendations were developed along with a recommended procedure for installing the adhesive anchor connectors. The findings from TxDOT Project 0-6719 built upon earlier work conducted in TxDOT Projects 0-4124 and 5-4124 (Kwon et al. 2007, Kwon et al. 2009).

During this first phase of TxDOT Project 5-6719, the findings from this research were used to evaluate and conduct a strengthening design for an existing continuous non-composite steel I-girder bridge in Lakeport, Texas. Additionally, a live load test was conducted on the bridge prior to later compare the pre- and post-strengthening behavior. The second phase of this project will include monitoring of the construction process and conducting a load test following the strengthening of the bridge.

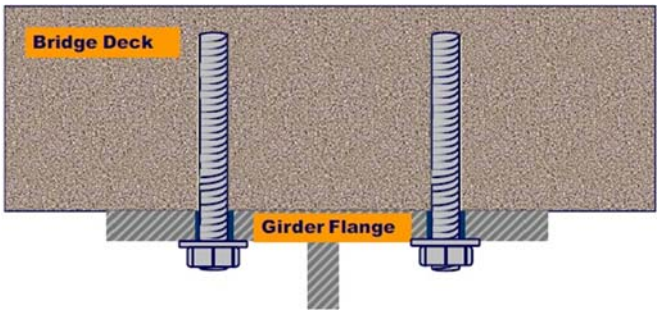

Figure 1.1 Post-Installed Adhesive Anchor Shear Connectors (Kwon et al. 2007)

1.2 Project Objectives and Report Outline

The main goal of this research project was to implement the findings and recommendations from TxDOT Project 0-6719 to strengthen an existing continuous non-composite steel I-girder bridge. To accomplish this objective, the following major tasks were carried out:

- Select a bridge for strengthening, determine strengthening targets, and evaluate the existing non-composite bridge,
- Develop a 3D finite element model of the bridge,
- Complete a design of the strengthening system for the bridge, and
- Conduct a load test on the existing non-composite bridge.

This report is organized into seven chapters. Following this introductory chapter, Chapter 2 provides pertinent background information about post-installed adhesive anchor shear connectors, inelastic moment redistribution, and load rating procedures. Chapter 3 summarizes the recommendations for design and construction procedures made by TxDOT project 0-6719. The bridge chosen for strengthening is described in Chapter 4, which also presents the results from the load rating of the existing non-composite structure. Chapter 5 discusses the design process and the final design of the strengthening system. A description of and results from the live load testing of the existing non-composite bridge are provided in Chapter 6, which also compares these results to the predicted behavior from finite element modeling. A summary of the report and conclusions from this project are given in Chapter 7. The Appendix provides design calculations for the strengthening system including details of the load rating calculations for the existing non-composite bridge.

Chapter 2. Background

2.1 Overview

This chapter provides pertinent background information regarding the evaluation and strengthening of continuous steel girder bridges using the proposed method. First, a summary of composite design is given. This is followed by a review of the behavior and design of post-installed adhesive anchor shear connectors. Next, an overview of the AASHTO provisions governing inelastic moment redistribution in continuous steel girder bridges is provided. Finally, an overview of load rating using the load factor method is given.

2.2 Composite Design

A steel-concrete composite girder has a floor system in which the concrete deck is mechanically attached to the supporting steel beams so that the two elements bend together (Oehlers and Bradford 1995). This mechanical attachment is achieved using shear connectors, which are fixed to the top flange of the steel beam and embedded into the concrete deck. Conventional shear connectors are comprised of headed studs, which are welded to the top flange prior to casting of the deck.

2.2.1 Fully and Partially Composite Behavior

A fully composite girder has enough shear connectors to develop the full strength of the composite cross section, which is controlled by the maximum plastic force that can be developed in either the steel beam or in the concrete deck. On the other hand, a partially composite girder has fewer shear connectors, so that the strength of the cross section is controlled by the shear connection. For both fully and partially composite girders, the shear connection must transfer the horizontal interface shear force (C_f), which is defined as the following for girders subjected to positive flexure:

$$C_f = min\begin{cases} 0.85\, f_c'\, A_c \\ (A_s\, F_y)_{girder} \\ \Sigma Q_n \end{cases} \qquad \textit{Equation 2.1}$$

where A_c is the area of the concrete deck within the effective width having a 28-day compressive strength of f_c', A_s is the cross-sectional area of the steel beam having a yield strength of F_y, and ΣQ_n is the sum of the static shear strength of all shear connectors between the points of zero and maximum moment.

In a fully composite girder, one of the top two expressions in Equation 2.1 will control. The number of shear connectors that must be located between points of zero and maximum moment to develop fully composite behavior (N_{full}) is defined as:

$$N_{full} = \frac{C_f}{Q_n} \qquad \textit{Equation 2.2}$$

where Q_n is the static strength of a single shear connector.

In a partially composite girder, the bottom expression in Equation 2.1 will always control. Partially composite girders are characterized by the composite ratio (η), which is defined as:

$$\eta = \frac{N}{N_{full}} \qquad \textit{Equation 2.3}$$

where N is the number of connectors provided between points of zero and maximum moment in the partially composite girder. A practical lower bound of approximately 0.3 is often set for the composite ratio in many specifications to ensure that both the steel beam and the shear connectors behave elastically under service-level loads and that significant ductility is provided beyond the ultimate strength (AISC 2010).

In fully composite girders, the "interface slip", or the relative longitudinal motion between the underside of the concrete deck and the top flange of the steel girder, is very small and is usually neglected in design. However, this interface slip can be of significant magnitude in partially composite girders due to the reduced number of shear connectors provided. The effects of this slip should be considered in the design of a partially composite girder.

2.2.2 Strength of Composite Girders

The plastic flexural strength of a compact, well-braced, fully or partially composite girder is calculated using the appropriate assumed plastic stress distribution from Figure 2.1 (AISC 2010). For fully composite girders, the plastic neutral axis can be located either in the concrete deck (a) or in the steel beam (b), while the plastic neutral axis in a partially composite girder will always be located in the steel section (c). All portions of the steel beam are assumed to be fully yielded in either compression or tension, depending on the neutral axis location. A compressive stress block with a resultant force equal to the horizontal interface shear force extends down from the top of the deck through a depth that satisfies force equilibrium. The deck is assumed to resist no tensile forces. The flexural capacity is determined by the summation of moments in this stress distribution.

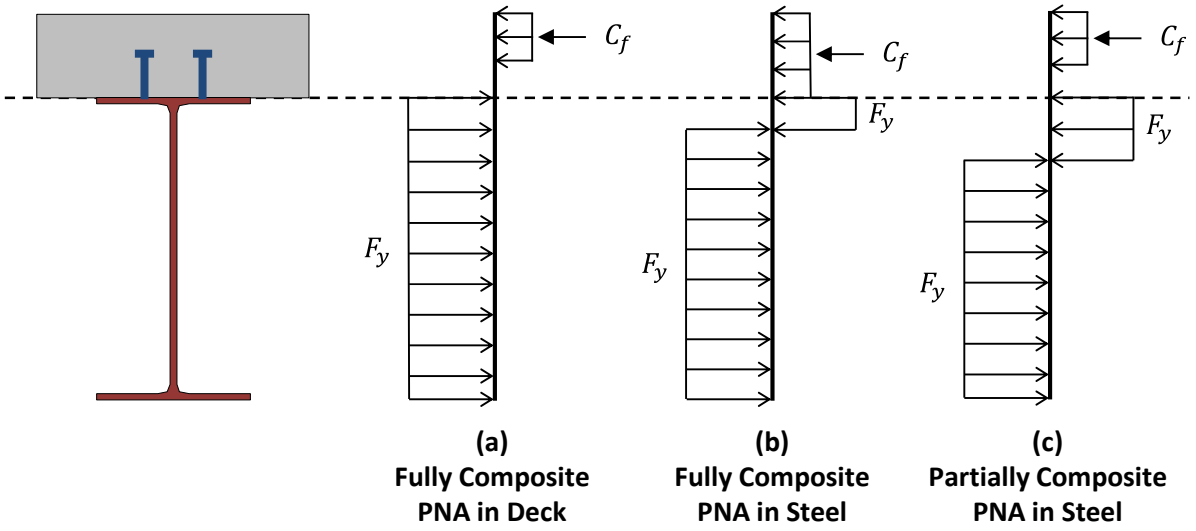

Figure 2.1 Plastic Stress Distributions in Composite Girders

Because the strength of a partially composite girder is controlled by the shear connection, the flexural strength will be reduced from that of a fully composite girder. However, this relationship between strength and composite ratio is not linear. In fact, partially composite action is very efficient, as small composite ratios can provide significant strength increases over a non-composite girder. As the composite ratio is increased, the increase in strength occurs at a

decreasing rate. The same trend is observed in the stiffness of partially composite girders, which is discussed in the following sections.

Because of the efficiency of partially composite action, many building structures are designed economically using partially composite girders. However, in bridge design, the fatigue strength of conventional welded shear studs tends to control the design, rather than the static strength requirements. Fatigue design usually requires enough shear connectors for fully composite action to develop in a bridge. Thus, the Association of American State Highway and Transportation Officials (AASHTO) *LRFD Bridge Design Specifications* do not currently allow for partial-composite action (AASHTO 2010).

2.2.3 Stiffness of Composite Girders

The moment of inertia of a fully composite girder is computed by statics as the transformed moment of inertia of the composite cross section. This ignores the negligible amounts of interface slip that occur in fully composite girders. However, the large amounts of interface slip that occur in partially composite girders can significantly reduce the cross-sectional stiffness. The American Institute for Steel Construction (AISC) *Commentary to the Specification for Structural Steel Buildings* recommends the following equation to estimate the effective moment of inertia (I_{eff}) of partially composite girders for the purposes of computing deflections (AISC 2010):

$$I_{eff} = I_s + \sqrt{\eta}\,(I_{tr} - I_s) \qquad \textit{Equation 2.4}$$

where I_s and I_{tr} are the moments of inertia of the steel section and of the fully composite uncracked transformed section, respectively. Note that the effective elastic section modulus (S_{eff}) can be estimated in the same manner for the purposes of computing stresses in partially composite girders.

2.3 Post-Installed Adhesive Anchor Shear Connectors

Figure 1.1 shows the adhesive anchor type of post-installed shear connector used in this research. This connector is installed entirely from the underside of the deck and requires the drilling of slightly oversized holes through the top flange of the steel beam and into the concrete deck. The connector is comprised of ASTM A193 B7 threaded rod, with a recommended diameter of 7/8 inch. A two-part structural adhesive is injected into the drilled hole prior to inserting the threaded rod. Hilti HIT-HY 200-R is recommended for use as the adhesive, as it performed well during the laboratory testing.

Design equations for post-installed adhesive anchor shear connectors at strength and fatigue limit states are given in Chapter 3, along with details regarding the installation of these connectors. Note that the fatigue design provisions have been modified from those given in the final report of TxDOT project 0-6719.

2.4 Inelastic Moment Redistribution

The inelastic moment redistribution provisions provided in the *AASHTO LRFD Bridge Design Specifications* are recommended for use in conjunction with this strengthening method (AASHTO 2010). These provisions are found in Appendix B6 of the specifications, and a summary is given here.

These provisions apply only to straight steel I-girder bridges with skew angles not exceeding 10 degrees and with no staggered cross frames. The cross section at all interior pier

locations from which moments will be redistributed must abide by certain web and flange slenderness limits. The web can be compact, noncompact, or slender, to a certain extent, but the flange must be compact. The compression flange must also be sufficiently braced to allow for large plastic rotations without lateral-torsional buckling occurring. The specifications also require that double-sided bearing stiffeners are present at these interior pier sections.

The general procedure for redistributing moments from the interior pier sections of continuous girder bridges is illustrated in Figure 2.2 and summarized as follows:

- Conduct an elastic analysis of the bridge girder for the load combination of interest. Moment redistribution is allowed for Service II and all Strength load combinations. Obtain the elastic moment envelope (M_e).
- Compute the effective plastic moment capacity (M_{pe}) at each interior pier. This effective capacity accounts for the slenderness of the section and ensures that an adequate amount of plastic rotation can be attained for moment redistribution to occur.
- If the magnitude of the elastic moment at the interior pier exceeds the effective capacity, the difference between the two is the amount of moment that needs to be redistributed. This "redistribution moment" (M_{rd}) is limited to 20% of the elastic moment.
- Draw the redistribution moment diagram by connecting the computed residual moments at each pier with straight lines.
- Add the redistribution moment diagram to the elastic moment envelope, and check that the capacity is not exceeded at any other point along the bridge.

Elastic Moment Envelope

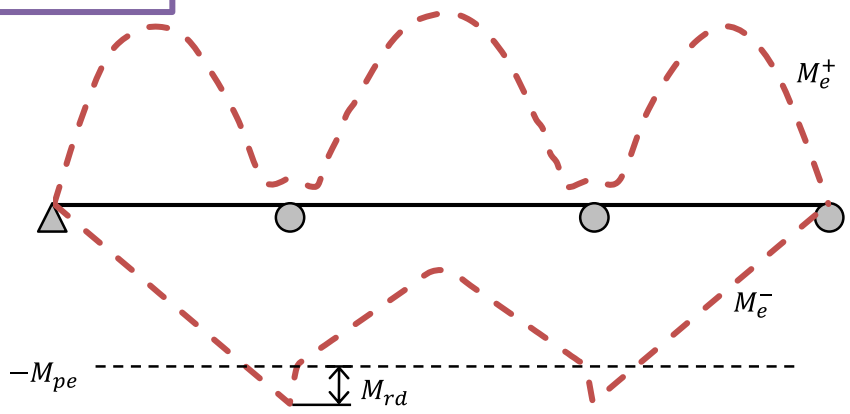

$$M_{pe} = \left(A - 2.3 \frac{b_{fc}}{t_{fc}} \sqrt{\frac{F_{yc}}{E}} - 0.35 \frac{D}{b_{fc}} + 0.39 \frac{b_{fc}}{t_{fc}} \sqrt{\frac{F_{yc}}{E} \frac{D}{b_{fc}}} \right) M_n \leq M_n$$

A = Constant between 2.63 and 2.90, depending on section properties and limit state
E = elastic modulus

b_{fc} = width of compression flange
t_{fc} = thickness of compression flange
D = web depth
F_{yc} = yield stress of compression flange

$$M_{rd} = |M_e| - M_{pe} \leq 0.2 M_e$$

Redistribution Moment Diagram

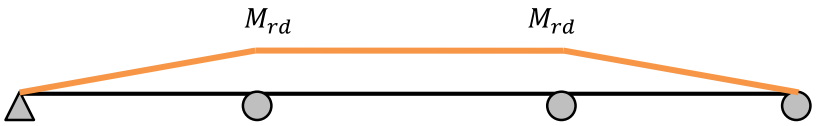

Resulting Moment Envelope

$$M_{total} = M_e + M_{rd}$$

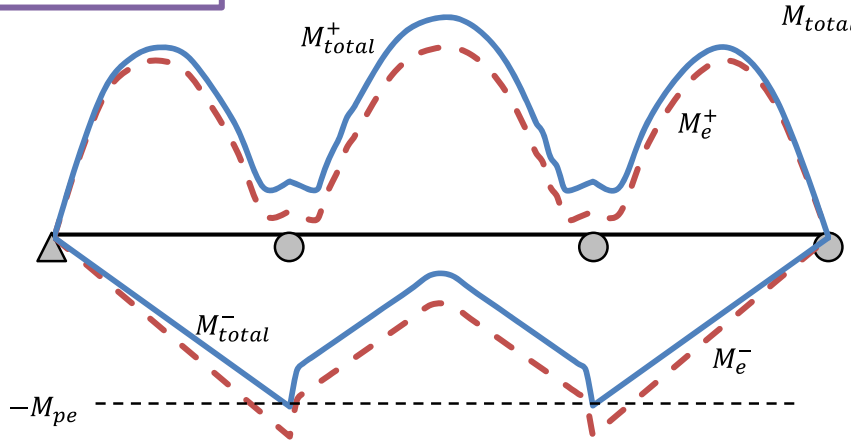

Figure 2.2 AASHTO Moment Redistribution Procedure

2.5 Load Factor Rating of Bridges

Load rating provides a comparison of the load-carrying capacity of an existing bridge to a particular bridge live load. This is a way to evaluate the safety of an existing bridge that was designed for different, usually smaller, loads. For the purposes of this research, load rating was used to evaluate the load-carrying capacities of both the existing non-composite bridges and the strengthened partially composite bridges.

The AASHTO *Manual for Bridge Evaluation* specifies procedures for conducting a load rating of an existing bridge using three methods: allowable stress rating, load factor rating, and load and resistance factor rating (AASHTO 2011). Load factor rating, based on the load factor design provisions from the most recent version of the AASHTO *Standard Specifications for Highway Bridges*, was chosen for the purposes of this research to be consistent with typical TxDOT practices (AASHTO 2002).

2.5.1 Rating Levels and Limit States

Load ratings for strength can be computed at both inventory and operating rating levels. The inventory rating is associated with load magnitudes used in the design of a new bridge and makes use of the same load factors. Live loads equivalent to the inventory rating should be able to be resisted indefinitely throughout the life of the bridge, barring any fatigue or durability-related failures. The operating rating represents the maximum load the bridge can sustain. Repeated application of this large level of load to the bridge is not recommended (AASHTO 2011).

The limit states considered in these load ratings were Overload and Maximum Load as defined by the AASHTO standard specifications (AASHTO 2002). The Overload limit state restricts permanent inelastic deformations from heavy permit vehicles that may be occasionally allowed on the bridge (Hansell and Viest 1971). It corresponds to the Service II limit state in the LRFD specifications, and restricts the maximum stresses in the steel girder to 80% and 95% of the yield stress for non-composite and composite sections, respectively. Because the AASHTO specifications do not allow for partially composite design, it is unclear what limiting stress should be used for partially composite sections, but a 95% limit was recommended by previous research (Kreitman et al. 2015). When moment redistribution is considered from the interior supports, the stress limit at the Overload limit state is ignored in those regions. The Maximum Load limit state is associated with the ultimate capacity of the bridge and corresponds to the Strength I limit state in the LRFD specifications when primarily considering gravity loads. Limit states involving serviceability, lateral loads, or other types of loads are generally not considered in load rating. The fatigue limit state can be investigated using provisions in the *Manual for Bridge Evaluation* if desired (AASHTO 2011).

2.5.2 Rating Procedures

A complete and thorough load rating would check flexure, shear, and axial forces at all locations in every member as well as the connections and any other details. The final reported load rating of a bridge would be the smallest rating calculated anywhere along the bridge. However, for a particular type of bridge, the controlling sections and limit states can often be easily identified beforehand to simplify the process. For the continuous steel I-girder bridges considered in this study, the flexural capacity of the girders will usually control, especially if the girders are comprised of rolled sections. For built-up sections with stiffeners and very thin webs, a load rating

for shear should also be considered. Connections, such as girder splices, are not normally considered in the rating process but can be if necessary or desired.

The first step in load rating is to conduct a structural analysis of the existing bridge using the live load corresponding to the chosen rating method. For the load factor rating reported here, this was an HS 20 live load as defined in the AASHTO standard specifications and summarized in Figure 2.3.

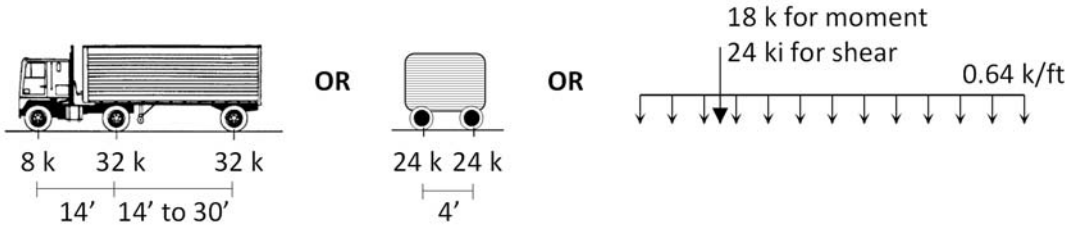

Figure 2.3 HS 20 Live Load (AASHTO 2002)

Next, the flexural capacities of the critical sections of the bridge are calculated. For load factor rating, the capacity is calculated using the design provisions in the AASHTO standard specifications. For a compact, sufficiently braced section in flexure, the capacity is taken as the plastic moment (M_p) for the Maximum Load limit state. This flexural capacity may be reduced based on local or lateral-torsional buckling. For the Overload limit state, the capacity refers to the limits on the maximum stress in the steel beam. Actual or estimated in situ material properties should be used in the load rating calculations. If these properties are unknown, recommended values from the *Manual for Bridge Evaluation* can be used (AASHTO 2011).

The next step is to compute the rating factor, which represents the fraction of the live load that the bridge can safely carry. The bridge can adequately resist the full live load if the rating factor is greater than or equal to unity. A rating factor is calculated for every critical section for both the inventory and operating rating levels. Generally, the rating factor (RF) is defined as the ratio of the capacity available to resist live loads to the factored live load:

$$RF = \frac{C - A_1 D}{A_2 (L + I)} \qquad \textit{Equation 2.5}$$

where C is the capacity of the section, D is the dead load force effect, $(L + I)$ is the live load force effect including the impact factor or dynamic allowance, and A_1 and A_2 are load factors that depend on the type and level of the load rating. For load factor rating, A_1 is taken as 1.3 for both the inventory and operating levels, and A_2 is taken as 2.17 for the inventory rating and 1.3 for the operating rating. Because the only difference between the inventory and operating load rating calculations is the load factor on the live load (A_2), the two ratings will differ by a constant factor for all bridges. The operating rating will always be 1.67 times greater than the inventory rating.

The final step in the rating procedure is to express the rating factor in terms of the live load. This is simply done by multiplying the rating factor by the magnitude of the HS load used in the structural analysis. For example, for an HS 20 load, the rating factor is multiplied by 20. The lowest inventory and operating load ratings from every section along the bridge are then chosen as the final load ratings for the bridge.

2.6 Summary

This chapter has provided relevant background information to supplement the information in the remainder of this report. In particular, an overview of composite design as well as post-installed shear connectors was provided, along with a summary of the inelastic moment redistribution provisions in the AASHTO LRFD specifications and a description of load factor rating procedures.

Chapter 3. Strengthening Design and Construction Recommendations

3.1 Recommended Strengthening Design Procedure

The recommended design procedure for strengthening continuous non-composite bridges with post-installed shear connectors is summarized in Figure 3.1. This procedure was described in detail in the report from TxDOT project 0-6917, and is repeated here for completeness. Note that these recommendations were developed for bridge girders primarily governed by flexural strength requirements and include fatigue considerations only for the post-installed shear connectors. Shear strength of the girders, fatigue strength of other details, and behavior of other bridge components are not explicitly included here, but should be checked as needed.

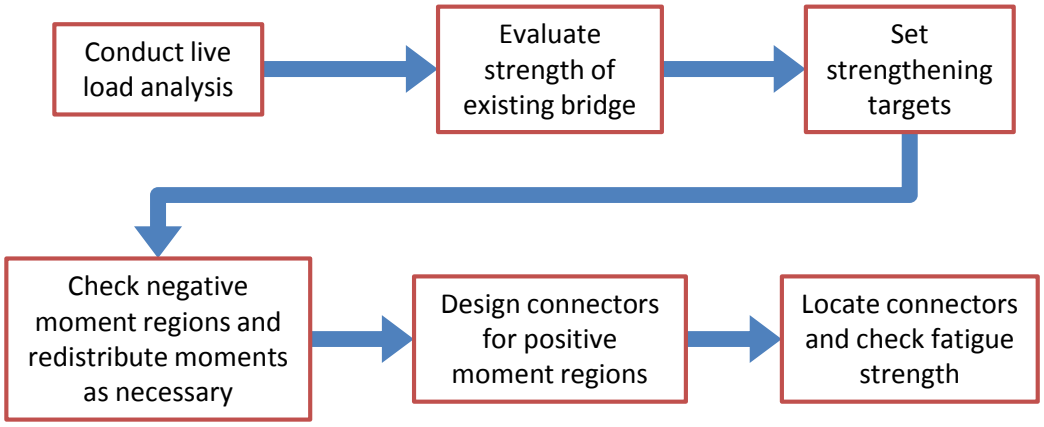

Figure 3.1 Design Procedure

3.1.1 Live Load Analysis

The first step that should be taken is to conduct a structural analysis on the bridge under the live load that will be used to evaluate the existing bridge and design the strengthened girders. This loading pattern can be chosen to meet the needs of a particular bridge or situation, allowing for flexibility in the procedure for a variety of cases. In this project, an AASHTO HS 20 live load was used to be consistent with the Load Factor Design and Rating methods and general TxDOT practices.

The moving load analysis can be conducted in any manner desired by the designer. For the purposes of determining the live load moment envelopes, researchers have found that a simple line element analysis using the flexural stiffness of the non-composite girder along the entire length of the bridge adequately represents the distribution of forces in both the existing non-composite bridge as well as the partially composite strengthened bridge for typical straight girder bridges in which post-installed connectors are added in all spans (Kreitman 2016). The appropriate distribution factors should be applied for interior and exterior girders.

Alternatively, a more rigorous live load analysis can be conducted using software with 3D modeling capabilities, such as SAP2000, which can explicitly model the steel beams, concrete deck, and shear connectors (CSI 2011). This type of analysis may be particularly useful for bridges with complex geometries. However, it requires that an initial guess of the number and layout of the shear connectors is made, leading to an iterative design procedure. It is recommended to run

separate analyses for the non-composite existing bridge and for the partially composite strengthened bridge, because the moment envelopes may vary based on the location of the shear connectors. This may be especially true for asymmetric span layouts or if the composite ratio varies greatly along the length of the strengthened bridge. In any 3D model, it is recommended to represent the adhesive anchor shear connectors as linear elastic springs with a stiffness of 900 kips per inch.

3.1.2 Evaluation of Existing Bridge

Using the results from the live load analysis, the strength of the existing bridge can be determined. For the purposes of this research, the Load Factor Rating method was used, as specified in the *AASHTO Manual for Bridge Evaluation* (AASHTO 2011). Limit states of Overload and Maximum Load were both considered in the load rating process. The Overload limit state prevents excessive permanent deformations of the bridge under typical levels of load and corresponds to the Service II limit state in the *AASHTO LRFD Bridge Design Specifications* (AASHTO 2010). The Maximum Load limit state is a reflection of the maximum carrying capacity of the bridge and corresponds to the Strength I limit state in the LRFD specifications when only considering gravity loads.

Fatigue of particular details not related to the post-installed shear connectors was not considered in the evaluation of existing bridges discussed in this report, but can be if desired. The *Manual for Bridge Evaluation* provides guidelines on evaluating the remaining fatigue life for critical details of existing bridges (AASHTO 2011). Recently proposed revisions to these guidelines are available through research conducted by the National Cooperative Highway Research Program (NCHRP 2012).

3.1.3 Targets for Strengthened Bridge

Once the existing bridge has been evaluated, targets for the strength and remaining life of the strengthened bridge should be set before beginning the design process. These targets can be chosen to accommodate any particular case, but it is recommended that both strength and fatigue limit states are considered. For fatigue purposes, a projected average daily truck traffic in a single lane ($(ADTT)_{SL}$) of the bridge over the expected remaining life should be estimated.

A strengthening target of attaining an inventory load rating of HS 20 was chosen by the researchers as an upper bound of the strengthening requirements that a bridge owner might consider. A bridge with an inventory rating of HS 20 has a load-carrying capacity meeting the design requirements for a new bridge designed with the Load Factor Design method from the *AASHTO Standard Specifications for Highway Bridges* (AASHTO 2002). No specific strengthening targets for fatigue were consistently used by the researchers. This will vary depending on the desired remaining bridge life and the projected truck traffic over that bridge life for the particular bridge of interest.

3.1.4 Check Negative Moment Regions and Redistribute Moments

To begin the design of the strengthened bridge, the first step is to check the negative moment regions around the interior piers. If the capacity of the existing non-composite girder exceeds the demand from the moment envelope at all pier locations, the negative moment regions can be deemed acceptable in terms of strength, and the design can proceed to the positive moment regions.

Otherwise, if the demand from the moment envelope at any of the pier locations exceeds the capacity of the existing non-composite girder, inelastic moment redistribution is required. It is recommended that the provisions of Appendix B6 of the AASHTO LRFD specifications be used for moment redistribution, as discussed in Section 2.4. These provisions require that the bridge is straight with no more than a 10 degree skew, and that the interior pier sections are well-braced, meet fairly unrestrictive slenderness limits, and have bearing stiffeners. Based on observations from previous research, the majority of these provisions are often already satisfied in typical existing bridges with the exception of the skew angle limit and the requirements for lateral bracing and bearing stiffeners. In many cases, bearing stiffeners and/or additional cross frames will need to be added to the bridge as part of the strengthening process.

The provisions also limit the amount of moment redistribution to 20% of the elastic moment. By following the procedure outlined in Section 2.4, the "redistribution moment diagram" can be drawn. These redistribution moments are then added to the design moment envelope for the remainder of the design. Note that inelastic moment redistribution can occur at both the Overload and Maximum Load limit states, although the capacities and moment envelopes will be different between the two cases. This process is illustrated in detail in the calculations provided in the Appendix.

3.1.5 Design Connectors for Positive Moment Regions

The next step in the design is focused on strengthening the positive moment regions near the middle of the spans by adding shear connectors and creating composite action. To begin this process, the required strength in these regions is determined from the design moment envelope, including the redistribution moments if applicable. Simple plastic cross-sectional analysis is then used to determine the number of connectors needed to attain the required strength, as illustrated in the design calculations in the Appendix. The design static strength of a single post-installed adhesive anchor shear connector (Q_n) is (Kwon et al. 2007):

$$Q_n = 0.5\, A_{sc} F_u \qquad \textit{Equation 3.1}$$

where A_{sc} is the effective cross-sectional area of the connector, taken as 80% of the nominal area of the threaded rod, and F_u is the specified nominal tensile strength of the threaded rod.

Note that the maximum strength that can be attained by creating composite action is ultimately controlled by the properties of the steel girder and concrete deck, rather than the shear connectors. If the required strength in any of the positive moment regions exceeds the fully composite cross-sectional strength, adding more shear connectors will not result in any further strength gain. Along with the 20% limit on moment redistribution, the strength of the fully composite section places an upper limit on the potential strength increase that can be achieved for a particular bridge.

3.1.6 Locate Connectors along Bridge

After the strength design is complete, the connectors must be laid out along the girders before the fatigue limit state can be checked. The following preliminary recommendations for connector layout, illustrated in Figure 3.2, are made based on analytical and experimental investigation from the present research and from previous research (Kwon et al. 2007, 2009):

- Connectors should be placed in pairs, with one on either side of the web at every location. It is recommended that general AASHTO requirements regarding clear cover, edge distance, and minimum transverse spacing are followed. A transverse

spacing of approximately 6 inches was used in all laboratory testing for beams with 10- to 11-inch wide flanges.

- It is recommended that connectors are concentrated near points of zero or low moment, rather than distributed uniformly through the positive moment regions, to improve the ductility of the strengthened girders.
- A longitudinal spacing of approximately 12 inches is recommended between pairs of concentrated connectors, although analysis indicates that the behavior is not significantly affected by slight changes in spacing, provided that the connectors are still effectively concentrated near points of low moment. All laboratory testing was conducted with a 12- or 24-inch spacing. Choosing a connector spacing that is a multiple of the transverse rebar spacing will help avoid bars during construction.
- At the ends of continuous units, the connector group should be located as close as possible to the end of the steel beam. The minimum longitudinal distance from the centerline of the support to the first connector pair used in the experimental testing was 6 inches.
- The most efficient location for interior connector groups is typically when the connector closest to the interior support is located approximately 15% of the span length away from that support.
- Constructability and accessibility in the field should be considered when choosing a connector layout. If possible, the site should be visited to identify potential problems that may arise during connector installation. The use of a rebar locator is highly recommended to choose a layout that avoids reinforcing bars.

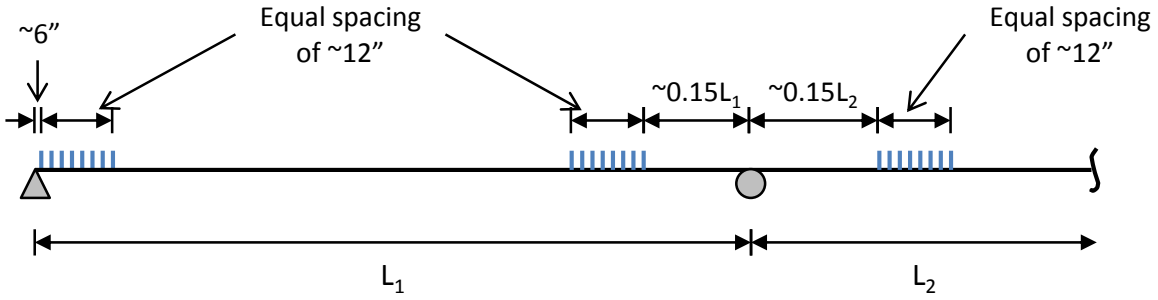

Figure 3.2 Recommended Connector Layout

3.1.7 Check Fatigue Strength of Connectors

The preliminary fatigue design provisions that were recommended previously have been revised to a format that follows the procedures in the AASHTO LRFD specifications for general fatigue design, rather than fatigue design for conventional welded stud shear connectors. The new recommendations are as follows.

A limiting value of the projected average annual daily truck traffic in a single lane ($(ADTT)_{SL}$) is provided to determine the appropriate load combination to use for the fatigue design. This limiting value is dependent on the number of years of remaining life desired for the bridge (Y):

$$(ADTT)_{SL\ limit} = \frac{8{,}700{,}000}{Y} \qquad \textit{Equation 3.2}$$

If the projected $(ADTT)_{SL}$ is greater than this limiting value, the Fatigue I load combination is used to design for infinite fatigue life. Otherwise, the Fatigue II load combination is used to design for finite fatigue life. The limiting value of truck traffic was determined by equating the infinite life and finite life fatigue shear resistances, accounting for the different load factors in the two load combinations, and corresponds to the values in Table 6.6.1.2.3-2 of the LRFD specifications. This limit assumes that the number of stress cycles per truck passage (n) is equal to one, and should be divided by the value of n if this is not the case. For continuous bridges with span lengths greater than 40 feet, n is taken as 1.0 for all connectors located more than one-tenth of the span length away from an interior support. For connectors located within one-tenth of the span length from an interior support, n is taken as 1.5. Note that Equation 3.2 tends to result in very large limiting values, indicating that the Fatigue II limit state will control in essentially all cases.

For infinite life and the Fatigue I limit state, the nominal fatigue resistance for adhesive anchor connectors ($(\Delta F)_n$) is equal to the constant-amplitude fatigue threshold value ($(\Delta F_n)_{TH}$):

$$(\Delta F_n) = (\Delta F)_{TH} = 15\ ksi \qquad \textit{Equation 3.3}$$

For finite life and the Fatigue II limit state, the nominal fatigue resistance for adhesive anchor connectors is determined using the following equation.

$$(\Delta F_n) = \left(\frac{A}{N}\right)^{1/m} \qquad \textit{Equation 3.4}$$

where $A = 4.24\ x\ 10^{15}\ ksi$, $m = 7$, and the number of cycles (N) is computed as:

$$N = (365)(Y)(n)(ADTT)_{SL} \qquad \textit{Equation 3.5}$$

The constant-amplitude fatigue threshold in Equation 3.3 corresponds to the endurance limit of 15 ksi that was observed during the small-scale testing conducted in TxDOT projects 0-4124 and 0-6719 (Kwon et al. 2007, Kreitman et al. 2015). Equation 3.4 was derived from a best fit to this experimental data. The exponent $(1/m)$ in this equation has been modified from 1/3 in the current LRFD specifications to 1/7 for post-installed adhesive anchor shear connectors. The small-scale testing that formed the basis for these design equations was conducted on 3/4- and 7/8-inch diameter connectors, and caution should be used in applying these equations outside of this range.

The fatigue analysis should be conducted using a procedure that explicitly considers the slip at the steel-concrete interface in partially composite girders, which can significantly reduce the force demand on the connectors as compared to conventional shear connector analysis techniques. While this analysis is more complex than the typical approach to designing shear connectors, it will provide more realistic connector forces for design and is easily programmed in a simple spreadsheet. Through the course of this research, an Excel-based program called UT-Slip has been developed to conduct this type of analysis (Ghiami Azad 2016). UT-Slip will be available for download on the FSEL website following the publication of this report (FSEL 2016).

Alternatively, the fatigue analysis can be done computationally through reasonably simple 3D models that discretely represent the shear connectors as spring elements. In this case, the force range in the connectors can be determined directly from the forces in the spring elements. A spring stiffness of 900 kips per inch is recommended for a single shear connector in a 3D model.

3.2 Recommended Connector Installation Procedure

The adhesive anchor shear connectors, shown in Figure 1.1, are composed of 7/8-inch diameter ASTM A193 B7 threaded rods. A two-part structural adhesive (Hilti HIT-HY 150-MAX or 200-R) was used in all of the experimental testing. The connectors are installed with the following procedure, illustrated in Figure 3.3:

1. Drill a 1-inch diameter hole through the top flange of the steel beam at the connector location (Figure 3.3(a)). This can be done using a portable drill with a magnetic base.
2. Through the hole in the flange, drill a 15/16-inch diameter hole into the concrete deck to the desired depth (Figure 3.3(b)). This can be done using a rotary hammer drill. A 2-inch cover to the top of the concrete deck was maintained in all laboratory testing, leaving an embedment depth of 4.5 inches into the deck.
3. Clean the hole with a wire brush and compressed air, as specified by the adhesive installation procedures (Figure 3.3(c)).
4. Inject the adhesive into the hole using the appropriate dispenser (Figure 3.3(d)). Take care that the hole is filled from the top down so that no air bubbles are present. The Hilti adhesive was viscous enough to not run downwards out of the hole after injection.
5. Place the threaded rod into the hole using a twisting motion so the adhesive fills the threads (Figure 3.3(e)). The Hilti adhesive was able to hold the connector in place immediately after installation and has a 9-minute working time at 70°F.
6. Allow the adhesive to cure. The Hilti adhesive has a 1-hour cure time at 70°F.
7. Tighten the nut to the torque specified by the adhesive (Figure 3.3(f)). The Hilti adhesive specifies a torque of 125 foot-pounds for 7/8-inch diameter rods.
8. Strike the exposed threads below the nut with a grinder. Although it is unlikely to occur, this will prevent any nuts that inadvertently loosen over time from potentially falling onto traffic or pedestrians passing under the bridge.

Figure 3.3 Connector Installation

Generally, this procedure follows the installation process recommended by the Hilti adhesive product with a few exceptions, namely the use of a 15/16-inch diameter hole in the deck instead of the prescribed 1-inch diameter. Due to the slightly enlarged head of the hammer drill bits, a 1-inch bit does not fit through the 1-inch diameter hole in the top flange. To minimize the oversized hole in the flange, a 15/16-inch diameter bit was used for the hole drilled into the deck.

Chapter 4. Lakeport Bridge

4.1 Overview

With assistance from bridge engineers at TxDOT, a bridge in Lakeport, Texas was chosen for strengthening using the proposed method from TxDOT project 0-6719. In this chapter, information about the geometry and properties of this bridge is first provided. Additionally, results from the load rating of the non-composite bridge are summarized along with the targets set for strengthening this bridge.

4.2 Bridge Geometry and Properties

The Lakeport Bridge provides a crossing for state highway 149 over the Sabine River in Lakeport, Texas. A three-span continuous steel unit comprises the portion of the bridge that crosses the river. The 32 approach spans are constructed of simply supported prestressed girders and are not the focus of this project. An estimated 24,110 vehicles cross the bridge each day, 4% of which are trucks. Over the next 30 years, this number is expected to rise to 33,760 vehicles per day.

A four-girder, two-lane bridge was originally constructed at this location in 1943 and was designed for H-15 loading. These original girders are 36WF150 sections with riveted cover plates on the top and bottom flanges at the piers and in the middle of the interior span. Cover plates are also located in the middle of the exterior spans on the interior girders. In 1961, the bridge was symmetrically widened to an eight-girder, four-lane bridge using 36WF160 girders with the additional lanes designed for H-20 loading. The additional girders have welded cover plates located on the top and bottom flanges at the piers and at the middle of the interior span.

Figure 4.1 is a photograph taken from the southeast side of the bridge showing primarily the three spans of the steel girder unit. Cross section and elevation views of the steel unit are shown in Figure 4.2 and Figure 4.3, respectively. Because the steel unit is symmetric both longitudinally and transversely, only half of the bridge is shown in these figures.

Figure 4.1 Photograph of the Lakeport Bridge

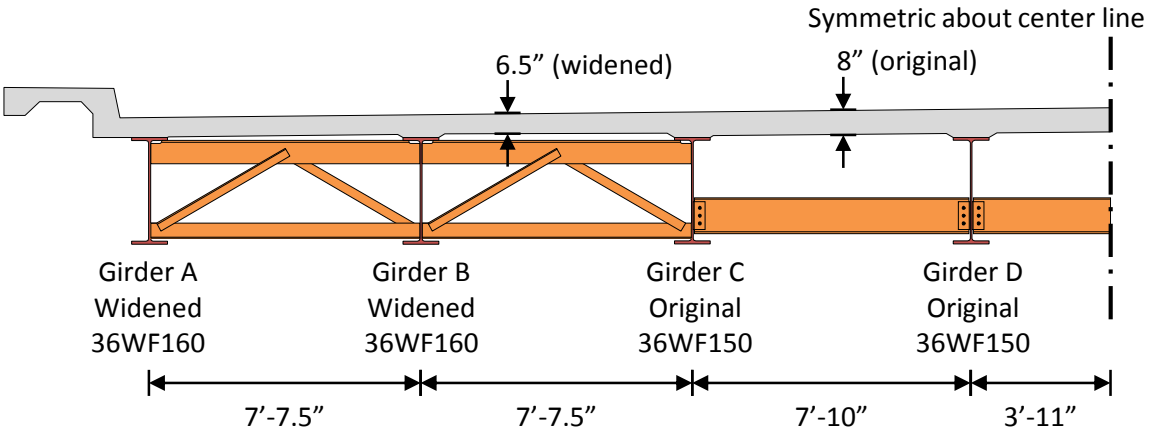

Figure 4.2 Cross Section View of Half of the Bridge

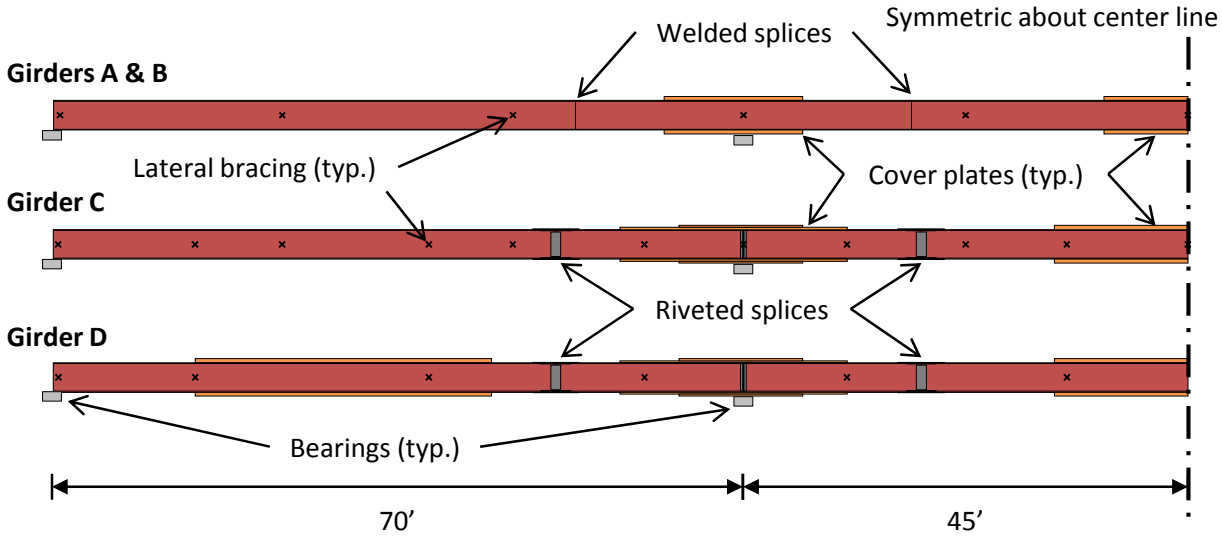

Figure 4.3 Elevation View of Half of the Girders

Although the available design drawings do not specify much information about materials used in construction, conservative estimates of the material properties can be made based on typical practices at the time of construction (AASHTO 2011, THD 1951). The girders in both the original and widened portions of the structure are likely comprised of ASTM A7 steel with a minimum yield stress of 33 ksi. The drawings call for the use of Class A concrete for the deck, which has a specified minimum compressive strength of 3000 psi. The reinforcing bars likely have a minimum yield stress of 33 ksi in the original portion of the deck and 40 ksi in the widened portion of the deck.

After more than 60 years of service life, this bridge remains in relatively good condition, as indicated by the most recent available inspection report. The superstructure is rated as a 6 (satisfactory), with minor surface rusting on the steel beams, cross frames, and bearings. The deck is rated at a 7 (good), with minor cracking of the soffit and wear on the asphalt surface. The substructure is rated at 6 (satisfactory), with some cracking and spalling of the abutments and bents. Moderate to severe impact damage of the railing at several locations along the bridge will

be fixed in an upcoming retrofit which will include widening of the sidewalk, replacement of the exterior railing, and the addition of a new barrier between the traffic lanes and the sidewalk.

During the design phase for this upcoming retrofit, it was discovered that the extra weight from the new concrete barrier separating the traffic lanes and the sidewalk, along with the thick asphalt overlay that has previously been placed over the deck, may require the bridge to be load-posted with restricted axle weights. Strengthening with post-installed shear connectors was proposed to avoid load-posting this bridge.

4.3 Evaluation of Existing Bridge and Strengthening Targets

The continuous steel girder spans of the existing bridge were load rated to evaluate the current load-carrying capacity of the bridge. This rating includes the strength limit states of Overload and Maximum Load, as discussed in Section 2.5.1. Load ratings at the inventory level are reported here, because they directly correspond to the level of live load used in the design of new bridges. The effects of the planned retrofits to the bridge including the expanded sidewalk and new railings are included in this evaluation. Detailed calculations for this load rating, which was carried out in part using the software BAR7, are provided in the Appendix (PennDOT 2010).

The load rating results are summarized in Figure 4.4. These column graphs plot the load rating at points of maximum moment and at section transitions, or ends of the cover plates, for each girder. In Girders A, B, and D, the Overload limit state controls the rating in regions dominated by positive bending while the Maximum Load limit state controls the rating in regions near the interior supports dominated by negative bending. This is because lateral-torsional buckling due to wide spacing of the cross frames around the interior supports reduces the flexural capacity in negative bending. Because the cross frames from the original construction and from the widened portion of the bridge are not aligned along the length of the bridge, Girder C has more closely spaced lateral bracing to prevent lateral-torsional buckling in negative bending. Thus, the Overload limit state controls the rating at all sections in Girder C.

The lowest load rating for each girder is denoted on the figure and occurs in positive bending in the exterior span in all cases. The lowest load rating for all girders is HS 11.5, near the middle of the exterior span in girder C. This is the controlling rating for the entire steel unit of the bridge.

To safely extend the remaining service life of this bridge, a goal of increasing the inventory load factor rating to HS 20 was targeted. This value is denoted by a horizontal dotted line on the graphs for comparison. At a minimum, a remaining life of 25 years is desired for the purposes of fatigue design. These targets were determined based on guidance from TxDOT bridge engineers.

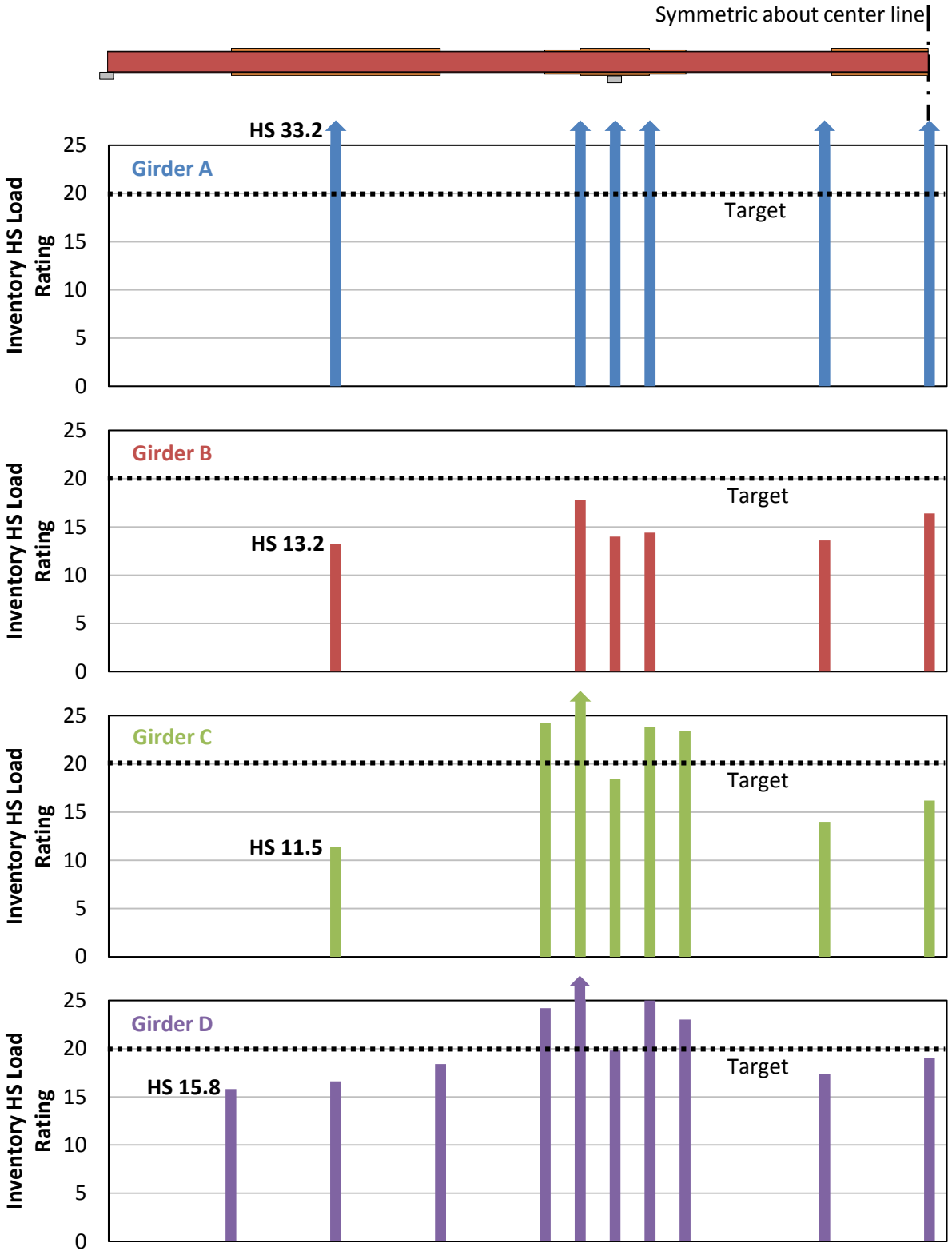

Figure 4.4 Results from Load Rating of Existing Non-Composite Girders at Locations of Maximum Moment and Section Transitions

4.4 Summary

A three-span continuous steel unit of a four-lane bridge in Lakeport, Texas was chosen for strengthening using post-installed shear connectors and inelastic moment redistribution. The existing structure has an inventory load rating of HS 11.5. It is desired to increase this load rating to HS 20, reflecting a nearly 75% increase in the load-carrying capacity. A remaining service life of at least 25 years is targeted.

Chapter 5. Design of Strengthening System

5.1 Overview

This chapter describes the design process and results for strengthening of the Lakeport Bridge. Detailed design calculations that produced these results are provided in the Appendix. After evaluating the existing non-composite bridge, as discussed in Section 4.3, the recommended design process consists of the following primary steps:

1. Check negative moment regions and redistribute moments as necessary at strength limit states,
2. Design post-installed shear connectors for positive moment regions at strength limit states, and
3. Locate the connectors and check fatigue limit states.

5.2 Design Considerations

The design was conducted following the procedures laid out in Section 3.1. It is based on the flexural strength of the steel girders and the fatigue strength of the post-installed shear connectors. Strength and fatigue considerations of additional bridge components, such as the piers supporting the steel girder unit, may be necessary.

Initially, it was assumed that all spans would be strengthened with post-installed shear connectors, so that the same design moments from the evaluation of the existing non-composite girders would be valid. This assumption was verified to be true following the completion of the design. A simple line girder analysis approach was taken for the structural analysis, which had already been completed using the software BAR7 during the load rating of the existing girders (PennDOT 2010). For determining the fatigue demands on the post-installed connectors, the interface slip was directly included in the analysis, as discussed in Section 3.1.7. This analysis was completed using the software UT-Slip, which was developed during the course of TxDOT project 0-6719 (Ghiami Azad 2016). This software will be available for download via the website of the Ferguson Structural Engineering Laboratory at the University of Texas at Austin following the publication of this report (FSEL 2016).

In this design, the deck was assumed to provide continuous bracing for the top flange, so lateral-torsional buckling limit states were not considered under positive flexure. Under negative flexure, the unbraced lengths for lateral-torsional buckling were taken as the distance between the cross frames. However, Girders C and D, which were erected during the original construction of this bridge, have cross frames that alternate between channel sections near the bottom flange of the girders (shown in Figure 4.2) and I-beams near the top flange of the girders (not shown in Figure 4.2). For the purposes of this design, only the channel sections located near the bottom flange of the girders were considered to act as lateral bracing in negative flexure. The K-type cross frames, which were constructed when Girders A and B were added to widen the bridge and are also depicted in Figure 4.2, effectively brace the bottom flange at all locations.

A minimum composite ratio of 0.3 was employed in the design. Additionally, the layout of the connectors abided by the recommendations provided in Section 3.1.6. When locating the connectors, care was also taken to avoid the cover plates on all girders and the riveted splice plates on Girders C and D. Although it may be possible to install the connectors in locations of welded cover plates in Girders A and B, these were avoided, as this condition has not been tested

experimentally. The closely spaced rivets in the splice and cover plates of Girders C and D prohibit placement of the connectors in these regions, partially due to the difficulty of using a portable magnetic drill on a riveted surface.

A longitudinal spacing of 12 inches was chosen for the connectors to prevent conflicts with the transverse reinforcing bars in the deck. The use of a rebar finder is highly recommended prior to installing these connectors, and slight modifications in the layout can be made to avoid the deck reinforcement. As shown in Figure 5.1, a transverse spacing of 6 inches was chosen for the two connectors in a cross section. However, the exact layout of the longitudinal deck reinforcement is unclear from the available design drawings for this bridge, although it seems that there are longitudinal bars located directly above the flange of each girder. Since these bars may be difficult to find using a rebar locator, it is recommended that either radar testing be done to locate these bars, or trial holes should be drilled to ensure that the rebar will be avoided prior to installing the connectors.

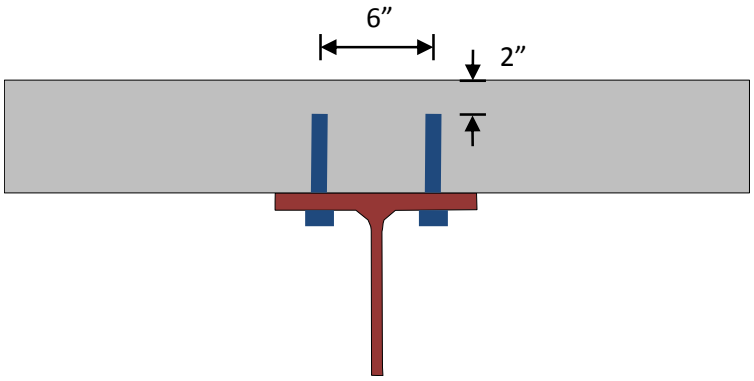

Figure 5.1 Cross-Sectional Layout of Connectors

5.3 Design Results

The results of the design are summarized in Figure 5.2. Because the exterior girders (A) are not subjected to significant traffic loading, the target HS 20 load rating was achieved by the non-composite girder, as indicated in Figure 4.4, and no strengthening was necessary. The non-composite section of the remaining three girders in the half cross-section required strengthening to some extent.

A total of 372 post-installed adhesive anchor shear connectors are required to satisfy both strength and fatigue requirements for the entire steel unit of this bridge. Only small amounts of moment redistribution, not exceeding 5% of the factored design moment, are required from the interior pier sections for this bridge. The controlling inventory load factor rating for the steel girders in the strengthened bridge is HS 20.0, occurring at the interior pier sections of Girder B. This is an increase of nearly 75% over the HS 11.5 rating of the existing non-composite steel girder unit.

A summary of the load rating results of the strengthened bridge are presented in Figure 5.3. The ratings in this figure can be directly compared to the load ratings of the non-composite girders shown in Figure 4.4. The controlling load rating for each girder is located near the middle of the exterior span, with the exception of Girder B in which the controlling load rating occurs at the interior support. As with most of the non-composite girders prior to strengthening, the Overload limit state controls for all ratings dominated by positive flexural demands, while the Maximum

Load limit state controls for all locations near the interior piers dominated by negative flexural demands.

The post-installed shear connectors satisfy the remaining fatigue life requirement of at least 25 years. Unlike conventional shear stud design, the fatigue demands did not control the design of these post-installed shear connectors. The maximum stress range expected to be experienced by any connector along the bridge corresponds to an actual predicted remaining fatigue life of 32 years. Note that the connectors are concentrated in groups near the ends of the positive moment regions in each span. This has been shown to improve the ductility of partially composite girders and to reduce the maximum demand on connectors under elastic levels of load (Kwon et al. 2007, Kreitman et al. 2015). The layouts avoid placing connectors at the locations of any splice plates or cover plates.

For strength purposes, the number of shear connectors required in each span was controlled by the minimum recommended composite ratio of 0.3. Most load ratings in positive bending exceed the HS 20 requirement because of this minimum composite ratio. The exception to this is the exterior spans of Girder C, which require a composite ratio of 0.66 to reach a load rating of just greater than HS 20.

Because small amounts of moment redistribution are required at the interior pier sections of Girders B, C, and D, particular requirements outlined in Appendix B6 of the *LRFD Bridge Design Specifications* must be fulfilled to allow the steel section to undergo plastic rotation required for moment redistribution, without premature local or lateral-torsional buckling (AASHTO 2010). Additional cross frames need to be added around the interior piers to reduce the unbraced lengths in these regions for adequate ductility during moment redistribution. A suggested layout for these cross frames is shown in Figure 5.4, and additional details are provided in the Appendix. A double-sided bearing stiffener must also be installed at the interior pier of Girder B. Bearing stiffeners are already present at the interior pier sections of Girders C and D.

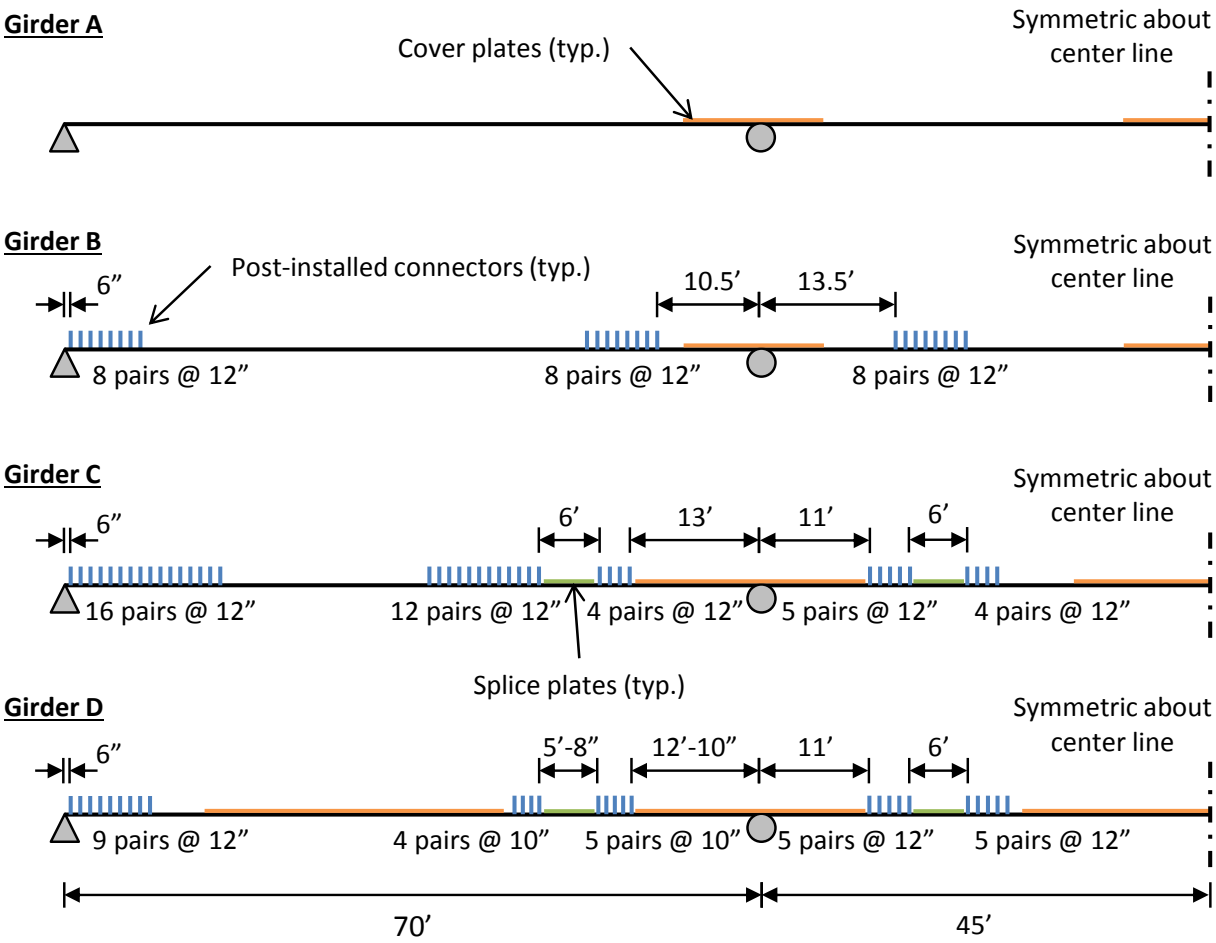

Figure 5.2 Summary of Design Results

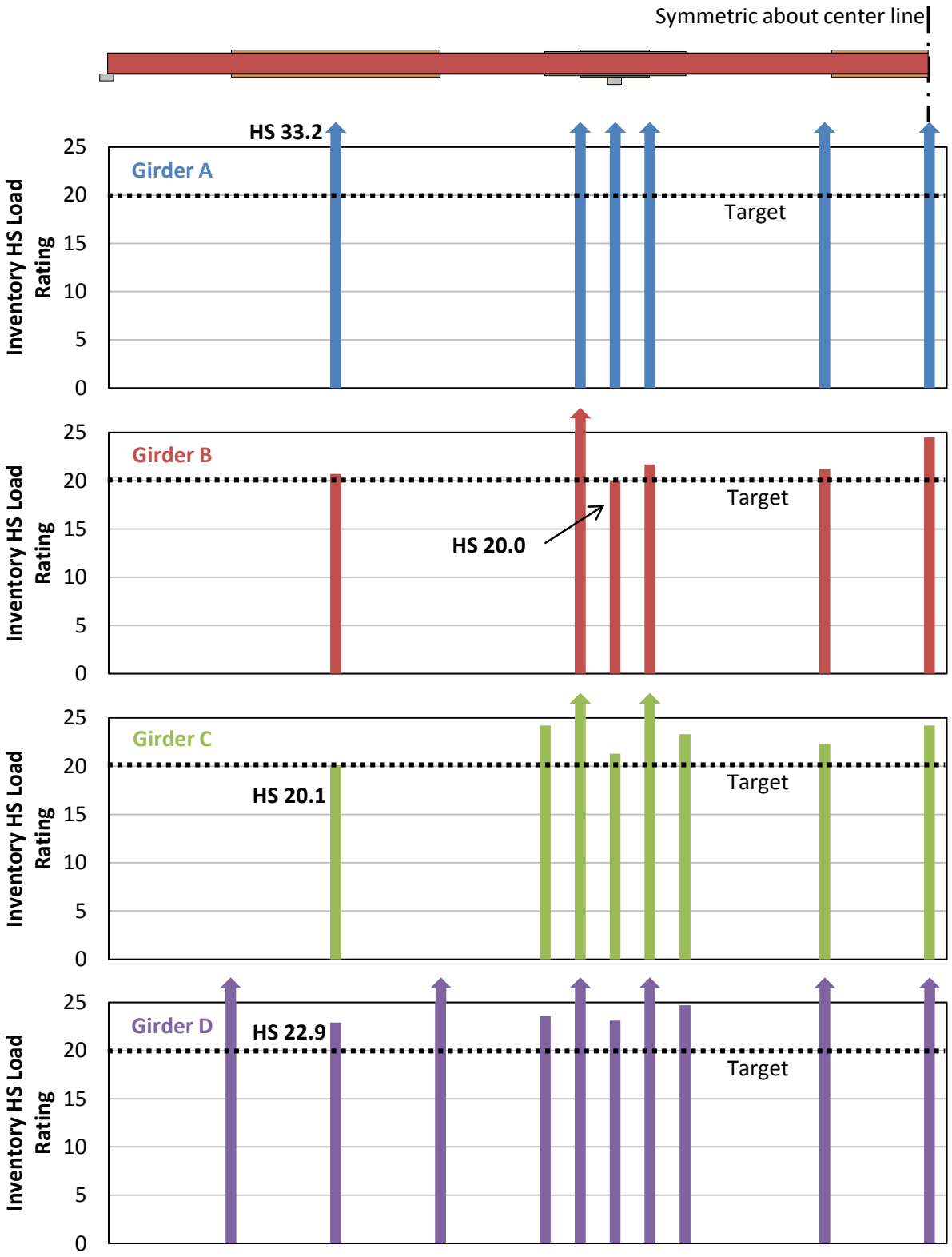

Figure 5.3 Results from Load Rating of Strengthened Girders at Locations of Maximum Moment and Section Transitions

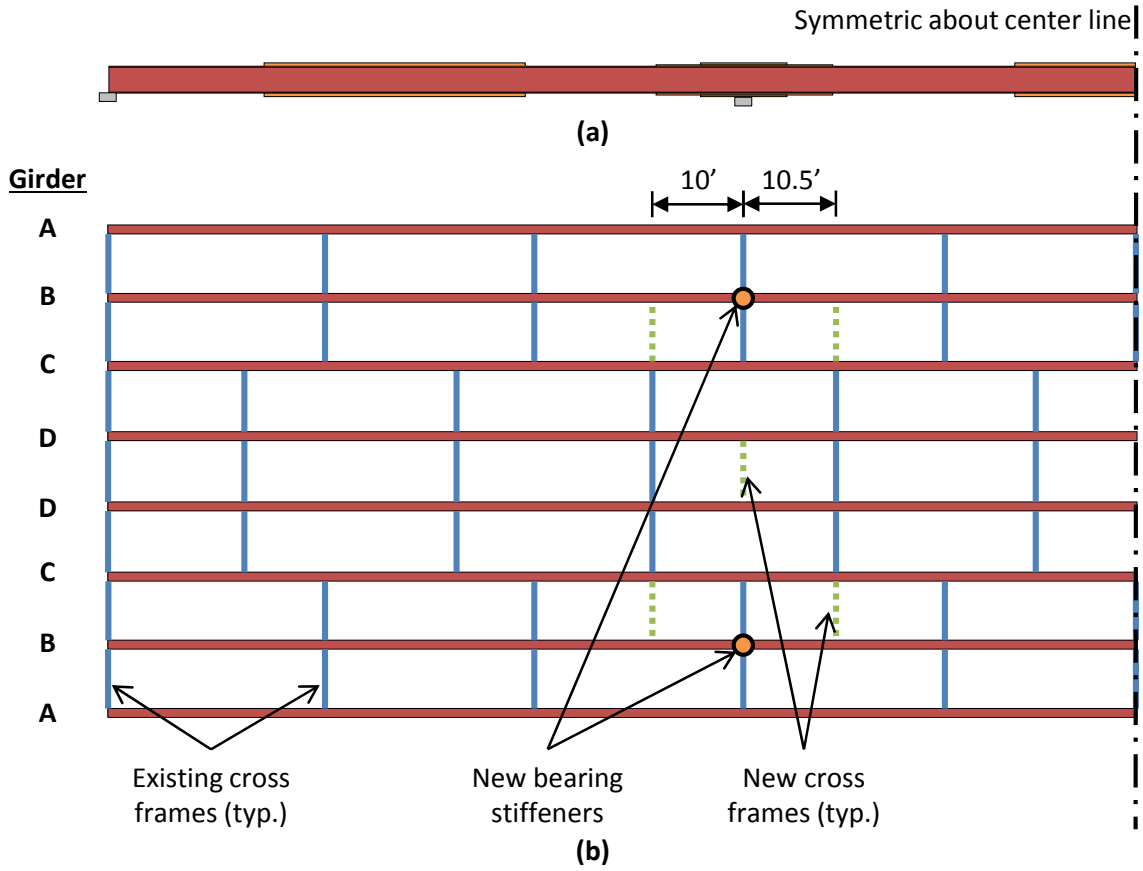

Figure 5.4 Suggested Locations of New Cross Frames and Bearing Stiffeners Required for Moment Redistribution – (a) Elevation View and (b) Plan View of Girders

5.4 Summary

A strengthening design was conducted for the three-span continuous steel unit of the Lakeport Bridge. A total of 372 post-installed shear connectors and minimum amounts of moment redistribution are required to increase the inventory load factor rating from HS 11.5 to the target strength of HS 20.0. A remaining life of 32 years was estimated for the post-installed connectors in fatigue, which exceeds the target of 25 years.

To allow for moment redistribution, additional cross frames must be added to reduce the unbraced lengths in the vicinity of the interior pier sections for two of the girders. This results in a minimum of 10 cross frames that must be added along the entire length of the bridge. Double-sided bearing stiffeners must also be added to the interior pier sections of Girder B to prevent local distortions of the steel section. This is required in four locations along the entire length of the bridge.

Chapter 6. Live Load Testing of the Non-Composite Lakeport Bridge

6.1 Overview

The ultimate goals of the live load test were to provide data on the response and behavior of the non-composite Lakeport Bridge and to compare the behavior of the existing bridge with that predicted by a finite element model of the bridge. This data can also be compared with data obtained from future live load testing of the strengthened bridge to assess the effectiveness of the retrofit.

This chapter documents the load test that was conducted on the bridge prior to any strengthening. First, details on the location and installation of the instrumentation are given. Next, the loading configurations that were used are discussed, followed by a description of the computational model developed to predict the behavior of the bridge. The results of the data collected during the test are then presented and compared to the predictions.

6.2 Instrumentation of the Lakeport Bridge

The instrumentation plan for the bridge was affected by the water level of the Sabine River, which flows underneath the bridge. This is because access to the bridge girders for installing instrumentation was gained using three scaffolding towers that were erected under the bridge just prior to the load test, as shown in Figure 6.1. Figure 6.2 shows how the water level changed drastically throughout the year. According to USGS water resources data, the water level was roughly 35 feet, 15 feet, and 3 feet deep in January (a), June (b), and August (c) of 2016, respectively (USGS 2016). The low level of water when the load test was conducted in August allowed for full access to the south span of the bridge. However, even at this very low level, water covered nearly the entire area under the middle span and extended slightly into the north span. Thus, it was only possible to install instrumentation in the south span of the bridge for the load test.

Figure 6.1 Scaffolding Towers Erected for Instrumentation – (a) South Span and (b) Middle Span

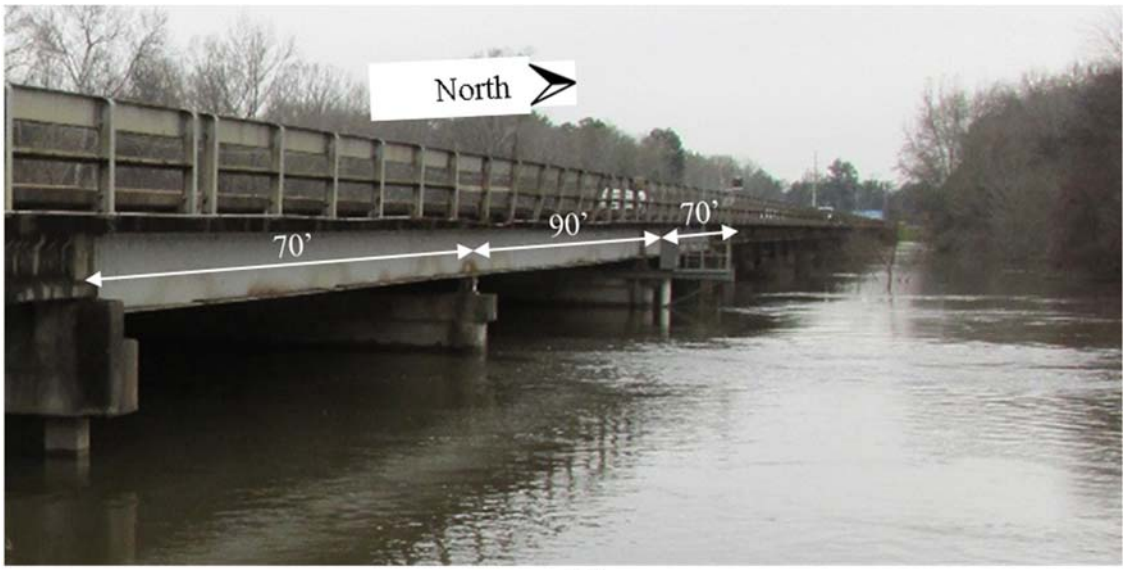

(a)

(b)

(c)

Figure 6.2 Photographs of the Bridge Prior To Instrumentation – (a) Jan 6, 2016 (b) Jun 6, 2016 (c) Aug 5, 2016

The three scaffolding towers were located roughly 4.5 feet, 28 feet, and 55.5 feet away from the exterior pier of the south span and allowed access to Girders B and C, as indicated in Figure 6.3. Exterior Girder A was not instrumented because it carries very little of the traffic load and does not require any strengthening. The behavior of interior Girder D was expected to be similar to that of Girder C, as both of these girders were part of the original construction of the bridge.

Figure 6.3 Installing Instrumentation on Girders B and C

Strain gages were installed on the top and bottom flanges of both Girder B and Girder C at 28 feet from the centerline of the southern-most pier, as shown in the photographs of Figure 6.4. Prior to installing the strain gages, a paste-type paint remover was applied to a small portion of the surface of the flanges at the desired locations. Approximately 18 hours later, the paint was easily scraped off at these locations. Next, a die grinder was used to smooth the surface of the flanges (a,b), and these areas were cleaned with acetone. The strain gages were glued to the flanges using a cyanoacrylate adhesive, and a light coating of wax was applied to protect the gages from moisture. Figure 6.4 (c) and (d) show a typical bottom and top flange strain gage, respectively, after the installation was completed.

Figure 6.4 Installing Strain Gages on the Bridge – (a) Grinding the Bottom Flange, (b) Grinding the Top Flange, (c) Strain Gage on the Mid-Height of the Bottom Flange, and (d) Strain Gage on the Mid-Height of the Top Flange

Figure 6.5 shows photographs of the instruments used to measure displacements on the two girders during the test. To measure the deflection of the bridge girders, string potentiometers (a) were fixed to the scaffolding tower at a distance of 28 feet from the centerline of the southern-most pier. A magnet was used to attach the string, which was extended in length using piano wire, to the underside of the bottom flange of the girders. Linear potentiometers with a 2-inch stroke were used to measure the slip, or relative longitudinal motion of the top flange of the steel beam and the underside of the concrete deck (b,c). These slip measurements were made at 4.5 feet and at 55 feet from the centerline of the southern-most pier, which are near the middle of the regions in which the post-installed shear connectors will be placed in the future. As shown in the figure, each linear potentiometer was mounted on a piece of wood, which was glued to the concrete deck. The plunger of the potentiometer came into contact with a short piece of aluminum tubing which was glued to the underside of the top flange of the steel beam.

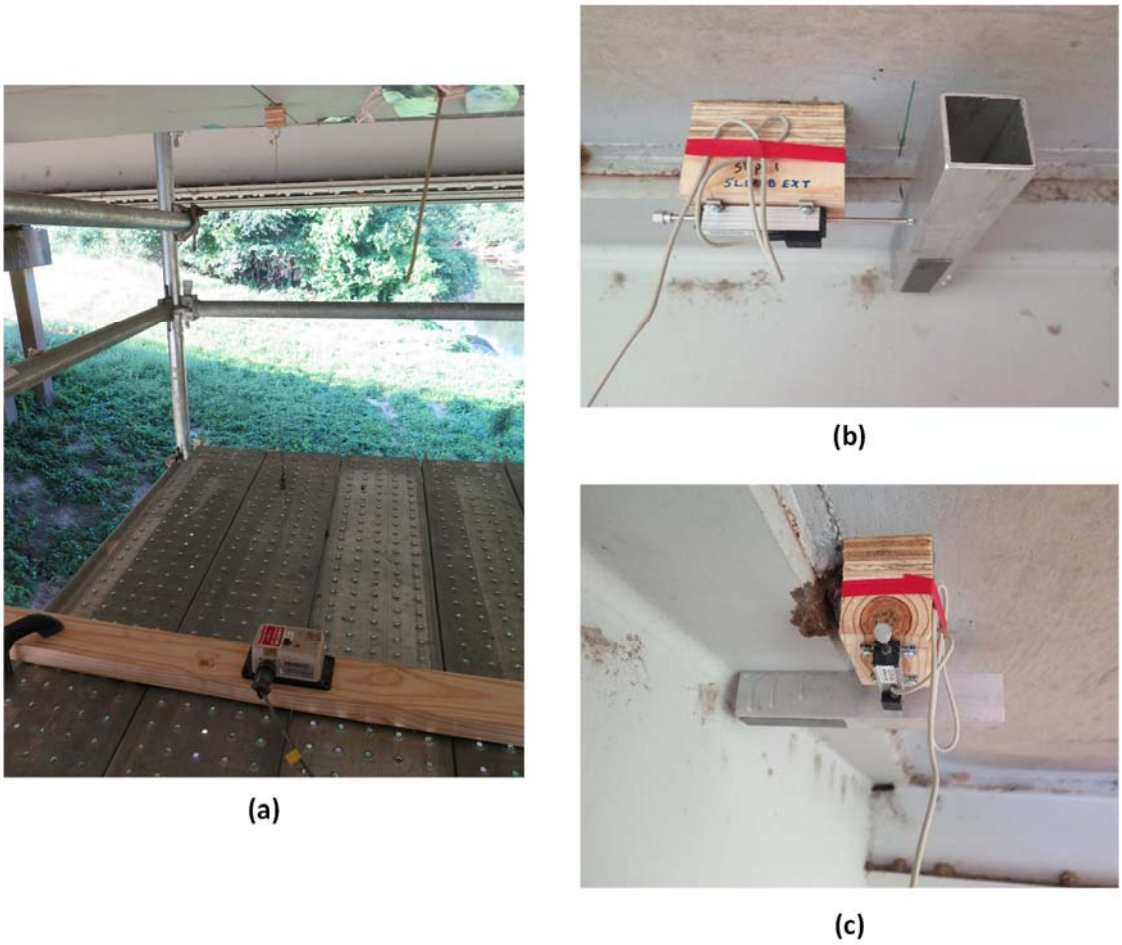

Figure 6.5 Bridge Instrumentation – (a) String Potentiometers Used to Measure Deflection (b) Longitudinal View of a Typical Slip Transducer (c) Transverse View of a Typical Slip Transducer

As shown in Figure 6.6, a Campbell Scientific CR5000 datalogger, powered by a 12-volt automotive battery, was used to collect data from these instruments during the load test. The datalogger communicated wirelessly to a laptop computer used to monitor the data during the test via a pair of Campbell Scientific RF401 radios. Data from each instrument was recorded at a frequency of 1 Hz during testing.

(a) (b)

Figure 6.6 Data Acquisition System – (a) Datalogger and (b) Laptop Computer

6.3 Load Test Program

Two dump trucks loaded with sand, one of which is pictured in Figure 6.7 were provided by the Texas Department of Transportation to apply load to the bridge during testing. These two trucks are referred to as Truck #1 and Truck #2 in this report. Figure 6.8 provides the relevant dimensions, which were identical for both trucks, and the axle weights, which varied slightly between the two trucks. Each truck has ten tires, eight of which are in the rear and two of which are in the front. The center-to-center distance between the front tires is approximately 82 inches.

Figure 6.7 Photograph of Typical Truck used in Load Test

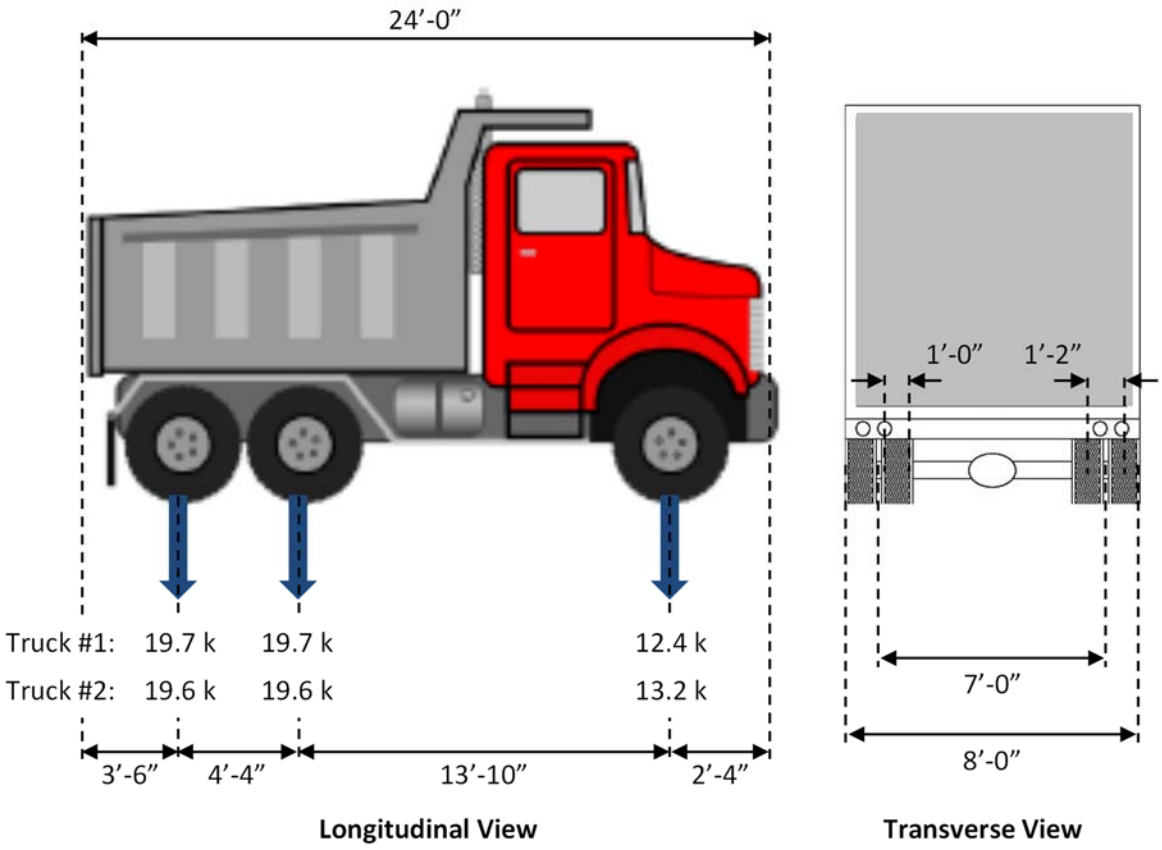

Figure 6.8 Dimensions and Axle Weights of Trucks Used in Load Test

The load test program consisted of six loading configurations, which are referred to in this report by a number representing the length of the loaded span in feet and a letter representing the primary girder(s) that were expected to resist the load. For example, "Test 70-B" consisted of a loading configuration in which the two trucks were placed back-to-back in the 70-foot long south span, approximately centered over Girder B, as shown in Figure 6.9. Similarly "Test 90-BC" consisted of a loading configuration in which both trucks were placed side-by-side in the 90-foot long middle span so that one truck was approximately centered over Girder B while the other truck was approximately centered over Girder C, as shown in Figure 6.14. The remaining four loading configurations are shown in Figure 6.10 through Figure 6.13, while Figure 6.15 provides photographs of the back-to-back (a) and side-by-side (b) configurations. The load test was run in the following order:

1. Test 70-B
2. Test 70-C
3. Test 70-BC
4. Test 90-B
5. Test 90-C
6. Test 90-BC

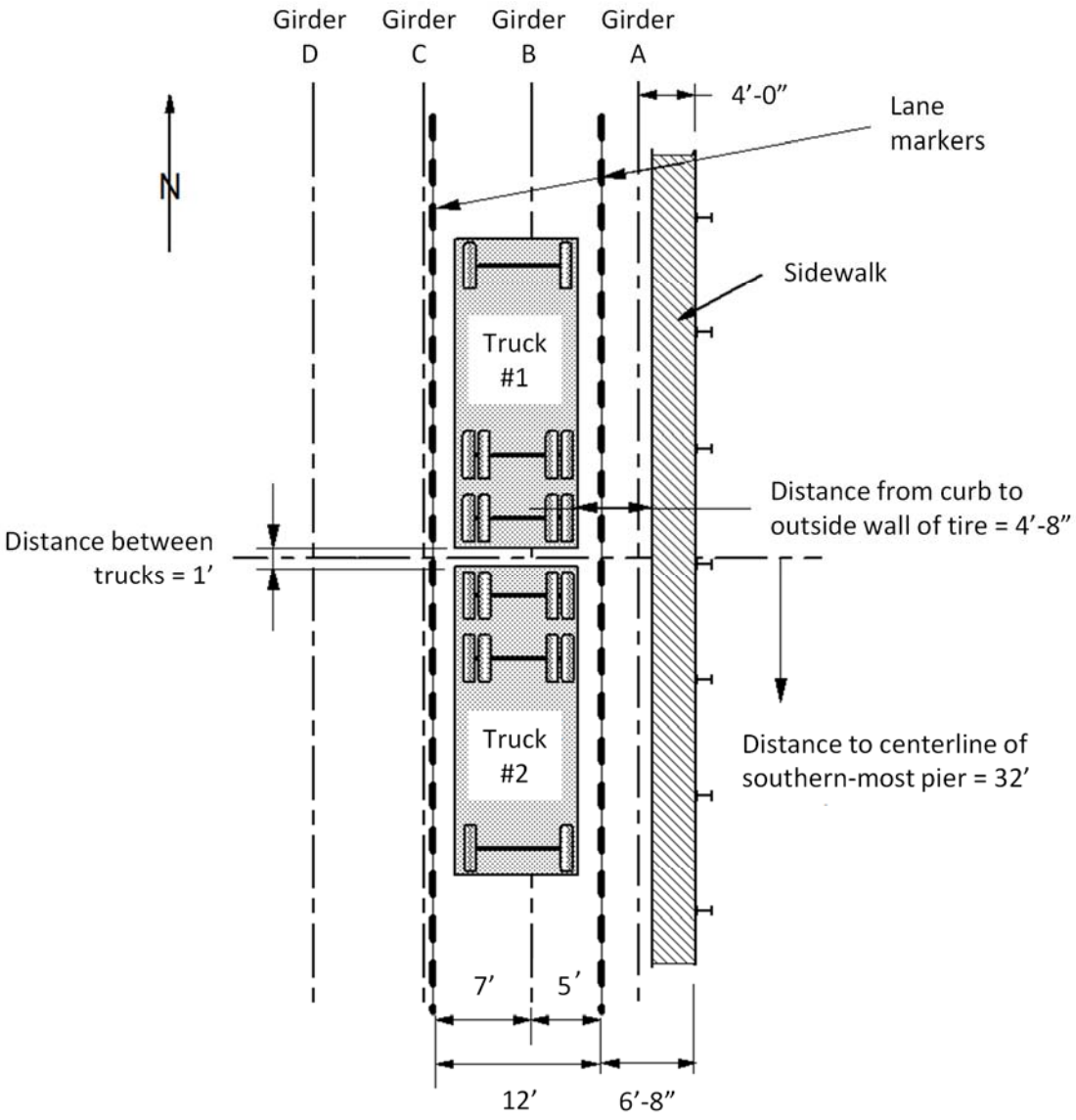

Figure 6.9 Test 70-B Setup

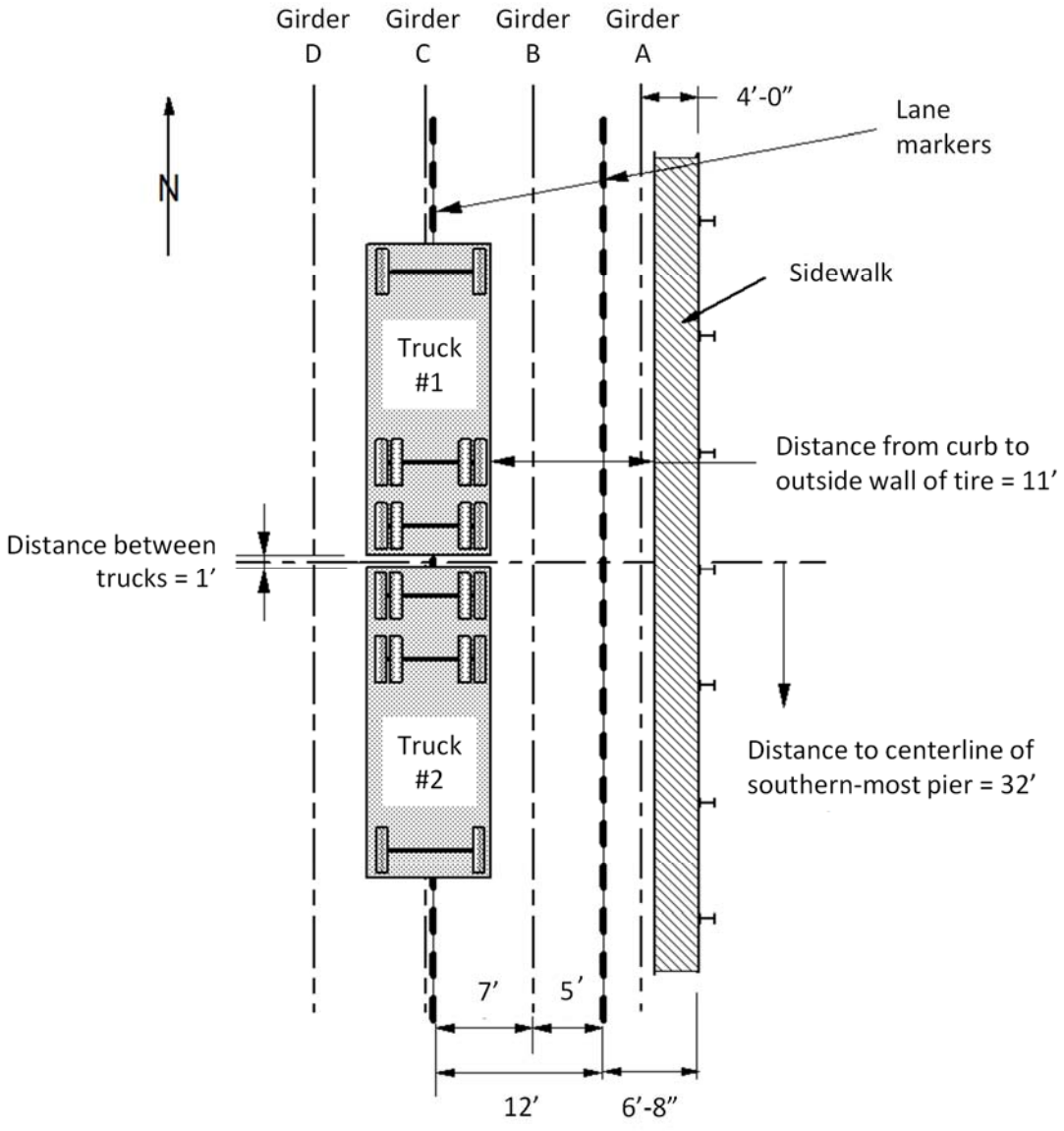

Figure 6.10 Test 70-C Setup

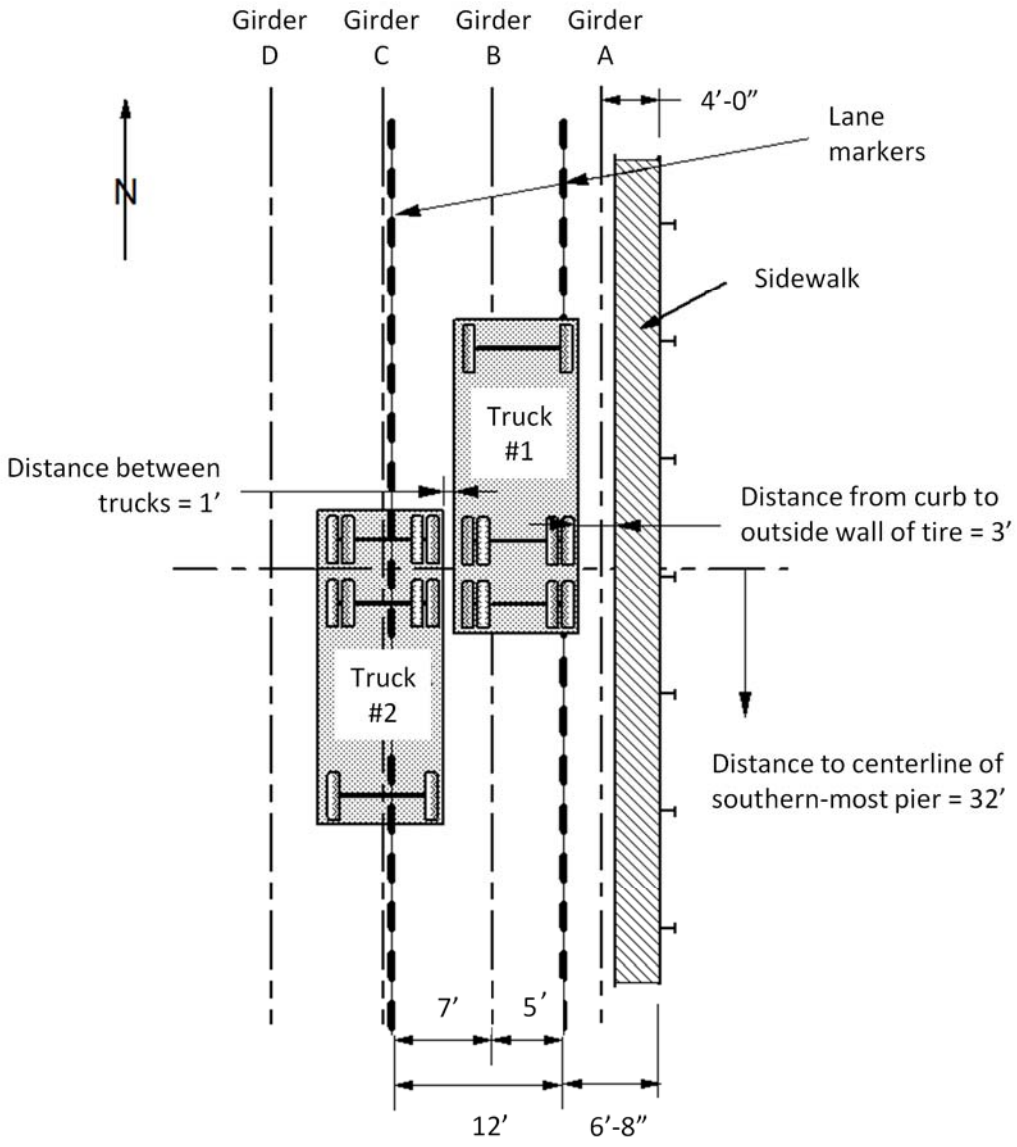

Figure 6.11 Test 70-BC Setup

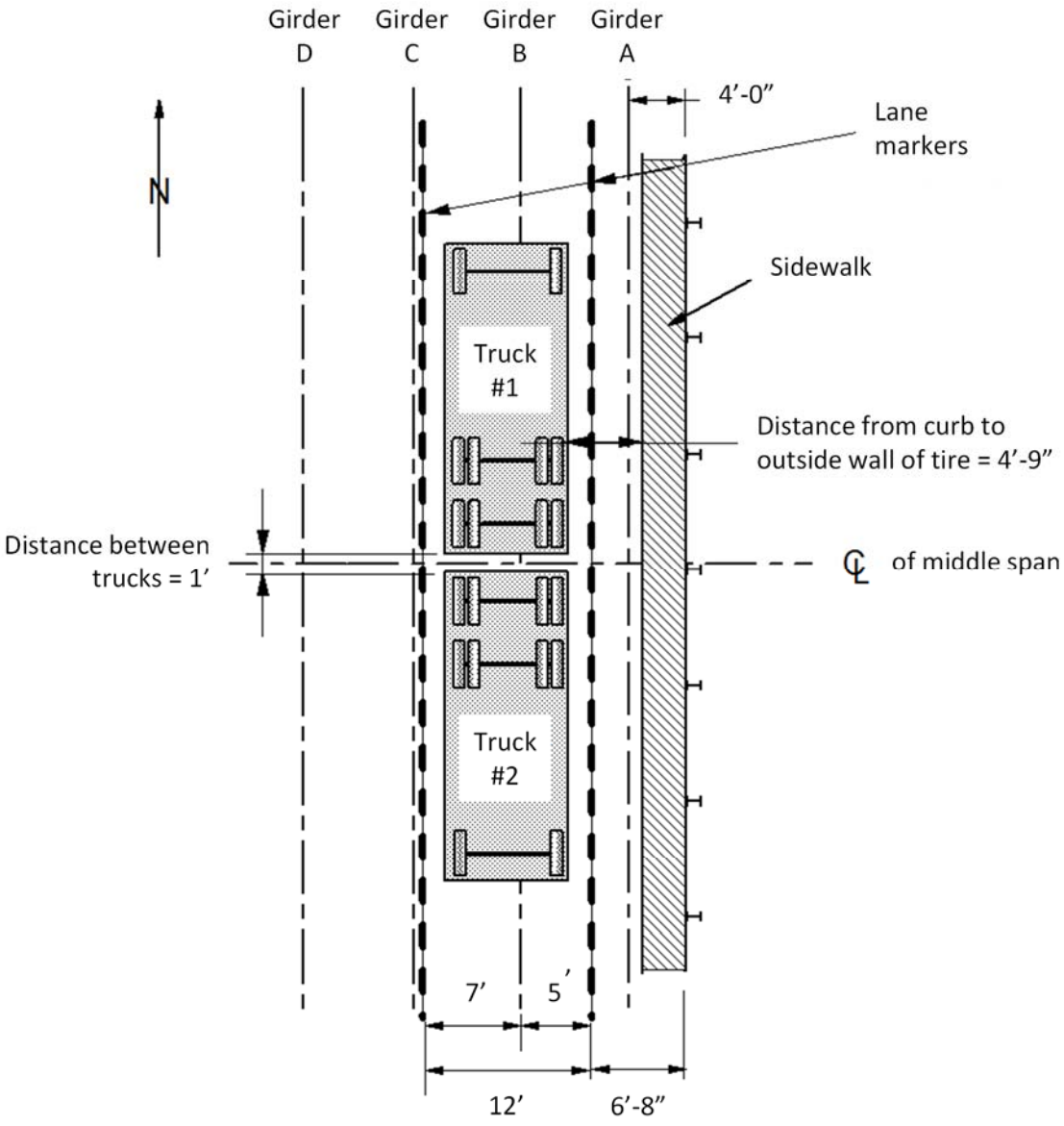

Figure 6.12 Test 90-B Setup

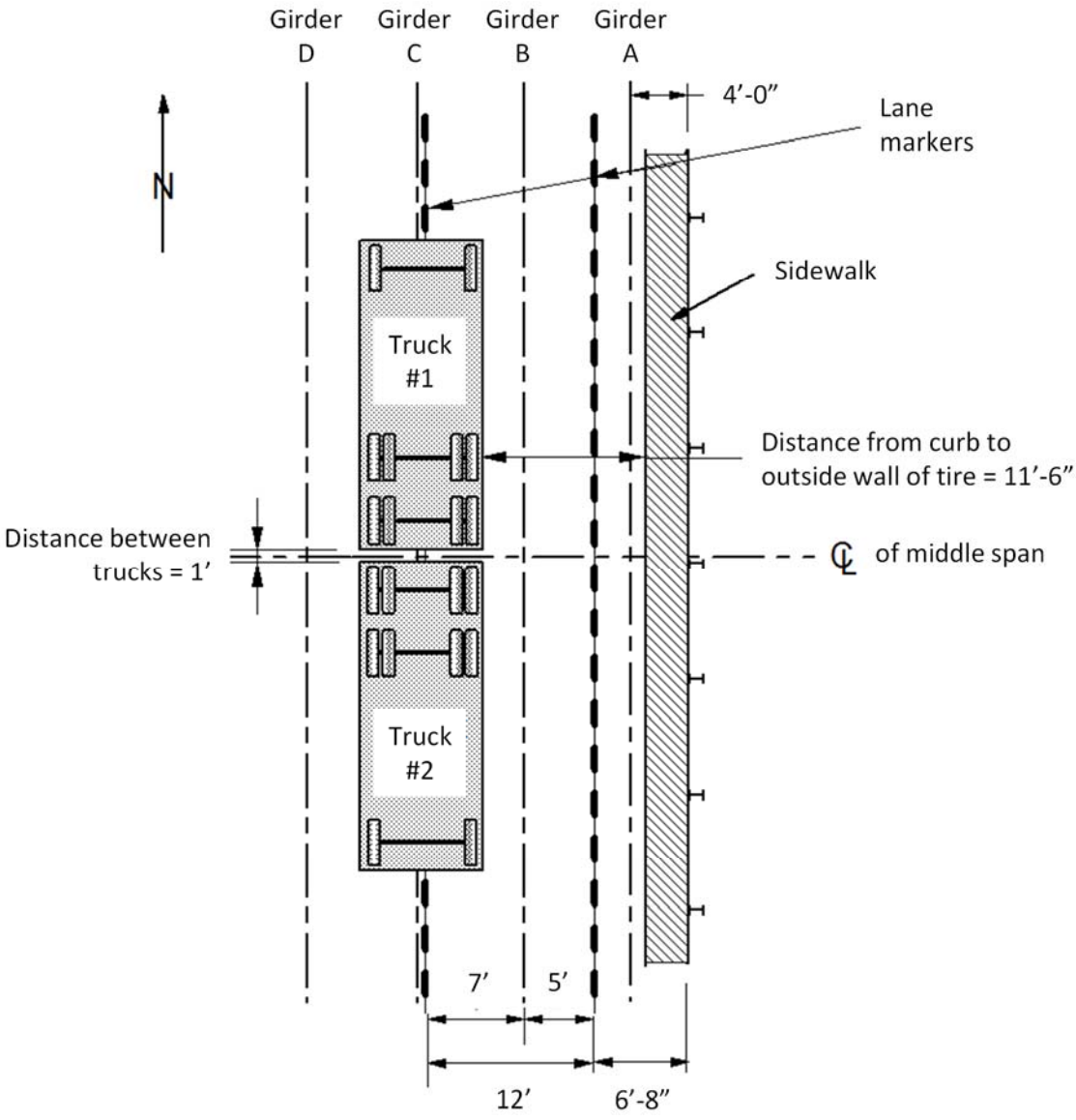

Figure 6.13 Test 90-C Setup

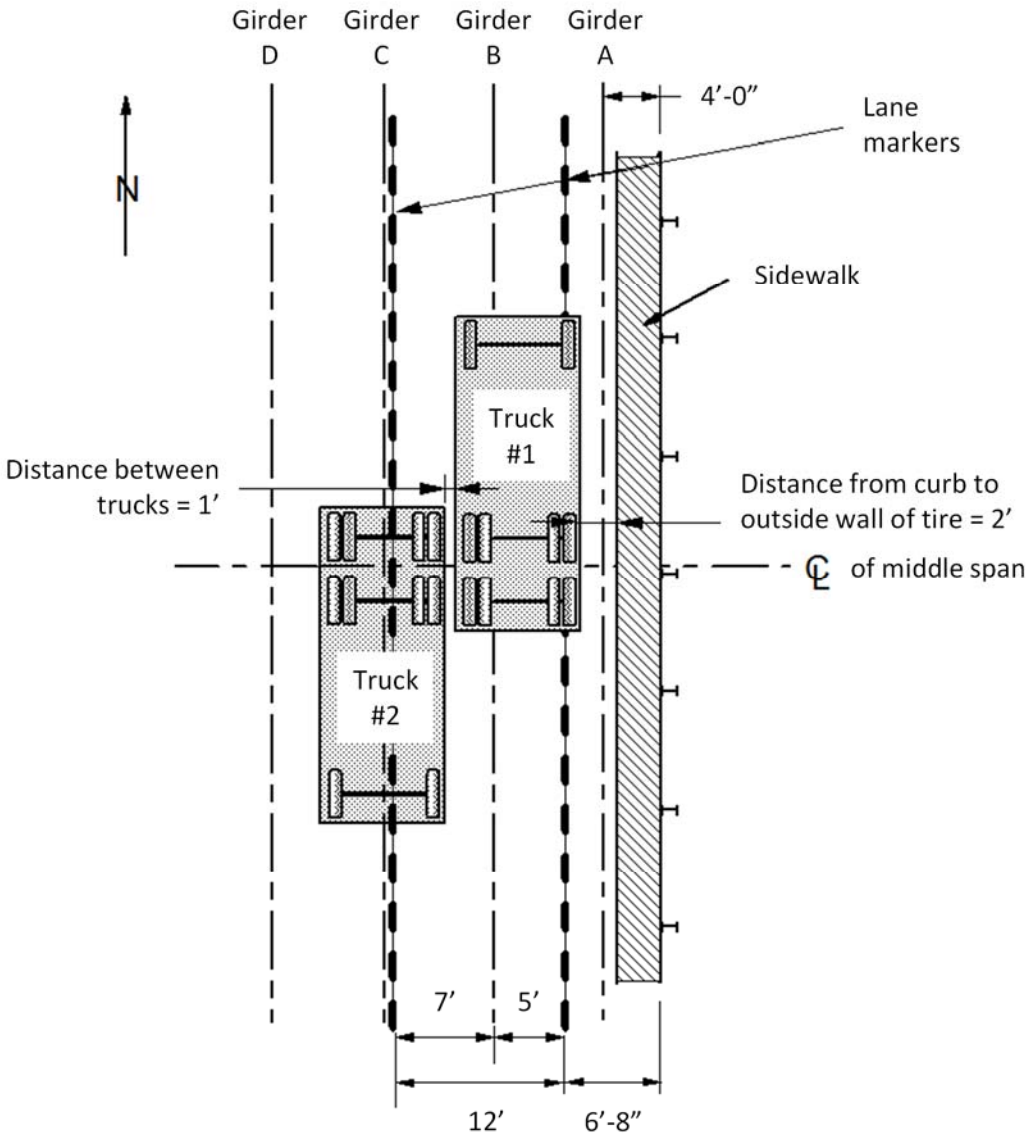

Figure 6.14 Test 90-BC Setup

(a) (b)

Figure 6.15 Photographs of (a) Back-to-Back Loading Configurations and (b) Side-by-Side Loading Configurations

Traffic on the bridge was stopped during the load test so that the two trucks were the only vehicles on the bridge. Prior to testing, a zero reading was taken with no vehicles on the bridge. During each loading configuration, the trucks were kept in place and data was recorded for one minute.

6.4 Finite Element Modeling

Computational analyses were conducted using the software SAP2000 to predict the behavior of the bridge during the load test (CSI 2011). The entire bridge was modeled as accurately as possible based on the available design drawings. Thin shell elements were used to model the web and flanges of the steel girders, as well as the cover plates. ASTM A36 steel was specified as the material for these elements. Similarly, the concrete deck was modeled with shell elements with a specified compressive strength of 3000 psi. All shell elements were positioned at the geometric centroid of the respective shape. The steel beam and concrete deck elements were meshed at 6-inch increments along the direction of traffic with a nearly one-to-one aspect ratio.

Frame elements were used to represent the cross frames in the model. These cross frames are spaced at approximately 23-foot intervals in the widened portion of the bridge (Girders A and B) and at 10- to 14-foot intervals in the original portion of the bridge (Girders C and D), as indicated in Figure 6.16. In the original portion of the bridge, these cross frames alternated in their location at the top and bottom of the web as illustrated in the cross-sectional views of Figure 4.2 and Figure 6.17.

The deck and the top flanges of the steel beams were connected by two-joint links at 6-inch increments along the length of the bridge to prevent vertical separation between the two materials. These links were fixed in the vertical direction and had zero stiffness in all other translational and rotational directions. In the model, it was assumed that no frictional force acts at the steel-concrete interface so that the behavior is purely non-composite.

Figure 6.17 and Figure 6.18 show a typical cross section and elevation of the 3D model of the bridge. The entire 3D model of the bridge is shown in Figure 6.19.

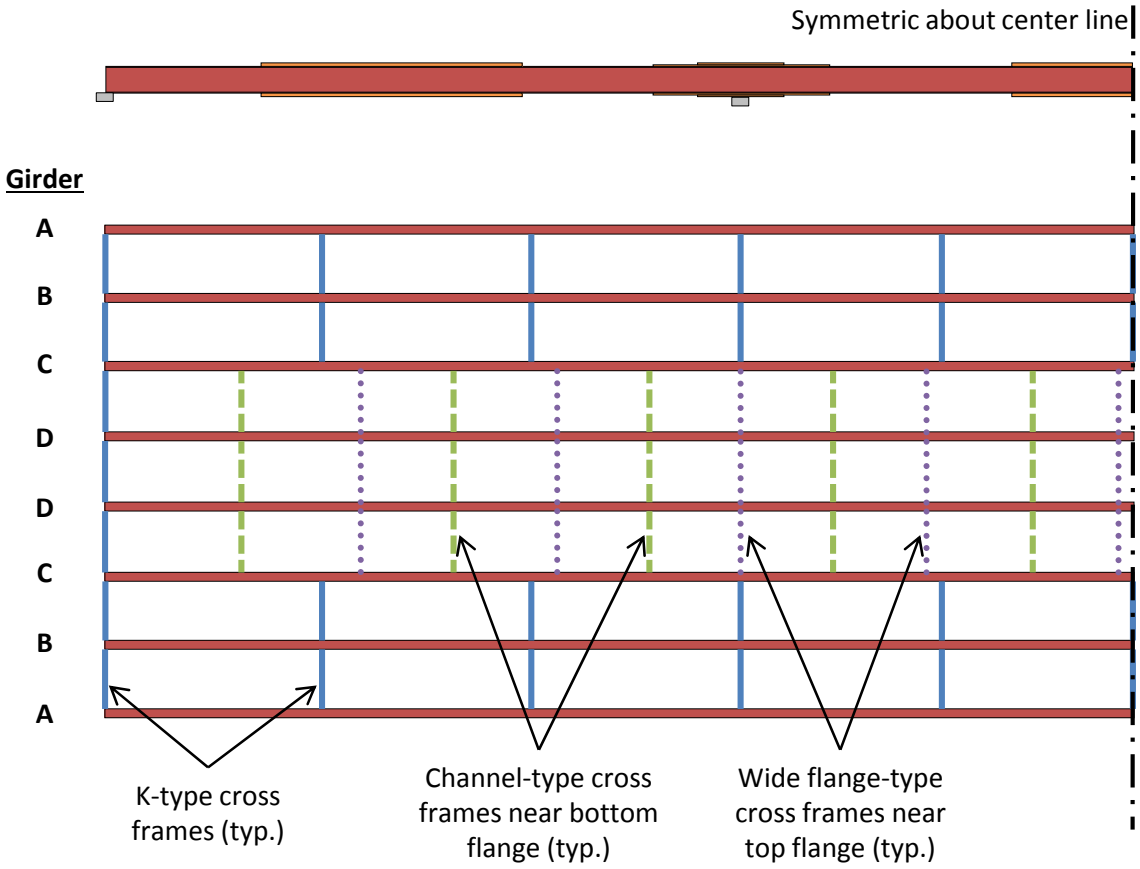

Figure 6.16 Plan View of Half of the Bridge Showing Locations of Different Types of Cross Frames

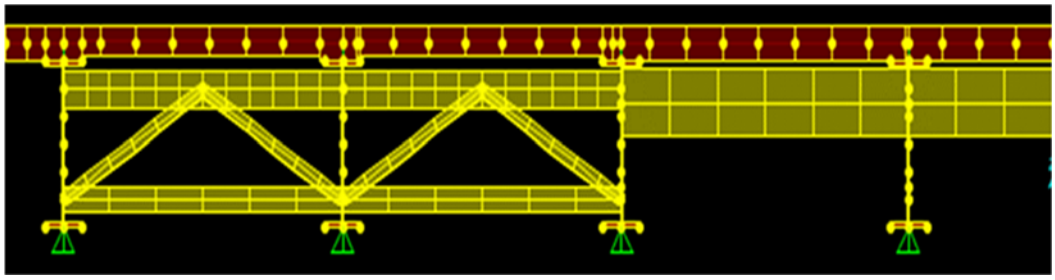

Figure 6.17 Typical Cross Section View of Half of the Bridge in SAP2000

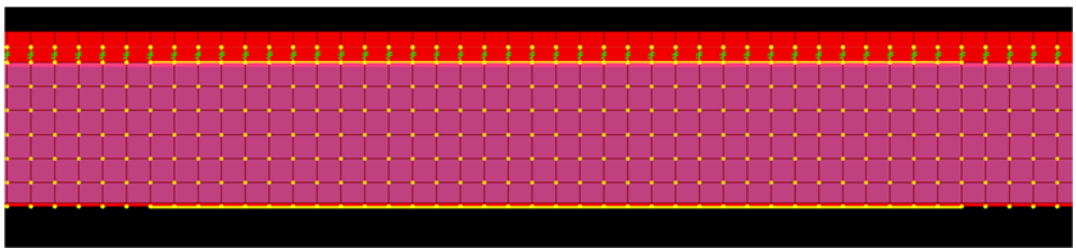

Figure 6.18 Typical Elevation View of the Bridge

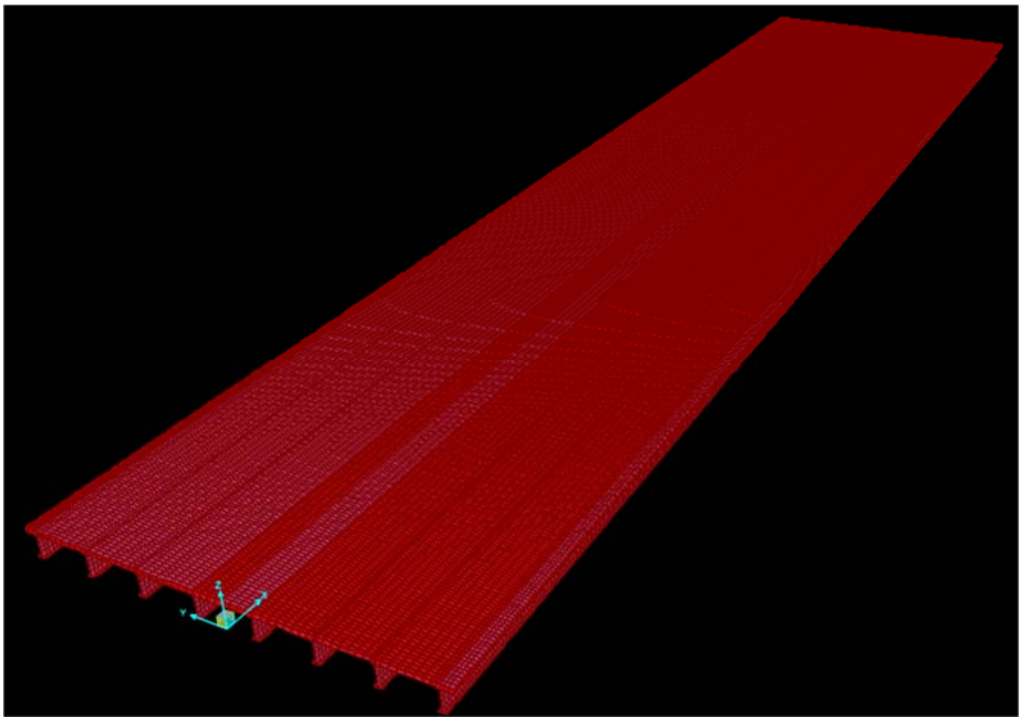

Figure 6.19 3D Model of the Bridge

6.5 Load Test Results

This section discusses the results from the six loading configurations that were used during the test, including the measured deflections and slips, along with the flange stresses, which were computed from the measured strains. These results are compared to the predictions from the finite element model of the bridge. This comparison provided insight into the behavior of the non-composite bridge prior to strengthening.

6.5.1 Deflection Results

Figure 6.20 and Figure 6.21 contain graphs of the measured and predicted deflection of Girders B and C under loading configurations in the south and middle spans, respectively. In all cases, the measured deflection matches the predicted deflection fairly well for Girder B. However, consistently smaller deflections were measured during the load test than were predicted for Girder C. This may indicate the presence of significant interface frictional or other forces acting to create some composite action in Girder C.

One possible explanation for the difference in behavior relative to the predictions of the two girders is that they were constructed at different times, with Girder C being part of the original construction and Girder B being part of the widening of the bridge roughly two decades later. It is possible that differences in construction practices and materials may have resulted in different properties at the steel-concrete interface. In particular, the use of riveted connections for the splice plates and cover plates that project upwards into the concrete deck in Girder C may induce a significant amount of unintended composite action. The welded splices in Girder B do not project into the deck, while the welded cover plates project only a small distance into the deck in this girder. Frictional forces at the interface may also have contributed to the development of some composite action.

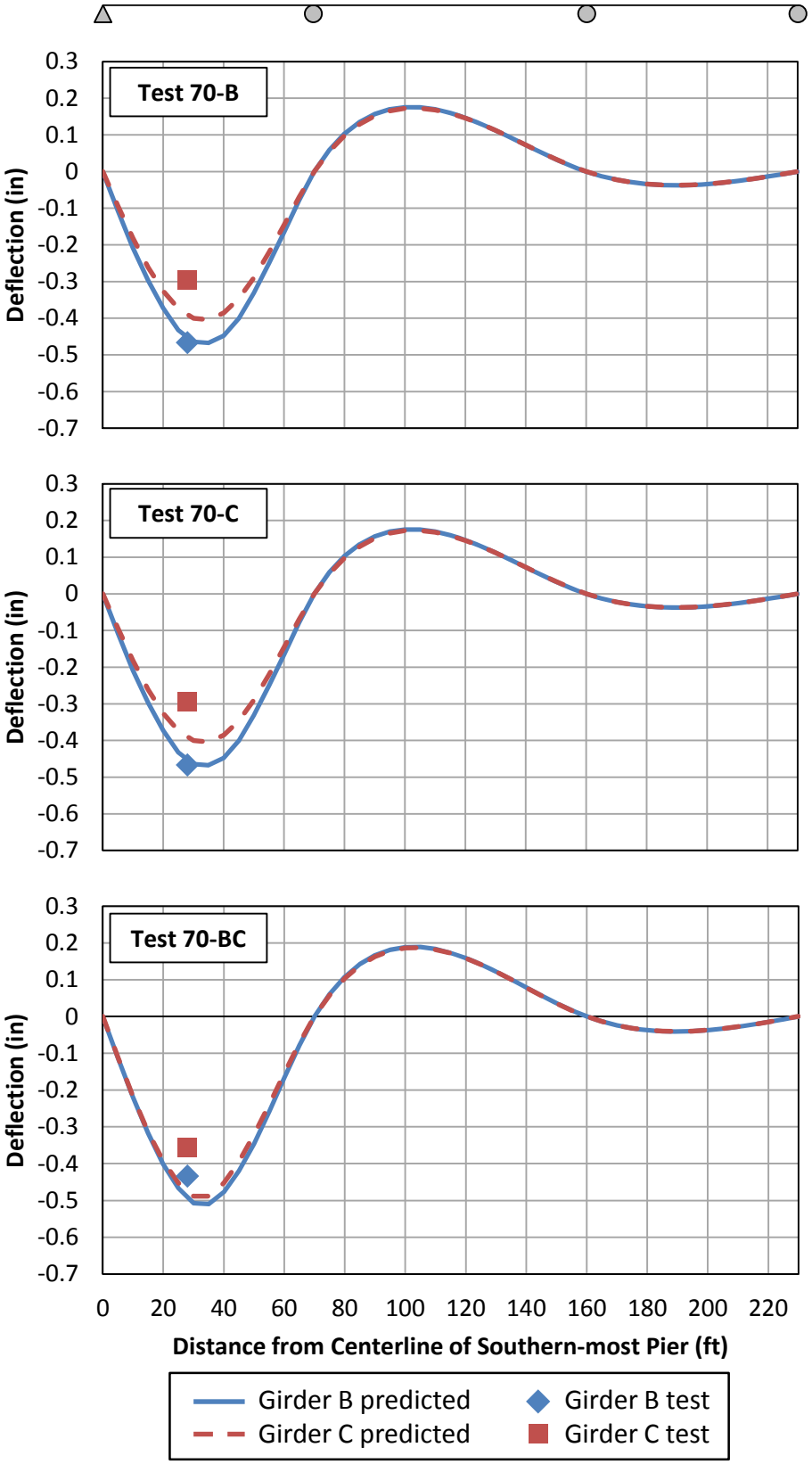

Figure 6.20 Deflection Results for Loading Configurations in the South Span

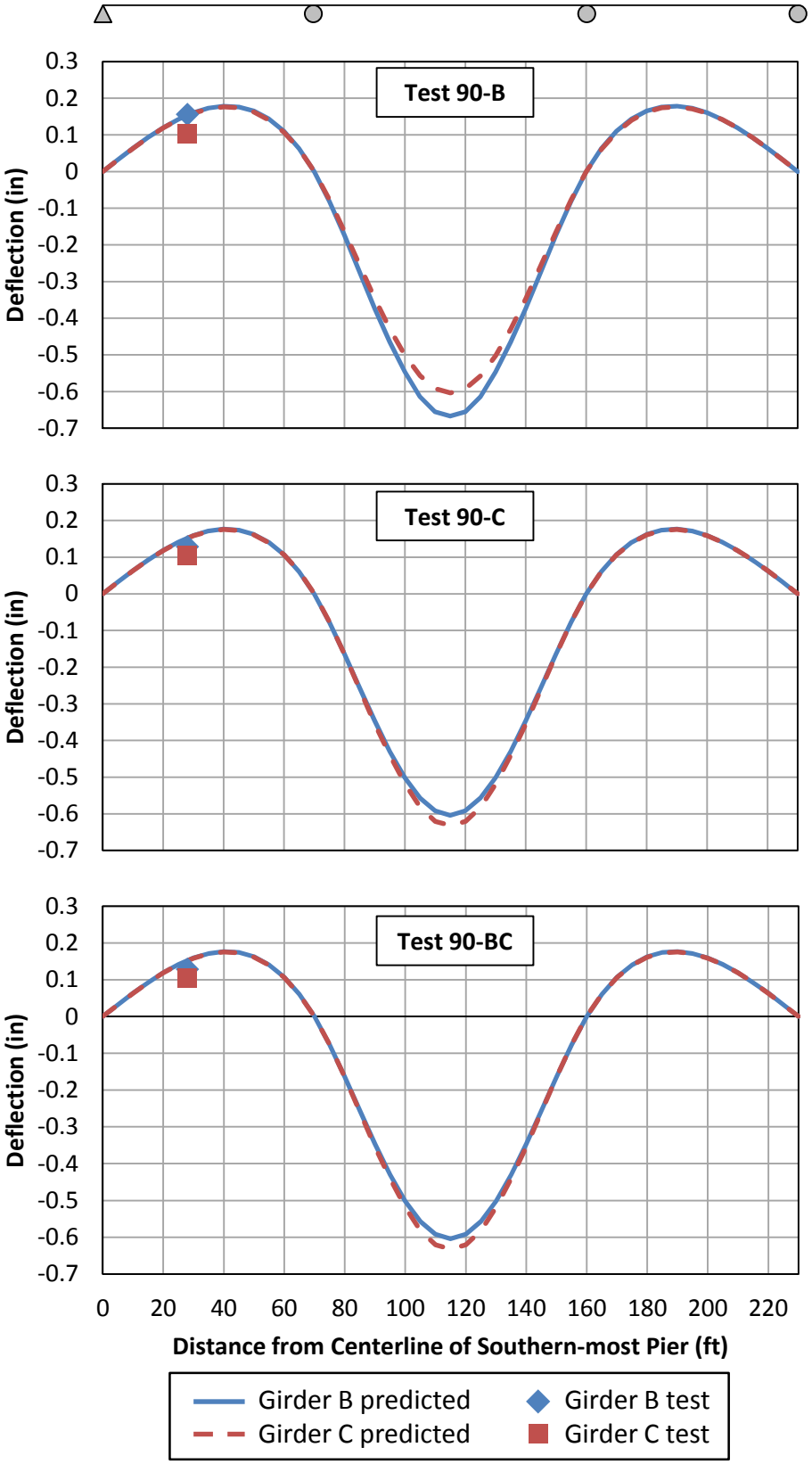

Figure 6.21 Deflection Results for Loading Configurations in the Middle Span

6.5.2 Slip Results

The measured interface slip values are compared to the predicted values in Figure 6.22 and Figure 6.23 for loading configurations in the south and middle spans, respectively. In most cases, the measured values of slip are significantly lower than that predicted for a non-composite girder. This is a further indication that some interface forces transferred through the connection plates or through friction are likely present, which create composite action to some extent. For Girder C, in which extremely small values of slip were measured, this is particularly true. Conversely, for Girder B in Test 70-B, the measured slip actually matched the predicted slip well at the location nearest the interior support, indicating that this girder may actually be behaving close to the non-composite assumption. However, the measured slip is significantly smaller than that predicted near the exterior girder in this test. Since slip measurements were only made at two locations along the entire girder, it is difficult to draw comprehensive conclusions from these results. In general, however, these observations are consistent with those made from the deflection results in the previous section.

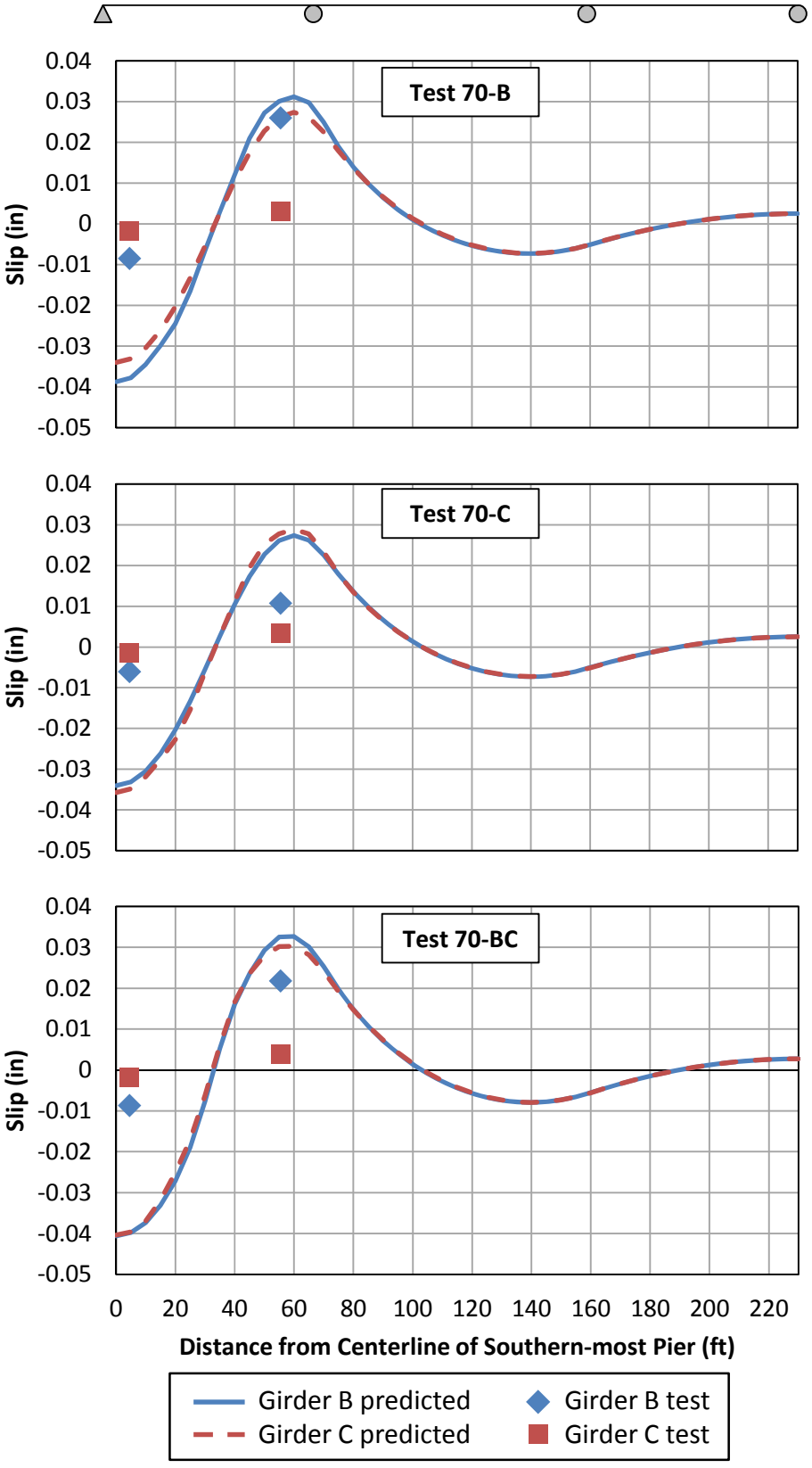

Figure 6.22 Slip Results for Loading Configurations in the South Span

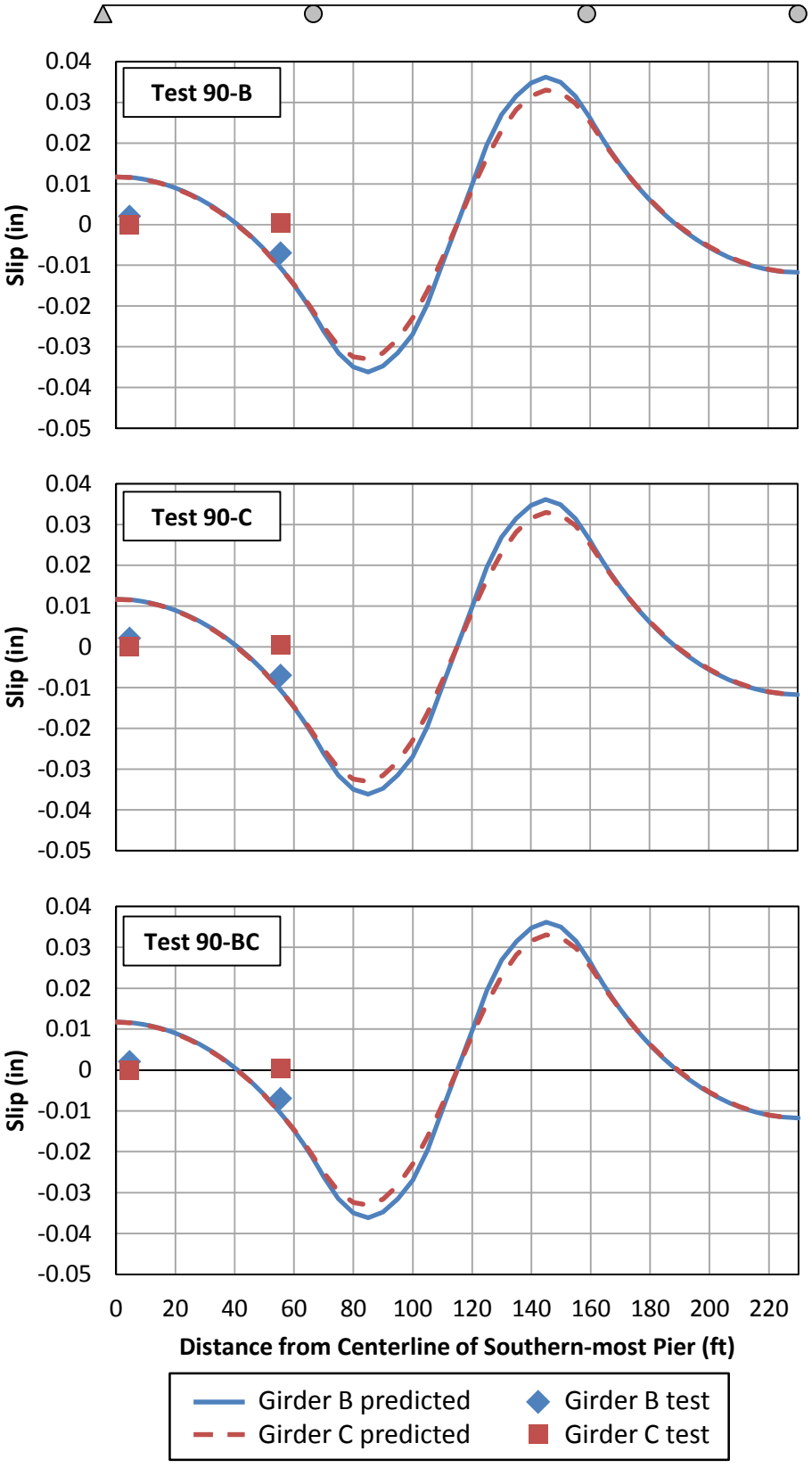

Figure 6.23 Slip Results for Loading Configurations in the Middle Span

6.5.3 Stress Results

The stress at mid-depth of the top and bottom flanges was computed from the strain gage readings at these locations, using an assumed elastic modulus of steel of 29,000 ksi. These results are compared with the stresses predicted by the finite element model in Figure 6.24 and Figure 6.25. Theoretically, for a non-composite girder comprised of a doubly-symmetric section, the flange stresses are of equal and opposite magnitudes so that the neutral axis is located at mid-depth of the steel beam. This was observed nearly exactly in the results from the finite element model. Thus, to facilitate comparison between the results from the top and bottom flanges, the absolute value of the stresses are plotted in all graphs.

As can be seen in the figure, the top flange stresses are smaller while the bottom flange stresses are larger than the predicted values for all cases on both girders. This means that the neutral axis is above mid-depth of the steel beam, indicating some level of composite behavior. The computed neutral axis location for all loading configurations is plotted in Figure 6.26. In all cases, the neutral axis is located closer to the top flange in Girder C than in Girder B, indicating that more composite behavior is occurring in Girder C than in Girder B, which is consistent with the observations made based on the deflection and slip results.

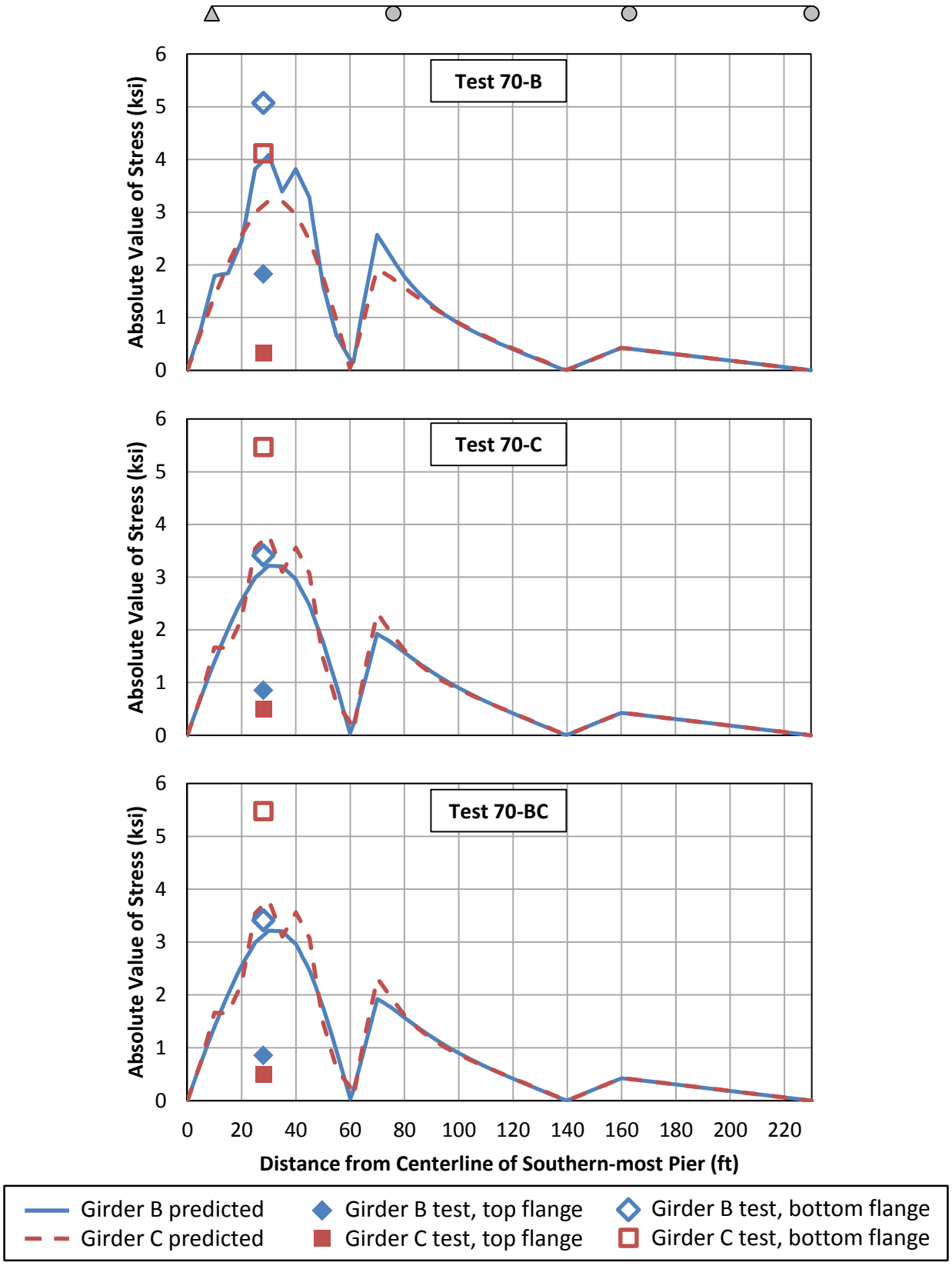

Figure 6.24 Stress Results for Loading Configurations in the South Span

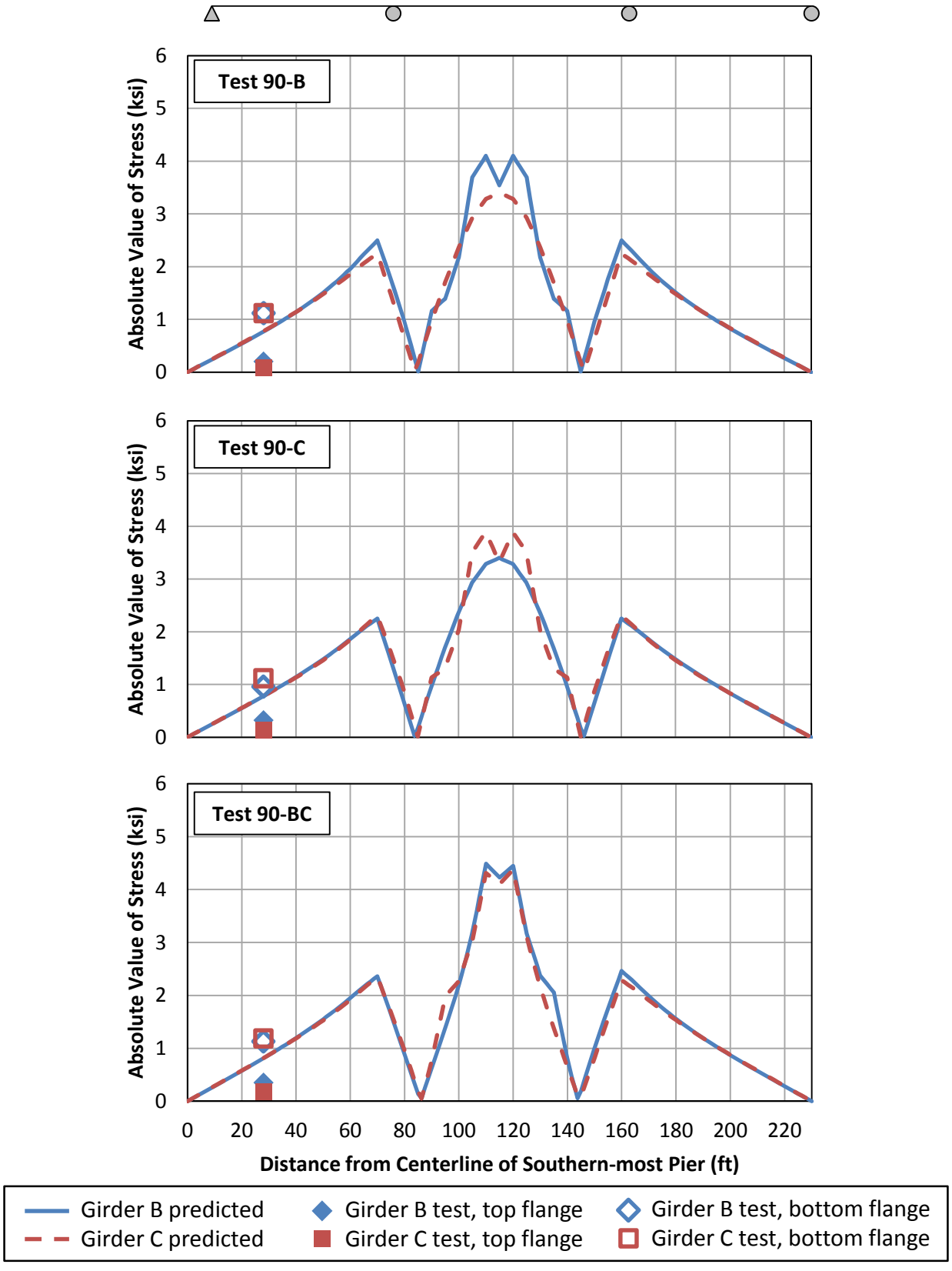

Figure 6.25 Stress Results for Loading Configurations in the Middle Span

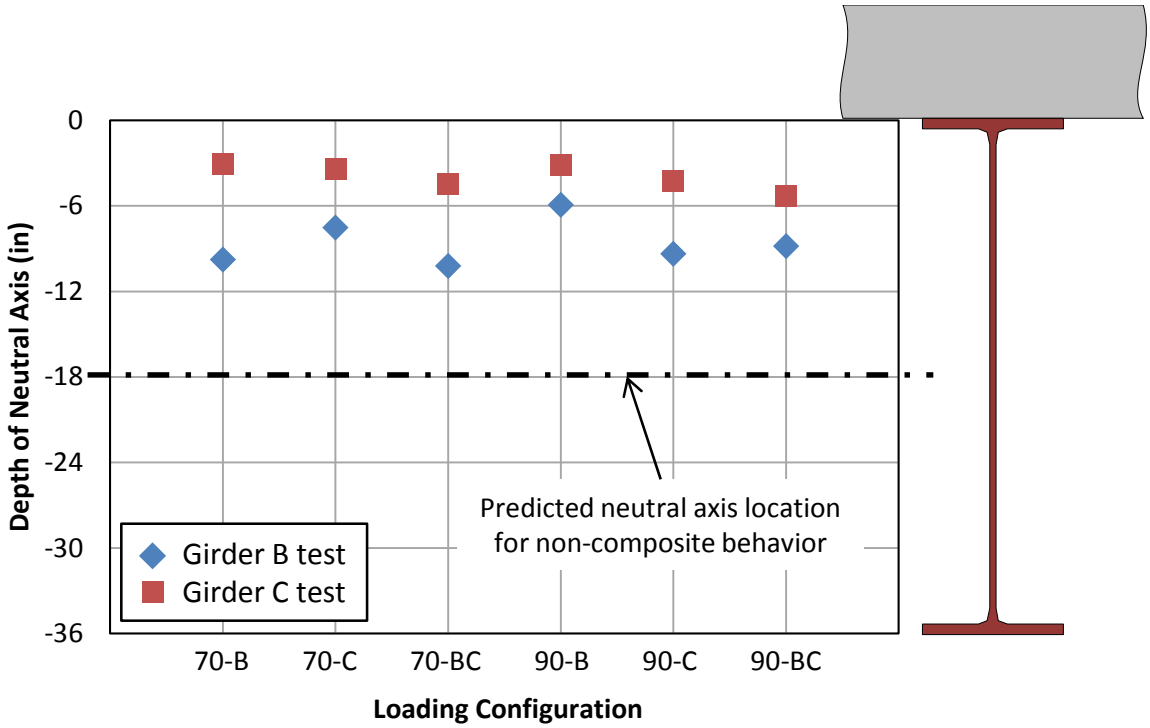

Figure 6.26 Estimated Neutral Axis Location for All Loading Configurations

6.6 Summary

A field load test was conducted on a three-span continuous steel girder unit in Lakeport, Texas. There are plans for this bridge to be strengthened with post-installed shear connectors in the future, and the results from this load test can be compared to a future load test conducted after the strengthening process is complete. Two girders on the bridge were instrumented with string potentiometers to measure deflections, linear potentiometers to measure interface slip, and strain gages. Data was collected from these instruments under six different loading configurations. The test results were compared to the predictions provided by the finite element model of the bridge.

This comparison indicated that while both of the instrumented girders behaved compositely to some extent, one of the girders exhibited significantly higher levels of composite action than the other. This difference is likely due to the different construction practices used for the two girders which were erected nearly two decades apart, as one was part of the original construction while the other was added when the bridge was widened. The riveted connections used for the girder splices and cover plates in the older girder project further up into the concrete deck, and may be inducing significant amounts of composite action, while the welded splices and cover plates protrude a smaller distance into the deck and have less of an effect on the behavior. Frictional forces at the steel-concrete interface may also play a role in creating some composite action in both girders.

Generally, it is not recommended to rely on any of this composite action that was observed during the load test when evaluating the bridge and conducting a strengthening design. It is advisable to assume that these girders act in a non-composite manner, despite indications that some composite behavior may be present in the bridge.

Chapter 7. Summary and Conclusions

7.1 Summary

This study has implemented the findings and recommendations from TxDOT project 0-6719 to conduct a strengthening design using post-installed shear connectors for an existing continuous non-composite steel I-girder bridge in Lakeport, Texas. Additionally, a pre-strengthening load test was conducted on the bridge to serve as a comparison to the behavior after the bridge is strengthened.

To strengthen the Lakeport Bridge to achieve an inventory load factor rating of HS 20, a total of 372 post-installed adhesive anchor shear connectors must be installed. This represents an increase of nearly 75% in the load factor rating from the existing non-composite bridge. Based on predicted future truck traffic, it is expected that these connectors will have a minimum of 32 years of fatigue life once installed on the bridge, which exceeds the desired extension of the service life of the bridge of 25 years. In addition to the post-installed shear connectors, a total of ten new cross frames and four sets of double-sided bearing stiffeners must be installed on the bridge to ensure that moment redistribution can occur in a safe manner.

The load test indicated that some composite action is already present in this non-composite bridge. In particular, it is likely that the riveted splices and cover plates in the girders comprising the original construction of the bridge induce some composite behavior by protruding upwards into the concrete deck. The level of composite action observed was significantly greater for Girder C, which was constructed as part of the original bridge, than for Girder B, which was added when the bridge was widened, and has welded splices and cover plates.

7.2 Conclusions

The following points summarize the major conclusions that have resulted from this study:

- Strengthening continuous non-composite steel I-girder bridges with post-installed shear connectors can provide significant increase in the load-carrying capacity. In the case of the Lakeport Bridge, a 75% increase in the load rating was attained using this method to eliminate the need to load-post the bridge with restricted axle weights.
- The design process, as illustrated in the detailed calculations in the Appendix, is straightforward and based on rational concepts of structural behavior. These design calculations can serve as a basis for strengthening designs for other similar bridges.
- In some cases, additional cross frames or bearing stiffeners must be added to the bridge to satisfy the requirements for moment redistribution in the *AASHTO LRFD Bridge Design Specifications*. These requirements ensure that there is an adequate amount of plastic rotation capacity at the interior supports to redistribute moments prior to the occurrence of local or lateral-torsional buckling.
- When locating the connectors, it is important to consider constructability and accessibility to facilitate the installation of the post-installed shear connectors. This includes avoiding splice plates or cover plates on the girders as well as reinforcing bars in the deck.

- Some composite behavior was observed during the load test conducted on the non-composite bridge. This is likely attributed to the protrusion of girder splice plates and cover plates into the concrete deck, with riveted connections inducing more composite action than welded connections. However, because only one bridge has been tested in this study, it is recommended that these effects be ignored in the evaluation and strengthening design of existing non-composite bridges.
- Overall, using post-installed shear connectors to strengthen continuous non-composite steel I-girder bridges seems to be an efficient method of increasing the load rating of such structures. Additional conclusions regarding the ease of construction and the cost of this type of retrofit will be possible following the second phase of this study, which plans to monitor the construction process and conduct a post-strengthening load test.

7.3 Recommendations for Future Research

The following recommendations are made for future research to improve this method of strengthening continuous non-composite steel I-girder bridges with post-installed shear connectors:

- Further study is needed to determine the particular cases in which additional cross frames and bearing stiffeners are necessary to allow for moment redistribution from interior pier sections of continuous steel girder bridges. Although these features are required by the provisions in Appendix B6 of the AASHTO LRFD specifications for new design, they may not be present in existing bridges. The addition of these features during a strengthening retrofit increases the cost, and the circumstances under which they are actually needed are unclear.
- Long-term monitoring of one or more strengthened bridges is needed to study the durability of the post-installed shear connectors over time and to monitor the actual permanent deformations that develop in the bridge from the inelastic redistribution of moments.
- Investigation into the application of this strengthening method to bridges with more complex geometries is needed to expand the scope of this strengthening method to a wider range of bridges. The research to date has focused on strengthening straight bridges with no skew or low skew angles. It would be beneficial to also apply this technique to bridges with heavily skewed supports and horizontal curvature.

References

AASHTO 2002, *Standard Specifications for Highway Bridges*, 17th edition, American Association of State Highway Officials, Washington, DC.

AASHTO 2010, *AASHTO LRFD Bridge Design Specifications*, 5th edition, American Association of State Highway and Transportation Officials, Washington, DC.

AASHTO 2011, *The Manual for Bridge Evaluation*, 2nd edition, American Association of State Highway and Transportation Officials, Washington, DC.

AISC 2010, *Commentary on the Specification for Structural Steel Buildings*, American Institute of Steel Construction, Chicago, Illinois.

Barth, KE, Hartnagel, BA, White, DW & Barker, MG 2004, 'Recommended Procedures for Simplified Inelastic Design of Steel I-Girder Bridges', *Journal of Bridge Engineering*, vol. 9, no. 3, pp. 230-242.

CSI 2011, *SAP2000*, Computers and Structures, Inc., Version 15, Walnut Creek, CA.

Ferguson Structural Engineering Laboratory (FSEL) 2016 (expected), Software Developed by FSEL, at <http://fsel.engr.utexas.edu/facilities/software/software>.

Ghiami Azad, AR 2016, *Fatigue Behavior of Post-Installed Shear Connectors used to Strengthen Continuous Non-composite Steel Bridge Girders*, PhD Dissertation, The University of Texas at Austin, Austin, Texas.

Hansell, WG & Viest, IM 1971, 'Load Factor Design for Steel Highway Bridges', *AISC Engineering Journal*, vol. 8, no. 4, pp. 113-123.

Kreitman, KL 2016, *Strengthening Continuous Steel Girder Bridges with Post-Installed Shear Connectors and Inelastic Moment Redistribution*, PhD Dissertation, The University of Texas at Austin, Austin, Texas.

Kreitman, K, Ghiami Azad, AR, Patel, H, Engelhardt, M, Helwig, T, Williamson, E & Klingner, R 2015, *Strengthening Existing Continuous Non-Composite Steel Girder Bridges using Post-Installed Shear Connectors*, Research report no. 0-6719-1, Center for Transportation Research, Austin, Texas.

Kwon, G, Engelhardt, M & Klingner, R 2009, *Implementation Project: Strengthening of a Bridge near Hondo, Texas using Post-Installed Shear Connectors*, Research report no. 5-4124-01-1, Center for Transportation Research, Austin, Texas.

Kwon, G, Hungerford, B, Kayir, H, Schaap, B, Ju, YK, Klingner, R & Engelhardt, M 2007, *Strengthening Existing Non-Composite Steel Bridge Girders Using Post-Installed Shear Connectors*, Research report no. 0-4124-1, Center for Transportation Research, Austin, Texas.

National Cooperative Highway Research Program (NCHRP) 2012, *Fatigue Evaluation of Steel Bridges*, Report 721, Transportation Research Board, Washington, DC.

Oehlers, DJ & Bradford, MA 1995, *Composite Steel and Concrete Structural Members: Fundamental Behavior*, 1st edition, Elsevier Science Inc., Tarrytown, New York.

PennDOT 2010, *BAR7 Bridge Analysis and Rating*, V7.13.0.0, Commonwealth of Pennsylvania Department of Transportation.

Texas Highway Department (THD) 1951, *Standard Specifications for Road and Bridge Construction*, Texas Highway Department.

U.S. Geological Survey (USGS) 2016, National Water Information System data available on the World Wide Web (USGS Water Data for the Nation), accessed [Jan 6, 2016 through Aug 5, 2016], at <http://waterdata.usgs.gov/nwis/uv?site_no=08020900>.

Appendix. Strengthening Design Calculations

Overview

These calculations detail the strengthening design of the Lakeport Bridge described in Chapter 4. . A half cross section of the symmetric bridge is shown in Figure 4.2. The four steel girders in the half section are denoted A, B, C, and D, with Girder A being the exterior girder and Girder D being the girder closest to the middle of the cross section. The steel unit, with 70-foot long exterior spans and a 90-foot long interior span, is also symmetric in the longitudinal direction, so only-one half of each girder is analyzed here.

General Design Information

The majority of the strength calculations and analyses are conducted using the load factor design method in the *Standard Specifications for Highway Bridges* (AASHTO 2002). All table, section, and equation references also refer to this document, unless otherwise specified. Although this is not the current design specification in the United States, it is often common practice to use the Standard specifications to evaluate bridges that were designed using those specifications.

However, the moment redistribution and fatigue provisions are taken from the *LRFD Bridge Design Specifications* for this example (AASHTO 2010). The moment redistribution provisions in the LRFD specifications are much simpler to use and apply to a wider range of geometries than those in the Standard specifications. Additionally, the fatigue design is conducted using the LRFD specifications to more accurately reflect the effect of realistic truck traffic at the time of the strengthening design.

Note that this design example is focused on the flexural strength of the non-composite and partially composite girders as well as the fatigue strength of the post-installed shear connectors. Although it is not explicitly shown here, a full strengthening design would consider all possible limit states for all members of the bridge. This includes but is not limited to the following:

- Shear strength of the steel girders
- Strength of the substructure and foundations
- Strength of the approach spans

The following material properties are used in these calculations. Because these properties were not directly specified on the available design drawings, the values used here are based on typical materials used at the time of construction and recommendations in the *Manual for Bridge Evaluation* (AASHTO 2011):

- Yield stress of steel beams, $F_y = 33\ ksi$ (ASTM A7 steel)
- Elastic modulus of steel beams, $E_s = 29000\ ksi$
- 28-day compressive strength of concrete deck, $f_c' = 3\ ksi$
- Elastic modulus of concrete deck,

$$E_c(ksi) = 57\sqrt{f'c\ (psi)} = 57\sqrt{3000\ psi} = 3222\ ksi$$

Scope of Design Example

Detailed design calculations and discussion are provided here for Girder B. A summary of the results for the other three girders is also provided in less detail, as the process is similar.

The general process for the design is as follows: (1) conduct structural analysis, (2) evaluate existing non-composite structure, (3) set strengthening targets, (4) check negative moment regions and redistribute moments as necessary, (5) design connectors for strength requirements in positive moment regions, and (6) locate connectors and check fatigue.

Detailed Design of Girder B

A half-elevation view of Girder B, which is equivalent to Girder A, is shown in Figure A.1. This girder was added as part of the widening of the bridge in 1961. It is constructed of a 36WF160 rolled steel shape, with welded splices and cover plates welded to the top and bottom flange at the interior pier and in the middle of the interior span. Table A.1 summarizes the section properties for design for the steel beam (Section 1), as well as for the steel beam with cover plates at the interior pier (Section 2) and in the interior span (Section 3).

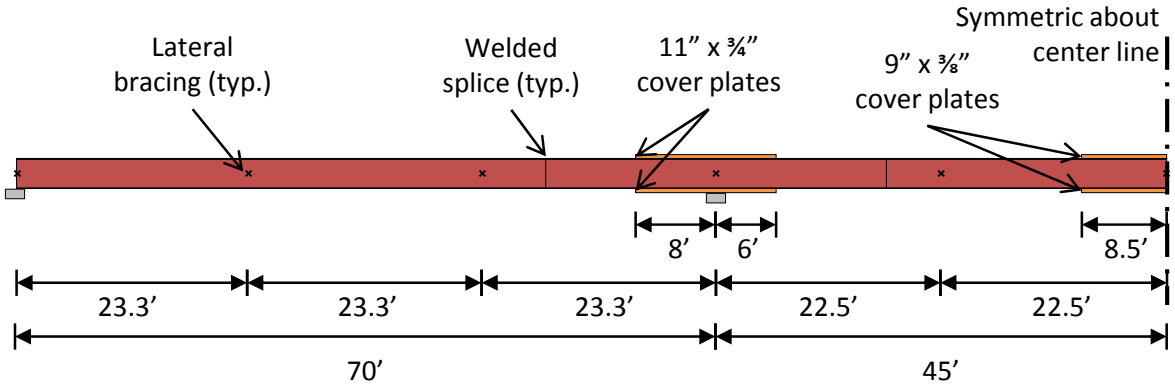

Figure A.1: Half-Elevation View of Girders A and B

Table A.1: Section Properties for Girders A and B

	Section 1	Section 2	Section 3
Cover plate width (b_{pl}, in)	0	11.0	9.00
Cover plate thickness (t_{pl}, in)	0	0.750	0.375
Flange width (b_f, in)	12.0	12.0	12.0
Flange thickness (t_f, in)	1.02	1.02	1.02
Flange area (A_f, in^2)	12.2	20.5	15.6
Flange moment of inertia (I_{yc}, in^4)	147	230	170
Total depth (d, in)	36.0	37.5	36.8
Web thickness (t_w, in)	0.650	0.650	0.650
Area (A_s, in^2)	47.0	63.5	53.8
Moment of inertia (I_x, in^4)	9760	15300	12000
Elastic section modulus (S_x, in^3)	542	818	653
Plastic section modulus (Z_x, in^3)	624	927	747
Radius of gyration (r_y, in)	2.51	2.70	2.52
Polar moment of inertia (J, in^4)	12.4	15.5	12.7
Web depth (D, in)	34.0	34.0	34.0
Depth of web in compression, elastic (D_c, in)	17.0	17.0	17.0
Depth of web in compression, plastic (D_{cp}, in)	17.0	17.0	17.0
Effective deck width (b_{deck}, in) and girder spacing (S, in)	91.5	91.5	91.5
Deck thickness (t_{deck}, in)	6.5	6.5	6.5
Deck area (A_{deck}, in^2)	595	595	595
Deck moment of inertia (I_{deck}, in^4)	2090	2090	2090

Conduct Structural Analysis

The structural analysis was done using a line girder analysis with the software BAR7. This software, which is commonly used for load rating of bridges, outputs the unfactored dead and live load moments, given the geometry of a given bridge girder, the magnitude of the live load, and the appropriate distribution factor. The load factor design and rating procedures are used in this example, so an HS 20 live load was chosen for the analysis.

The dead load was taken as the self-weight of the girder (including cover plates), the self-weight of the deck, the weight of a 4-inch asphalt overlay, and a portion of the curb, sidewalk, and railing weights. The tributary area for the deck and overlay was taken as half of the distance to the adjacent girders, and the overlay was assumed to contribute a load of 12 psf per inch of

thickness. The weight of the curb, sidewalk, and railings was even distributed over all of the girders, according to the recommendation in Section 3.23.2.3.1.1.

The vehicular live load used in the analysis was an HS 20 load, which is the target load rating for the bridge after strengthening. The distribution factor for moment, is calculated as follows. Note that this calculated distribution factor represents the fraction of a wheel line of the design truck that is distributed to the girder of interest. The software BAR7 defines the distribution factor as the fraction of the total design truck distributed to the girder of interest. Thus, the distribution factor entered into the software is one-half of this calculated value:

$$DF = \frac{S}{5.5} = \frac{(91.5\ in)\left(\frac{1\ ft}{12\ in}\right)}{5.5} = 1.39$$ *Table 3.23.1*

The unfactored dead load moments and live load moment envelope are plotted in Figure A.2. Table A.2 indicates the values of these moments at the critical sections of the girder. The critical sections for flexural strength are at the points of maximum positive moment near the center of each span, at the points of maximum negative moment at the centerline of each interior support, and at the points of section transitions, which only occur on this girder at the termination of the cover plates. The moments at the lateral brace points in the unbraced lengths adjacent to the interior pier are also given in the table. Recall that because of symmetry, only one-half of the girder is analyzed here. Each section is denoted by its location relative to the end of the continuous steel unit. Thus, the section at the centerline of the interior pier is denoted as 70'.

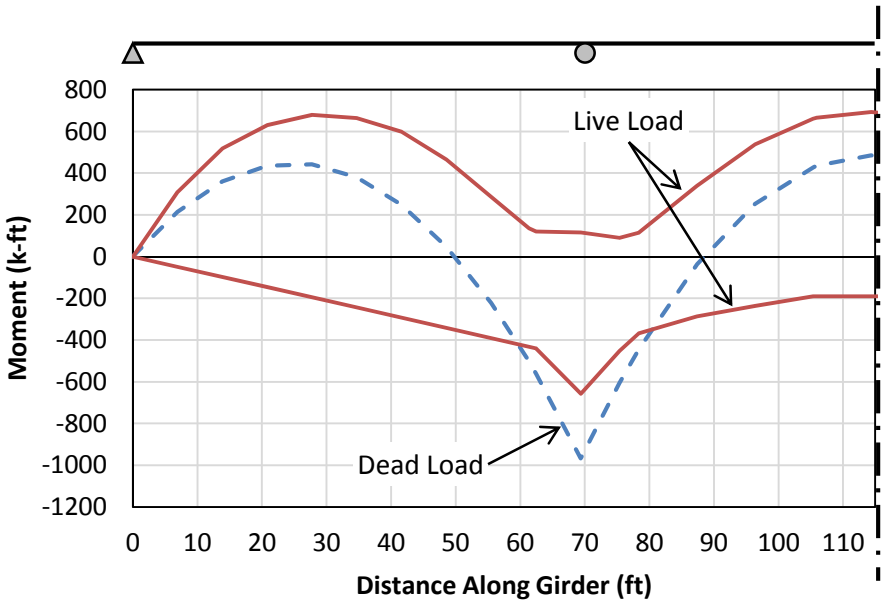

Figure A.2: Plot of Unfactored Moments for Girder B

Table A.2: Unfactored Moments at Critical Sections and at Lateral Brace Locations around the Interior Pier Section in Girder B

Location (ft)	Section Type	Section Number	Unfactored Moment (k-ft)		
			Dead Load	Live Load	
				Pos.	Neg.
28	Critical, Span	1	442	679	-195
46.7	Lateral Brace	1	121	514	-324
62	Critical, Transition	1	-503	136	-432
70	Critical, Pier Lateral Brace	2	-967	116	-657
76	Critical, Transition	1	-606	89	-452
92.5	Lateral Brace	1	108	439	-261
106.5	Critical, Transition	1	434	666	-191
115	Critical, Span	3	486	694	-191

Evaluate Existing Non-composite Girder

The evaluation of the non-composite girder is done through a load rating at the critical sections listed in Table A.2 using the Load Factor Rating method. The rating factor (RF) is calculated using the following equation:

$$RF = \frac{C - A_1\, DL}{A_2(LL + I)}$$

MBE Equation 6B.4.1-1

where C represents the capacity of the section, DL is the dead load force effect, $LL + I$ is the live load force effect including the dynamic impact factor, and A_1 and A_2 are constants depending on the type of rating and the limit state considered.

This rating factor represents the fraction of the live load applied during the structural analysis that can be safely resisted by the girder, which in this case is an HS 20 live load. The corresponding load factor rating (RT) is determined by multiply the rating factor by the magnitude of the live load used in the analysis in tons, which in this case is 20.

$$RT = (RF)(W) = (RF)(20)$$

MBE Equation 6B.4.1-2

Both the Overload and Maximum Load limit states are considered here. The values of the coefficients A_1 and A_2 for an inventory-level rating for the two limit states are as follows:

$$Overload: \quad A_1 = 1.0; \quad A_2 = 1.67$$

$$Maximum\ Load: \quad A_1 = 1.3; \quad A_2 = 2.17$$

MBE Equation 6B.4.3

The capacity at the Overload limit state is based on a limiting value for the stresses in the steel beam. Because the entire girder is non-composite at this point, the stress in the extreme fiber of the steel beam is limited to 80% of the yield stress. This is equivalent to limiting the moment to 80% of the yield moment (M_y) because all of the stresses are carried by the non-composite section. Thus, in general, the flexural capacity at the Overload limit state (C_{OL}) is:

$$C_{OL} = 0.80\, M_y = 0.80\, S_x\, F_y$$ *Section 10.57.1*

The capacity at the Maximum Load limit state (C_{ML}) is the smaller of the local buckling capacity, lateral torsional buckling capacity, and the plastic moment of the section, as defined in Section 10.48. The following calculations determine the capacity at both the Overload and Maximum Load limit states for the critical sections listed in Table A.2:

Critical Location at 28' (Section #1)

The Overload capacity is calculated as:

$$C_{OL\,28'} = 0.80\, S_x\, F_y = 0.80(542\ in^3)(33\ ksi)\left(\frac{1\ ft}{12\ in}\right) = 1190\ k.ft$$

To calculate the Maximum Load capacity, the compression (top) flange can be considered to be continuously braced by the deck so that lateral-torsional buckling will not control the strength. Thus, the steel section is classified as compact if:

$$\frac{b_f}{t_f} \le \frac{4{,}100}{\sqrt{F_y}} \rightarrow \frac{12.0\ in}{1.02\ in} \le \frac{4{,}100}{\sqrt{33{,}000\ psi}} \rightarrow 11.8 \le 22.6$$ *Equation 10-93*

$$\rightarrow \textit{compression flange is compact}$$

$$\frac{D}{t_w} \le \frac{19{,}230}{\sqrt{F_y}} \rightarrow \frac{34.0\ in}{0.650\ in} \le \frac{19{,}230}{\sqrt{33{,}000\ psi}} \rightarrow 52.3 \le 106$$ *Equation 10-94*

$$\rightarrow \textit{web is compact}$$

This section qualifies as a compact section, so the flexural strength is defined as the plastic moment of the section. The Maximum Load capacity is:

$$C_{ML\,28'} = Z_x\, F_y = (624\ in^3)(33\ ksi)\left(\frac{1\ ft}{12\ in}\right) = 1720\ k.ft$$ *Section 10.48.1*

The rating factor and load rating for the Overload and Maximum Load limit states for this critical location are:

$$RF_{OL\,28'} = \frac{1190\ k.ft - (1.0)(442\ k.ft)}{(1.67)(679\ k.ft)} = 0.660$$

$$RT_{OL\,28'} = (0.660)(20) = 13.2 \rightarrow HS\ 13.2$$

$$RF_{ML\,28'} = \frac{1720\ k.ft - (1.3)(442\ k.ft)}{(2.17)(679\ k.ft)} = 0.777$$

$$RT_{ML\,28'} = (0.777)(20) = 15.5 \quad \rightarrow \quad HS\ 15.5$$

Critical Location at 62' (Section #1)

The Overload capacity is equivalent to that at 28', although it will be given a negative sign since this location is dominated by negative flexure:

$$C_{OL\,62'} = -1190\ k.ft$$

The unbraced length (L_b) for the compression (bottom) flange is 23.3 feet, or 280 inches. The steel section is the same as that at 28', so the compression flange and web meet the compact limits. Thus, the steel section is classified as compact if:

$$\frac{L_b}{r_y} \leq \frac{\left[3.6 - 2.2\left(\frac{M_1}{M_p}\right)\right] x10^3}{F_y} \qquad \textit{Equation 10-96}$$

$$M_1 = (1.3)(121\ k.ft) + (2.17)(-324\ k.ft) = -546\ k.ft$$

$$M_p = -Z_{x\,70'}\,F_y = (927\ k.ft)(33\ ksi)\left(\frac{1\ ft}{12\ in}\right) = -2550\ k.ft$$

$$\rightarrow \ \frac{280\ in}{2.51\ in} \leq \frac{\left[3.6 - 2.2\left(\frac{-546\ k.ft}{-2550\ k.ft}\right)\right] x10^3}{33\ ksi} \ \rightarrow \ 111 \not\leq 94.8$$
$$\rightarrow \quad LTB\ not\ OK$$

In the above equation for the lateral-torsional buckling check, M_1 is the smaller of the brace moments and M_p is the plastic moment capacity at the other brace point. The ratio of M_1 to M_p is taken as positive if the factored moments cause single curvature within the unbraced length, which is the case here.

Because the unbraced length is too large, the section is not compact. The steel section is classified as a braced noncompact section if the following equation is true. Note that because the compression flange and web are known to meet the compact limits, only the lateral-torsional buckling check needs to be done here:

$$L_b \leq \frac{20{,}000A_f}{F_y\,d} \quad \rightarrow \quad 280\ in \leq \frac{20{,}000(12.2\ in^2)}{(33\ ksi)(36.0\ in)} \qquad \textit{Equation 10-101}$$
$$\rightarrow \quad 280\ in \not\leq 205\ in \quad \rightarrow \quad LTB\ not\ OK$$

Again, because the unbraced length is too large, the section does not qualify as a braced noncompact section. Thus, it is a partially braced member, and the capacity is calculated as follows:

$$C_{ML\,62'} = -M_r R_b$$ *Equation 10-103a*

$$M_r = (91\ x\ 10^3) C_b \left(\frac{I_{yc}}{L_b}\right) \sqrt{0.772 \frac{J}{I_{yc}} + 9.87 \left(\frac{d}{L_b}\right)^2} \leq M_y$$ *Equation 10-103c*

$$C_b = 1.75 + 1.05\left(-\frac{M_1}{M_2}\right) + 0.3\left(-\frac{M_1}{M_2}\right)^2 \leq 2.3$$

$$M_1 = (1.3)(121\ k.ft) + (2.17)(-324\ k.ft) = -546\ k.ft$$

$$M_2 = (1.3)(-967\ k.ft) + (2.17)(-657\ k.ft) = -2680\ k.ft$$

$$C_b = 1.75 + 1.05\left(-\frac{-546\ k.ft}{-2680\ k.ft}\right) + 0.3\left(-\frac{-546\ k.ft}{-2680\ k.ft}\right)^2 = 1.55$$

$$M_y = S_x F_y = (542\ in^3)(33\ ksi)\left(\frac{1\ ft}{12\ in}\right) = 1490\ k.ft$$

$$M_r = (91x10^3)(1.55)\left(\frac{147\ in^4}{280\ in}\right)\sqrt{0.772\left(\frac{12.4\ in^4}{147\ in^4}\right) + 9.87\left(\frac{36.0\ in}{280\ in}\right)^2}$$

$$= 35400\ k.in\left(\frac{1\ ft}{12\ in}\right) = 2950\ k.ft \not\leq M_y \quad \rightarrow \quad M_r$$

$$= 1490\ k.ft$$

$$R_b = 1 - 0.002\left(\frac{D_c\ t_w}{A_f}\right)\left[\frac{D_c}{t_w} - \frac{\lambda}{\sqrt{\frac{M_r}{S_x}}}\right] \leq 1.0$$

$$= 1 - 0.002\frac{(17.0\ in)(0.650\ in)}{12.2\ in^2}\left[\frac{17.0\ in}{0.650\ in} - \frac{15{,}400}{\sqrt{33{,}000\ psi}}\right]$$

$$= 1.11 \not\leq 1.0 \quad \rightarrow \quad R_b = 1.0$$

$$C_{ML\,62'} = -(1490\ k.ft)(1.0) = -1490\ k.ft$$

Note that because M_r is equal to M_y, the ratio of M_r to S_x under the square root in the equation for R_b is simply equal to F_y. In the equation for C_b, M_1 and M_2 are the smaller and larger of the factored brace point moments, respectively. The ratio of M_1 to M_2 is taken as negative if the moments cause single curvature, which is the case here.

The rating factor and load rating for the Overload and Maximum Load limit states for this critical location are:

$$RF_{OL\,62'} = \frac{-1190\ k.ft - (1.0)(-503\ k.ft)}{(1.67)(-432\ k.ft)} = 0.952$$

$$RT_{OL\,62'} = (0.952)(20) = 19.0 \quad \rightarrow \quad HS\ 19.0$$

$$RF_{ML\,62'} = \frac{-1490\ k.ft - (1.3)(-503\ k.ft)}{(2.17)(-432\ k.ft)} = 0.892$$

$$RT_{ML\,62'} = (0.892)(20) = 17.8 \quad \rightarrow \quad HS\ 17.8$$

Critical Location at 70' (Section #2)

The Overload capacity is calculated as:

$$C_{OL\,70'} = -0.80\ S_x\ F_y = 0.80(818\ in^3)(33\ ksi)\left(\frac{1\ ft}{12\ in}\right) = -1800\ k.ft$$

Because there is a cross frame at this location, the unbraced lengths on both sides of this critical location need to be checked. The unbraced length (L_b) for the compression (bottom) flange is 23.3 feet, or 280 inches, in the direction of the exterior span and 22.5 feet, or 270 inches, in the direction of the interior span. However, from the calculations at 62', it is already known that the unbraced length adjacent to the interior pier in the exterior span is classified as a partially braced member, so the compact and braced noncompact checks do not need to be made here. The capacity for a partially braced member is calculated for the unbraced lengths on either side of the interior pier are:

$$C_{ML\,70'} = -M_r R_b \qquad \textit{Equation 10-103a}$$

$$M_r = (91\ x\ 10^3) C_b \left(\frac{I_{yc}}{L_b}\right)\sqrt{0.772\frac{J}{I_{yc}} + 9.87\left(\frac{d}{L_b}\right)^2} \leq M_y \qquad \textit{Equation 10-103c}$$

$$C_b = 1.75 + 1.05\left(-\frac{M_1}{M_2}\right) + 0.3\left(-\frac{M_1}{M_2}\right)^2 \leq 2.3$$

$$M_{1\,ext} = -546\ k.ft$$

$$M_{1\,int} = (1.3)(108\ k.ft) + (2.17)(-261\ k.ft) = -426\ k.ft$$

$$M_2 = -2680\ k.ft$$

$$C_{b\,ext} = 1.55$$

$$C_{b\,int} = 1.75 + 1.05\left(-\frac{-426\ k.ft}{-2680\ k.ft}\right) + 0.3\left(-\frac{-426\ k.ft}{-2680\ k.ft}\right)^2 = 1.59$$

$$M_y = S_x F_y = (818\ in^3)(33\ ksi)\left(\frac{1\ ft}{12\ in}\right) = 2250\ k.ft$$

$$M_{r\,ext} = (91x10^3)(1.55)\left(\frac{230\ in^4}{280\ in}\right)\sqrt{0.772\left(\frac{15.5\ in^4}{230\ in^4}\right) + 9.87\left(\frac{36.0\ in}{280\ in}\right)^2}$$
$$= 53700\ k.in\left(\frac{1\ ft}{12\ in}\right) = 4480\ k.ft \nleq M_y \quad \rightarrow \quad M_{r\,ext}$$
$$= 2250\ k.ft$$

$$M_{r\,int} = (91x10^3)(1.59)\left(\frac{230\ in^4}{270\ in}\right)\sqrt{0.772\left(\frac{15.5\ in^4}{230\ in^4}\right) + 9.87\left(\frac{36.0\ in}{270\ in}\right)^2}$$
$$= 58800\ k.in\left(\frac{1\ ft}{12\ in}\right) = 4900\ k.ft \nleq M_y \quad \rightarrow \quad M_{r\,int}$$
$$= 2250\ k.ft$$

$$R_b = 1 - 0.002\left(\frac{D_c\ t_w}{A_f}\right)\left[\frac{D_c}{t_w} - \frac{\lambda}{\sqrt{\frac{M_r}{S_x}}}\right] \leq 1.0$$
$$= 1 - 0.002\frac{(17.0\ in)(0.650\ in)}{20.5\ in^2}\left[\frac{17.0\ in}{0.650\ in} - \frac{15{,}400}{\sqrt{33{,}000\ psi}}\right]$$
$$= 1.06 \nleq 1.0 \quad \rightarrow \quad R_b = 1.0$$

$$C_{ML\,70'} = -(2250\ k.ft)(1.0) = -2250\ k.ft$$

The rating factor and load rating for the Overload and Maximum Load limit states for this critical location are:

$$RF_{OL\,70'} = \frac{-1800\ k.ft - (1.0)(-967\ k.ft)}{(1.67)(-657\ k.ft)} = 0.759$$

$$RT_{OL\,70'} = (0.759)(20) = 15.2 \quad \rightarrow \quad HS\ 15.2$$

$$RF_{ML\,70'} = \frac{-2250\ k.ft - (1.3)(-967\ k.ft)}{(2.17)(-657\ k.ft)} = 0.696$$

$$RT_{ML\,70'} = (0.696)(20) = 13.9 \quad \rightarrow \quad HS\ 13.9$$

Critical Location at 76' (Section #1)

The Overload capacity is equivalent to that at 62':

$$C_{OL\,76'} = -1190\ k.ft$$

The unbraced length (L_b) for the compression (bottom) flange is 22.5 feet, or 270 inches. The steel section is the same as that at 28' and 62', so the compression flange and web meet the compact limits. Some calculations for the unbraced length were conducted previously for the critical location at 70' and will not be repeated in detail here. The steel section is classified as compact if:

$$\frac{L_b}{r_y} \leq \frac{\left[3.6 - 2.2\left(\frac{M_1}{M_p}\right)\right] x10^3}{F_y} \qquad \textit{Equation 10-96}$$

$$M_1 = -426\ k.ft$$

$$M_p = -Z_{x\,70'}\,F_y = (927\ k.ft)(33\ ksi)\left(\frac{1\ ft}{12\ in}\right) = -2550\ k.ft$$

$$\rightarrow\ \frac{270\ in}{2.51\ in} \leq \frac{\left[3.6 - 2.2\left(\frac{-426\ k.ft}{-2550\ k.ft}\right)\right] x10^3}{33\ ksi}\ \rightarrow\ 108 \not\leq 98.0$$

$$\rightarrow\ LTB\ not\ OK$$

Because the unbraced length is too large, the section is not compact. Because the compression flange and web already satisfy the compact limits, the steel section is classified as a braced noncompact section if:

$$L_b \leq \frac{20{,}000A_f}{F_y\,d} \rightarrow 270\ in \leq \frac{20{,}000(12.2\ in^2)}{(33\ ksi)(36.0\ in)} \qquad \textit{Equation 10-101}$$

$$\rightarrow\ 270\ in \not\leq 205\ in \rightarrow\ LTB\ not\ OK$$

Again, because the unbraced length is too large, the section does not qualify as a braced noncompact section. Thus, it is a partially braced member, and the capacity is calculated as follows:

$$C_{ML\,76'} = -M_r R_b \qquad \textit{Equation 10-103a}$$

$$M_r = (91\ x\ 10^3)C_b\left(\frac{I_{yc}}{L_b}\right)\sqrt{0.772\frac{J}{I_{yc}} + 9.87\left(\frac{d}{L_b}\right)^2} \leq M_y \qquad \textit{Equation 10-103c}$$

$$C_b = 1.59$$

$$M_y = S_x F_y = (542\ in^3)(33\ ksi)\left(\frac{1\ ft}{12\ in}\right) = 1490\ k.ft$$

$$M_r = (91x10^3)(1.59)\left(\frac{147\ in^4}{270\ in}\right)\sqrt{0.772\left(\frac{12.4\ in^4}{147\ in^4}\right) + 9.87\left(\frac{36.0\ in}{270\ in}\right)^2}$$
$$= 38600\ k.in\left(\frac{1\ ft}{12\ in}\right) = 3220\ k.ft \not\leq M_y \quad \rightarrow \quad M_r$$
$$= 1490\ k.ft$$

$$R_b = 1 - 0.002\left(\frac{D_c\ t_w}{A_f}\right)\left[\frac{D_c}{t_w} - \frac{\lambda}{\sqrt{\frac{M_r}{S_x}}}\right] \leq 1.0$$
$$= 1 - 0.002\frac{(17.0\ in)(0.650\ in)}{12.2\ in^2}\left[\frac{17.0\ in}{0.650\ in} - \frac{15{,}400}{\sqrt{33{,}000\ psi}}\right]$$
$$= 1.11 \not\leq 1.0 \quad \rightarrow \quad R_b = 1.0$$

$$C_{ML\ 76'} = -(1490\ k.ft)(1.0) = -1490\ k.ft$$

The rating factor and load rating for the Overload and Maximum Load limit states for this critical location are:

$$RF_{OL\ 76'} = \frac{-1190\ k.ft - (1.0)(-606\ k.ft)}{(1.67)(-452\ k.ft)} = 0.774$$

$$RT_{OL\ 76'} = (0.774)(20) = 15.5 \quad \rightarrow \quad HS\ 15.5$$

$$RF_{ML\ 76'} = \frac{-1490\ k.ft - (1.3)(-606\ k.ft)}{(2.17)(-452\ k.ft)} = 0.716$$

$$RT_{ML\ 76'} = (0.716)(20) = 14.3 \quad \rightarrow \quad HS\ 14.3$$

Critical Location at 106.5' (Section #1)

The Overload capacity is equivalent to that at 28':

$$C_{OL\ 106.5'} = 1190\ k.ft$$

To calculate the Maximum Load capacity, the compression flange and web have already been shown to meet the compact limits. Additionally, the compression (top) flange can be considered to be continuously braced by the deck so that lateral-torsional buckling will not control the strength. Thus, the steel section is classified as compact and the capacity is:

$$C_{ML\ 106.5'} = Z_x\ F_y = (624\ in^3)(33\ ksi)\left(\frac{1\ ft}{12\ in}\right) = 1720\ k.ft$$ *Section 10.48.1*

The rating factor and load rating for the Overload and Maximum Load limit states for this critical location are:

$$RF_{OL\ 106.5'} = \frac{1190\ k.ft - (1.0)(434\ k.ft)}{(1.67)(666\ k.ft)} = 0.680$$

$$RT_{OL\ 106.5'} = (0.680)(20) = 13.6 \quad \rightarrow \quad HS\ 13.6$$

$$RF_{ML\ 106.5'} = \frac{1720\ k.ft - (1.3)(434\ k.ft)}{(2.17)(666\ k.ft)} = 0.800$$

$$RT_{ML\ 106.5'} = (0.800)(20) = 16.0 \quad \rightarrow \quad HS\ 16.0$$

Critical Location at 115' (Section #3)

The Overload capacity is calculated as:

$$C_{OL\ 115'} = 0.80\ S_x\ F_y = 0.80(653\ in^3)(33\ ksi)\left(\frac{1\ ft}{12\ in}\right) = 1440\ k.ft$$

To calculate the Maximum Load capacity, the compression flange and web have already been shown to meet the compact limits. Additionally, the compression (top) flange can be considered to be continuously braced by the deck so that lateral-torsional buckling will not control the strength. Thus, the steel section is classified as compact and the capacity is:

$$C_{ML\ 115'} = Z_x\ F_y = (747\ in^3)(33\ ksi)\left(\frac{1\ ft}{12\ in}\right) = 2050\ k.ft$$ *Section 10.48.1*

The rating factor and load rating for the Overload and Maximum Load limit states for this critical location are:

$$RF_{OL\ 115'} = \frac{1440\ k.ft - (1.0)(486\ k.ft)}{(1.67)(694\ k.ft)} = 0.823$$

$$RT_{OL\ 115'} = (0.823)(20) = 16.5 \quad \rightarrow \quad HS\ 16.5$$

$$RF_{ML\ 115'} = \frac{2050\ k.ft - (1.3)(486\ k.ft)}{(2.17)(694\ k.ft)} = 0.942$$

$$RT_{ML\ 115'} = (0.942)(20) = 18.8 \quad \rightarrow \quad HS\ 18.8$$

Summary of Load Rating of Existing Non-Composite Girder

Table A.3 summarizes the results of the load rating calculations for the existing girder at the critical locations from Table A.2. The controlling load rating is HS 13.2, which occurs at the Overload limit state at the critical section at the maximum positive moment in the exterior span (28').

Table A.3: Load Rating Results of Existing Non-Composite Girder B

Location (ft)	Section Type	Capacity (k-ft)		Inventory Load Rating	
		Overload	Maximum Load	Overload	Maximum Load
28	Critical, Span	1190	1720	HS 13.2	HS 15.5
62	Critical, Transition	-1190	-1490	HS 19.0	HS 17.8
70	Critical, Pier	-1800	-2250	HS 15.2	HS 13.9
76	Critical, Transition	-1190	-1490	HS 15.5	HS 14.3
106.5	Critical, Transition	1190	1720	HS 13.6	HS 16.0
115	Critical, Span	1440	2050	HS 16.5	HS 18.8

Set Strengthening Targets

The bridge owner would like to ***increase the inventory load factor rating to HS 20***, which corresponds to the minimum strength of a new bridge designed using the Standard specifications. At a minimum, a ***remaining life of 25 years*** is desired for the purposes of fatigue design of the post-installed shear connectors. It is expected that an ***average annual daily truck traffic ($(ADTT)_{SL}$) of 1160 trucks per day*** will cross the bridge over the next 25 years.

Check Negative Moment Regions and Redistribute Moments

To start the strengthening process, first the strength of the negative moment regions at the interior piers (70') is evaluated and compared to the factored moments (M_u) to determine whether or not moment redistribution is necessary. As with the evaluation of the existing girder, both the Overload and Maximum Load limit states are considered here. The factored moments for these limit states are as follows, where DL is the dead load force effect and $LL + I$ is the live load force effect, including the dynamic impact factor:

$$M_{u\,OL} = 1.0DL + (1.67)(LL + I)$$
$$= 1.0(-967\ k.ft) + (1.67)(-657\ k.ft)$$
$$= -2060\ k.ft$$

Section 10.57

$$M_{u\,ML} = 1.3DL + 2.17(LL + I)$$
$$= 1.3(-967\ k.ft) + 2.17(-657\ k.ft) = -2680\ k.ft$$

Table 3.22.1A

If the factored moment at the interior pier exceeds the capacity of the section at that interior pier, moment redistribution can be considered to increase the load rating at that location. The

capacity at both limit states was calculated during the evaluation of the existing non-composite girder:

$$C_{OL\,70'} = -1800\ k.ft$$

$$C_{ML\,70'} = -2250\ k.ft$$

The magnitude of the factored moments exceed the calculated capacities at the interior pier section (70') for both the Overload (2060 k-ft > 1800 k-ft) and Maximum Load (2680 k-ft > 2250 k-ft) limit states. This means that ***moment redistribution should be considered at both limit states***.

The findings of this research recommend using the simple, rational moment redistribution provisions from Appendix B6 of the LRFD specifications, rather than the provisions that cover moment redistribution in the Standard specifications. The provisions in the LRFD specifications are much simpler to use and apply to a wider range of cases than those in the Standard specifications, based on research done in the mid-1990s (Barth et al. 2004). The following requirements are given in Section B6.2 of the LRFD specifications, and must be satisfied to allow for moment redistribution:

7. The bridge must be straight with supports not skewed more than 10° $\rightarrow$ OK
8. The specified minimum yield stress does not exceed 70 ksi $\rightarrow$ OK
9. Holes in the tension flange may not be present within a distance of twice the web depth from each interior pier section from which moments are redistributed $\rightarrow$ OK
10. The web proportions cannot violate the following requirements:

    $$\frac{D}{t_w} \leq 150 \rightarrow \frac{34.0\ in}{0.650\ in} \leq 150 \rightarrow 52.3 \leq 150 \rightarrow OK$$

    $$\frac{2D_c}{t_w} \leq 6.8\sqrt{\frac{E}{F_y}} \rightarrow \frac{2(17.0\ in)}{0.650\ in} \leq 6.8\sqrt{\frac{29000\ ksi}{33\ ksi}} \rightarrow 52.3 \leq 202 \rightarrow OK$$

    $$D_{cp} \leq 0.75D \rightarrow 17.0\ in \leq 0.75(34.0\ in) \rightarrow 17.0\ in \leq 25.5\ in \rightarrow OK$$

11. The compression flange proportions cannot violate the following requirements, the first of which ensures that the flange is compact:

    $$\frac{b_f}{2t_f} \leq 0.38\sqrt{\frac{E}{F_y}} \rightarrow \frac{12.0\ in}{2(1.02\ in)} \leq 0.38\sqrt{\frac{29000\ ksi}{33\ ksi}} \rightarrow 5.88 \leq 11.3 \rightarrow OK$$

    $$b_f \geq \frac{D}{4.25} \rightarrow 12.0\ in \geq \frac{34.0\ in}{4.25} \rightarrow 12.0\ in \geq 8\ in \rightarrow OK$$

    Note that the flange proportions here are checked without considering the contributions of the cover plates. Engineering judgement can be used to include any contribution from the cover plates, if desired.

12. The compression flange must be adequately braced to prevent lateral-torsional buckling and allow the section to achieve enough plastic rotation to adequately redistribute moments:

$$L_b \leq \left[0.1 - 0.06\left(\frac{M_1}{M_2}\right)\right]\frac{r_t E}{F_y}$$

The cover plate terminates within the unbraced length, so that two different sets of section properties are valid within the unbraced lengths in question. To be conservative, the section properties of the smaller section (Section #1) are used. The effective radius of gyration for lateral torsional buckling is defined in Appendix A6 of the LRFD specifications (Equation A6.3.3-10), and is calculated for Section #1 as:

$$r_t = \frac{b_f}{\sqrt{12\left(1 + \frac{1}{3}\frac{D_c t_w}{b_f t_f}\right)}} = \frac{12.0\ in}{\sqrt{12\left(1 + \frac{1}{3}\frac{(17.0\ in)(0.650\ in)}{(12.0\ in)(1.02\ in)}\right)}} = 3.04\ in$$

Because both the unbraced length and the brace point moments are different on either side of the interior pier, both must be checked at the Overload and Maximum Load limit states. However, because the load factors for the Maximum Load limit state are exactly 30% greater than those for the Overload limit state, the ratio of the factored brace moments (M_1 and M_2) will be the same for both limit states. Thus, only the Maximum Load limit state will be used here.

$$L_{b\ ext} \leq \left[0.1 - 0.06\left(\frac{1.3(121\ k.ft) + (2.17)(-324\ k.ft)}{1.3(-967\ k.ft) + (2.17)(-657\ k.ft)}\right)\right]\frac{(3.04\ in)(29000\ ksi)}{33\ ksi}$$
$$= (235\ in)\left(\frac{1\ ft}{12\ in}\right) = 19.5\ ft$$

$$L_{b\ int} \leq \left[0.1 - 0.06\left(\frac{1.3(108\ k.ft) + (2.17)(-261\ k.ft)}{1.3(-967\ k.ft) + (2.17)(-657\ k.ft)}\right)\right]\frac{(3.04\ in)(29000\ ksi)}{33\ ksi}$$
$$= (242\ in)\left(\frac{1\ ft}{12\ in}\right) = 20.1\ ft$$

In the above calculations, M_1 is the smaller of the brace point moments, while M_2 is the larger of the brace point moments. The ratio of M_1 to M_2 is taken as a positive value if the factored moments cause single curvature within the unbraced length, which is the case here.

The actual unbraced lengths exceed these calculated limiting values:

$L_{b\ ext} = 23.3\ ft > 19.5\ ft \ \rightarrow \ NOT\ OK$

$L_{b\ int} = 22.5\ ft > 20.1\ ft \ \rightarrow \ NOT\ OK$

Thus, the existing cross frames do not provide adequate lateral bracing to allow for moment redistribution. To redistribute moments in this girder, ***additional cross frames must be added on either side of the interior pier to reduce the unbraced length***. These cross frames must be located such that they reduce the unbraced length so that this requirement is satisfied.

In this design, the ***cross frames will be added at 10 feet from the interior pier in the exterior span and at 10.5 feet from the interior pier in the interior span***. These locations are chosen to match the existing cross frame locations on Girders C and D, which are different from those in Girders A and B because they were constructed at different times. Repeating the calculations for the limiting unbraced lengths using the new brace point moments, shown later in Table A.4, shows that the new unbraced lengths satisfy the lateral bracing requirements:

$L_{b\ ext} = 10.0\ ft < 15.1\ ft \ \rightarrow \ OK$

$L_{b\ int} = 10.5\ ft < 16.0\ ft \ \rightarrow \ OK$

13. There shall be no section transitions within the unbraced length of the interior pier section $\rightarrow \ NOT\ OK$

    Because the cover plates at the interior pier terminate within the adjacent unbraced lengths from the pier, this requirement is not satisfied. Although the exact reason for this requirement is unclear in the specification, it is likely there for a few reasons, which are discussed here.

    Firstly, if the section changes within the unbraced length, it is unclear which section properties should be used to check the lateral-torsional buckling capacity within that unbraced length. To be conservative, the properties of the smallest section within the unbraced length are used here (see number 6 on this list).

    Secondly, the moment redistribution provisions are based on the assumption that the critical section for negative flexure is at the centerline of the interior pier. If there is a section transition very near to the interior pier, that location could be the critical location for negative flexure instead. This means that the location of the section transition might reach its capacity first, and moments would be redistributed from that location instead of from the centerline of the interior pier. However, when evaluating the existing bridge, it was found that the load rating was in fact controlled by the section at the centerline of the interior pier, rather than at the ends of the cover plates, indicating that this will not be a concern for this bridge.

    Finally, and most importantly, the LRFD specifications eliminate the requirements to satisfy flexural stress checks at the Overload limit state within the entire negative moment region as well as flexural capacity checks at the Maximum Load limit state within the unbraced lengths adjacent to the interior

pier from which moments are redistributed (LRFD Sections B6.3.2.1 and B.6.4.1.1). Thus, if there is a transition to a smaller section within that unbraced length, it is possible that the reduced flexural strength of that section may be exceeded by the factored moments or stresses. However, a simple additional check that the flexural capacity at both the Overload and Maximum Load limit states exceeds the factored moment after redistribution at any section transitions within the unbraced length adjacent to the interior pier will eliminate this possibility. Note that for the Overload limit state, the stress limits should be abolished and the capacity should be taken as the same nominal moment capacity used in the check for at Maximum Load limit state.

Because of the conservative use of section properties in calculating the maximum unbraced length to prevent lateral-torsional buckling and the assessment that the controlling section in negative flexure will be the centerline of the interior pier, rather than at any nearby section transitions, this requirement that no section transitions occur within the unbraced lengths of the pier section is ignored. The reduced flexural capacity at each transition will be checked against the factored moments after redistribution to ensure that the section has adequate strength.

Note that alternatively, this requirement could be directly satisfied by placing the additional cross frames that are needed to reduce the unbraced length (see number 6 on this list) at the location of the section transition or at a location even closer to the interior pier.

14. The shear limit state must not be exceeded within the unbraced length adjacent to the interior pier regions. $\rightarrow \ OK$

    Although a check for shear is not shown here, the shear strength requirements are satisfied for this girder.

15. Bearing stiffeners must be present at the interior pier locations $\rightarrow \ NOT\ OK$

    Thus, bearing stiffeners must be added at the interior pier to allow for inelastic moment redistribution. It is recommended that these stiffeners are should be designed according to the provision in Article 6.10.11.2 of the LRFD specifications. These provisions require double-sided stiffeners that extend over the full depth of the web and as close to the outer edges of the flanges as is practical. Thus, choose a stiffener width of 5 inches and calculate the minimum thickness using the following equation from the LRFD specifications:

$$b_t \le 0.48 t_p \sqrt{\frac{E}{F_y}} \ \rightarrow \ t_p \ge \frac{b_t}{0.48}\sqrt{\frac{F_y}{E}} \ \rightarrow \ t_p \ge \frac{(5\ in)}{0.48}\sqrt{\frac{33\ ksi}{29000\ ksi}}$$

$$\rightarrow \ t_p \ge 0.35\ in$$

    Choose a thickness of 3/8 inches so that ***double-sided 5-inch by 3/8-inch bearing stiffeners should be installed at the interior pier sections of Girder B***. Strength considerations for the bearing stiffeners can be addressed by investigating the effects of the concentrated reaction force at the interior piers.

Equations for the strength of the stiffeners can also be found in Article 6.10.11.2 of the LRFD specifications.

By adding additional cross frames around the interior pier to satisfy number 6 in the preceding list and by adding bearing stiffeners at the interior pier section to satisfy number 9 on the preceding list, moment redistribution can be allowed for this girder. Following the provisions in Section B6.5 of the LRFD specifications, the effective plastic moment for the section is calculated, which accounts for the slenderness of the section to ensure an adequate amount of inelastic rotation capacity can be attained. This effective plastic moment differs for the Overload and Maximum Load limit states, which are referred to as the Service II and Strength I limit states, respectively, in the LRFD specifications. Sections that have "ultracompact" webs have been shown to exhibit enhanced moment-rotation characteristics and thus have a larger effective plastic moment. The section is classified as having an ultracompact web if:

$$\frac{2D_{cp}}{t_w} \le 2.3\sqrt{\frac{E}{F_y}} \rightarrow \frac{2(17.0\ in)}{0.650\ in} \le 2.3\sqrt{\frac{29000\ ksi}{33\ ksi}} \rightarrow 52.3 \le 68.2 \qquad \textit{LRFD Equation B6.5.1-1}$$

$$\rightarrow \quad web\ is\ ultracompact$$

The effective plastic moment at both the Overload and Maximum Load limit state is calculated as follows. Note that for the Overload limit state, the capacity is simply the nominal moment capacity of the section (M_n). Because the section has an ultracompact web, a compact flange (as determined in number 5 of the moment redistribution requirements), and additional lateral bracing will be added to satisfy the moment redistribution requirements, this nominal capacity is simply the plastic moment capacity (M_p) of the section. For the Maximum Load limit state, the capacity is equal to a calculated fraction of the nominal capacity:

$$M_{pe\ OL} = M_n = M_p = F_y Z_x = (33\ ksi)(927\ in^3)\left(\frac{1\ ft}{12\ in}\right) = 2550\ k.ft \qquad \textit{LRFD Equation B6.5.1-2}$$

$$M_{pe\ ML} = \left(2.78 - 2.3\frac{b_f}{t_f}\sqrt{\frac{F_y}{E}} - 0.35\frac{D}{b_f} + 0.39\frac{b_f}{t_f}\sqrt{\frac{F_y}{E}}\frac{D}{b_f}\right)M_n \le M_n \qquad \textit{LRFD Equation B6.5.1-3}$$

$$\rightarrow \quad \left(2.78 - 2.3\left(\frac{12.0\ in}{1.02\ in}\right)\sqrt{\frac{33\ ksi}{29000\ ksi}} - 0.35\left(\frac{34.0\ in}{12.0\ in}\right) + 0.39\left(\frac{12.0\ in}{1.02\ in}\right)\sqrt{\frac{33\ ksi}{29000\ ksi}}\left(\frac{34.0\ in}{12.0\ in}\right)\right)(2550\ k.ft)$$

$$= 3350\ k.ft > 2550\ k.ft \quad \rightarrow \quad 2550\ k.ft$$

In this case, the capacity at both the Overload and Maximum Load limit states considering moment redistribution is equal to the full plastic moment capacity of the section. This is common for girders comprised of rolled steel sections.

Once the effective plastic moment has been calculated, the redistribution moment at the interior pier is calculated for both limit states. The redistribution moment represents the portion of the factored moment that exceeds the effective plastic moment. Thus, the redistribution moment must be positive, as redistribution is only necessary when the factored moment is greater than the effective plastic moment. Note that only gravity loads are considered in this design, so no lateral forces are included in this calculation.

$$M_{rd\ OL} = |M_{u\ OL}| - M_{pe\ OL} = |-2060\ k.ft| - 2550\ k.ft$$
$$= -490\ k.ft \quad \rightarrow \quad 0\ k.ft$$

LRFD Equation B6.4.2.1-1

$$M_{rd\ ML} = |M_{u\ ML}| - M_{pe\ ML} = |-2680\ k.ft| - 2550\ k.ft$$
$$= 130\ k.ft$$

LRFD Equation B6.4.2.1-1

Although it was determined previously that moment redistribution is necessary at both the Overload and the Maximum Load limit states, the redistribution moment at Overload is calculated to be zero. This is because of the significant increase in the strength that is attributed to this section from the original capacity, defined as 80% of the moment at first yield, and the effective plastic moment, which in this case is the full plastic moment capacity. Thus, although moment redistribution needs to be considered at the Overload limit state, and all of the requirements from Section B6.2 of the LRFD specifications must be satisfied, no actual redistribution of moments is needed at the Overload limit state.

At the Maximum Load limit state, however, the effective plastic moment is only slightly larger than the capacity calculated prior to considering moment redistribution. In fact, with the addition of the extra cross frames required to satisfy the redistribution requirements, there would be no difference in the capacity prior to considering redistribution and the effective plastic moment, at least in this case. This is because the girder at 70' would be classified as a compact section and would have a capacity equal to the plastic moment of the steel section.

The calculated redistribution moment is limited to 20% of the factored moment, which is confirmed by the following check. The actual percentage of the factored elastic moment that is redistributed is also calculated here:

$$M_{rd\ ML} \leq 0.2|M_{u\ ML}| = 0.2|-2680\ k.ft| = 536\ k.ft$$
$$\rightarrow \quad 130\ k.ft < 536\ k.ft \quad \rightarrow \quad OK$$

LRFD Equation B6.4.2.1-3

$$\frac{M_{rd\ ML}}{|M_{u\ ML}|} = \frac{130\ k.ft}{2680\ k.ft} = 4.9\%$$

The redistribution moment diagram is constructed by first plotting the redistribution moments calculated at the interior piers, and then connecting them by straight lines, with zero moment at the end of the girder. Figure A.3 plots the redistribution moment diagram at the Maximum Load limit state, along with the same dead load and live load moments from Figure A.2. Table A.4 summarizes the value of the redistribution moment at each of the critical sections, along with the dead and live load moments at the critical sections from Table A.2. For the remainder of the design, the redistribution moments will be added to the dead and live load

moments for the Maximum Load limit state. Note that the redistribution moments always have a load factor of 1.0.

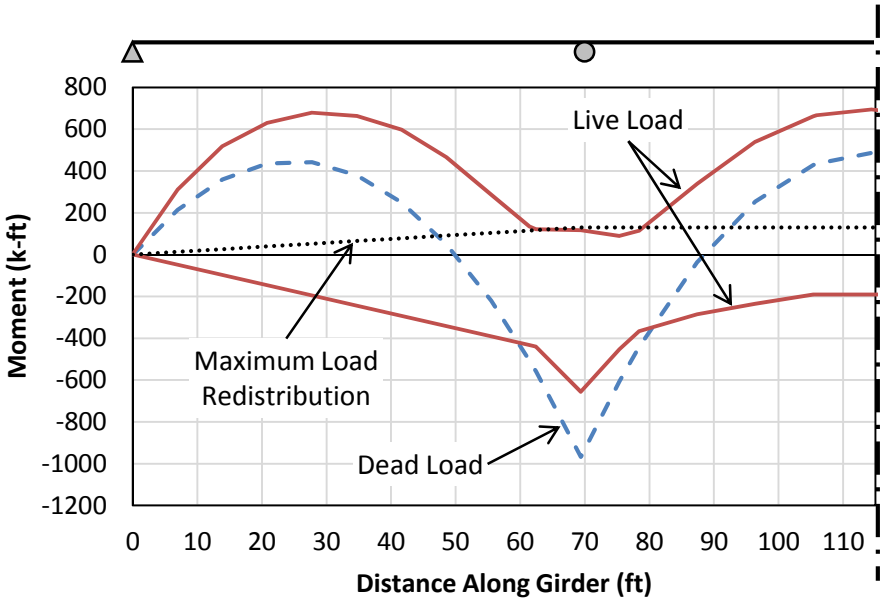

Figure A.3: Plot of Unfactored and Redistribution Moments for Girder B

Table A.4: Unfactored and Redistribution Moments at Critical Sections in Girder B

Location (ft)	Section Type	Section Number	Unfactored Moment (k-ft)			Redistribution Moment (k-ft)	
			Dead Load	Live Load			
				Pos.	Neg.	OL	ML
28	Critical, Span	1	442	679	-195	0	52
60	Lateral Brace	1	-405	188	-418	0	111
62	Critical, Trans.	1	-503	136	-432	0	115
70	Critical, Pier Lateral Brace	2	-967	116	-657	0	130
76	Critical, Trans.	1	-606	89	-452	0	130
80.5	Lateral Brace	1	-378	151	-354		130
106.5	Critical, Trans.	1	434	666	-191	0	130
115	Critical, Span	3	486	694	-191	0	130

Finally, check that the factored moment at the section transitions near the interior pier do not exceed the capacity after redistribution at the Maximum Load limit state. This is a necessary check in this case because the cover plates terminate within the unbraced length adjacent to the interior pier section from which moments are redistributed.

Critical Location at 62' (Section #1)

After the addition of a cross frame at 10 feet from the interior pier section in the exterior span, the unbraced length (L_b) for the compression (bottom) flange is now 10 feet, or 120 inches. The compression flange and web have already been shown to meet the compact limits. Thus, the steel section is classified as compact if:

$$\frac{L_b}{r_y} \leq \frac{\left[3.6 - 2.2\left(\frac{M_1}{M_p}\right)\right] x10^3}{F_y} \qquad \textit{Equation 10-96}$$

$$M_1 = (1.3)(-405\ k.ft) + (2.17)(-418\ k.ft) = -1430\ k.ft$$

$$M_p = -Z_{x\,70'}\, F_y = (927\ k.ft)(33\ ksi)\left(\frac{1\ ft}{12\ in}\right) = -2550\ k.ft$$

$$\rightarrow\ \frac{120\ in}{2.51\ in} \leq \frac{\left[3.6 - 2.2\left(\frac{-1430\ k.ft}{-2550\ k.ft}\right)\right] x10^3}{33\ ksi}\ \rightarrow\ 47.8 \leq 71.7\ \rightarrow\ LTB\ OK$$

Thus, the steel section is classified as compact and the Maximum Load capacity is:

$$C_{ML\,62'} = -Z_x\, F_y = -(624\ in^3)(33\ ksi)\left(\frac{1\ ft}{12\ in}\right) = -1720\ k.ft \qquad \textit{Section 10.48.1}$$

The factored moment at the Maximum Load limit state at this location is:

$$M_{u\,ML\,62'} = 1.3(-503\ k.ft) + 2.17(-432\ k.ft) + 1.0(111\ k.ft) = -1480\ k.ft \qquad \textit{Table 3.22.1A}$$

Because the capacity exceeds the factored moment at this section transition, the calculated 130 k-ft redistribution moment can be allowed.

Critical Location at 76' (Section #1)

After the addition of a cross frame at 10.5 feet from the interior pier section in the interior span, the unbraced length (L_b) for the compression (bottom) flange is now 10.5 feet, or 126 inches. The compression flange and web have already been shown to meet the compact limits. Thus, the steel section is classified as compact if:

$$\frac{L_b}{r_y} \leq \frac{\left[3.6 - 2.2\left(\frac{M_1}{M_p}\right)\right] x10^3}{F_y} \qquad \textit{Equation 10-96}$$

$$M_1 = (1.3)(-378\ k.ft) + (2.17)(-354\ k.ft) = -1260\ k.ft$$

$$M_p = -Z_{x\,70'}\, F_y = (927\ k.ft)(33\ ksi)\left(\frac{1\ ft}{12\ in}\right) = -2550\ k.ft$$

$$\rightarrow \ \frac{126\ in}{2.51\ in} \leq \frac{\left[3.6 - 2.2\left(\frac{-1260\ k.ft}{-2550\ k.ft}\right)\right] x10^3}{33\ ksi} \ \rightarrow \ 50.2 \leq 76.1 \ \rightarrow \ LTB\ OK$$

Thus, the steel section is classified as compact and the Maximum Load capacity is:

$$C_{ML\,76'} = -Z_x\,F_y = -(624\ in^3)(33\ ksi)\left(\frac{1\ ft}{12\ in}\right) = -1720\ k.ft \qquad \textit{Section 10.48.1}$$

The factored moment at the Maximum Load limit state at this location is:

$$M_{u\,ML\,76'} = 1.3(-606\ k.ft) + 2.17(-452\ k.ft) + 1.0(130\ k.ft) = -1638\ k.ft \qquad \textit{Table 3.22.1A}$$

Because the capacity exceeds the factored moment at this section transition, the calculated 130 k-ft redistribution moment can be allowed.

Design Connectors for Positive Moment Regions

Now that the redistribution moments are known, the partially composite positive moment regions are designed and checked at both the Overload and Maximum Load limit states. For this girder, a different design needs to be conducted for the exterior span, which has a critical section at 28', and for the middle span, which has a critical section at 115'. The design for the interior span also needs to be checked at the transition location at the termination of the cover plate at 106.5'. The Overload limit state involves stress-based calculations on the non-composite, short term composite, and long term composite sections which can make for a complicated way to begin the design. Thus, it is recommended to begin the design with the Maximum Load limit state.

<u>Design for the Maximum Load Limit State – Exterior Spans</u>

The factored moment, including redistribution moments, for the critical section in the exterior spans (28') at the Maximum Load limit state is:

$$M_{u\,ML\,28'} = 1.3(442\ k.ft) + 2.17(679\ k.ft) + 1.0(52\ k.ft) = 2100\ k.ft$$

The capacity at the Maximum Load limit state is simply the nominal moment capacity of the section (M_n). This is usually equal to the plastic moment of the partially composite cross section, because the deck provides continuous lateral support for the top flange of the girder to prevent lateral torsional buckling, and little to none of the steel section is required to resist large compressive forces so local buckling tends not to control.

First, the fully composite section is analyzed to determine the number of connectors required for full-composite action as well as the strength and stiffness of the fully composite section, indicated by the subscript "FC". The number of connectors needed is simply the compression force in the deck (C_f) divided by the strength of a single connector (Q_n), which is calculated from the effective cross sectional area (A_{sc}) and the ultimate tensile strength ($F_{u\,sc}$) of the ASTM A193 B7 threaded rod comprising the connector (Kwon et al. 2007):

$$A_{sc} = 0.8\left(\frac{\pi\ {d_{sc}}^2}{4}\right) = 0.8\left(\frac{\pi\left(\frac{7}{8}in\right)^2}{4}\right) = 0.481\ in$$

$$Q_n = 0.5\ A_{sc}\ F_{u\,sc} = 0.5(0.481\ in^2)(125\ ksi) = 30.1\ kips$$

Simple plastic cross-sectional analysis, is used to determine the properties of the fully composite section:

$$C_{f\,FC} = min\begin{cases}0.85f_c'A_{deck}\\ A_sF_y\end{cases} = min\begin{cases}0.85(3\ ksi)(595\ in^2)\\ (47.0\ in^2)(33\ ksi)\end{cases} = min\begin{cases}1520\ k\\ 1550\ k\end{cases}$$
$$= 1520\ k$$

$$N_{FC} = \frac{C_{f\,FC}}{Q_n} = \frac{1520\ k}{30.1\ k} = 50.5$$

Generally, the number of connectors in a design should be rounded up to the next even number, as they are installed in pairs. However, since the final design is unlikely to be fully composite, the number of connectors required for a fully composite girder can remain as a decimal for now. Also, because the first term in the equation for C_f is the smallest, the plastic neutral axis will be either in the top flange or top portion of the web of the steel beam. If the plastic neutral axis is in the web of the steel beam, the net plastic force in the top and bottom flanges will cancel out, since the section is doubly symmetric. Thus, the plastic neutral axis can only be in the web of the steel beam if the maximum plastic force that can be developed in the web ($P_{y\,web}$) is greater than the compressive force in the slab (C_f). Otherwise, the plastic neutral axis is located in the top flange of the steel beam, as is the case here, indicated by the following calculations:

$$P_{y\,web} = A_{web}\ F_y = \left(A_s - 2A_f\right)F_y = (47.0\ in^2 - 2(12.2\ in)^2)(33\ ksi)$$
$$= 743\ k$$

$$743\ k < 1520\ k \quad \rightarrow \quad P_{y\,web} < C_{f\,FC}$$
$$\rightarrow \quad Plastic\ neutral\ axis\ is\ in\ the\ top\ flange$$

The stress distribution at the plastic moment capacity is shown in Figure A.4. Force resultants, which act at mid-height of the corresponding stress block, are indicated by filled arrowheads and bold labels. For simplicity, an equivalent stress distribution, shown in the far right portion of the figure, will be used for the calculations. In this equivalent stress distribution, the entirety of the steel beam is shown under tensile yield stress, while the portion of the top flange above the plastic neutral axis is subjected to twice the yield stress in compression. Using the equivalent stress distribution helps to simplify the calculations while keeping the same net stresses on the section. The unknown distance "y" represents the depth of the top flange that is in compression and can be solved for by summing forces on the cross-section. The plastic moment capacity (M_p) is then calculated by summing moments on the section. Since there is no net axial force on the section, moments can be summed about any point. Here, the steel-concrete interface is chosen, and counterclockwise moments are taken as positive:

$$T_s = A_s F_y = (47\ in^2)(33\ ksi) = 1550\ k$$

$$C_s = b_f\ y\ F_y = (12.0\ in)(y)(33\ ksi) = \left(396\frac{k}{in}\right)(y)$$

$$\Sigma F = 0 \quad \rightarrow \quad T_s - C_s - C_{f\,FC} = 0 \quad \rightarrow \quad (1550\ k) - \left(396\frac{k}{in}\right)(y) - (1520k) = 0 \quad \rightarrow \quad y = 0.0758\ in$$

$$M_{p\,FC} = \Sigma M_{interface} = T_s\left(\frac{d}{2}\right) - C_s\left(\frac{y}{2}\right) + C_{f\,FC}\left(\frac{t_{deck}}{2}\right)$$
$$= (1550\ k)\left(\frac{36.0\ in}{2}\right) - \left(396\frac{k}{in}\right)(0.0758\ in)\left(\frac{0.0758\ in}{2}\right)$$
$$+ (1520\ k)\left(\frac{6.5\ in}{2}\right) = (32800\ k.in)\left(\frac{1\ ft}{12\ in}\right) = 2740\ k.ft$$

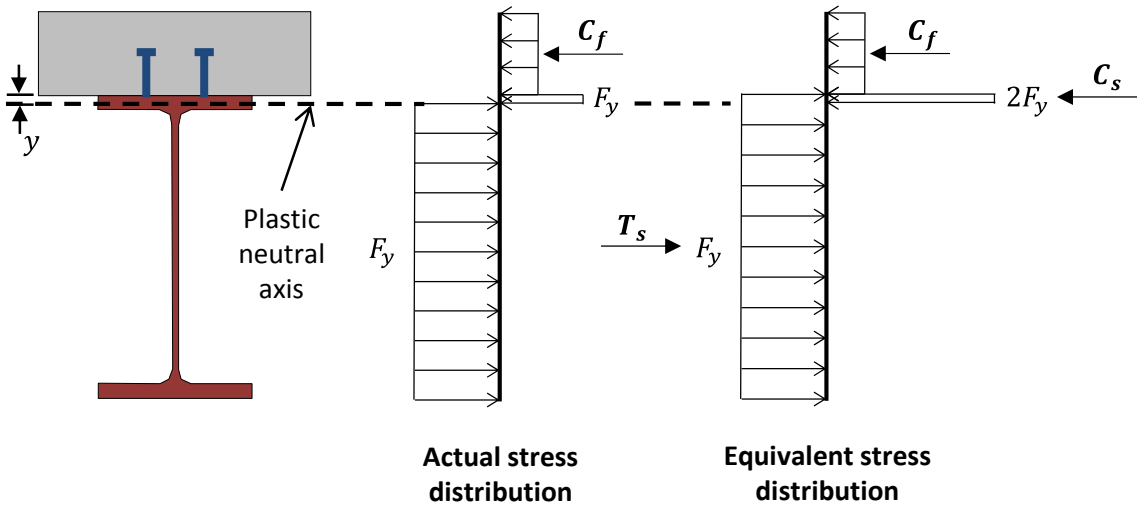

Figure A.4: Stress Distribution at Plastic Moment of Fully Composite Section – Exterior Span of Girder B

The transformed moment of inertia (I_{tr}) and elastic section modulus to the extreme bottom fiber of the steel beam (S_{tr}) of the fully composite section can also be calculated using basic concepts of mechanics of materials after locating the elastic neutral axis (at a distance of y_{NA} below the interface). Two sets of calculations follow, one of which corresponds to the short-term composite section and the other of which corresponds to the long-term composite section. The short-term composite section properties, indicated by the subscript "*ST*", are calculated using the short-term modular ratio of n while the long-term composite section properties, indicated by the subscript "*LT*", are calculated using the long-term modular ratio of $3n$:

Short-term section:

$$n = \frac{E_s}{E_c} = \frac{29000\ ksi}{3122\ ksi} = 9.3$$

$$y_{NA\ ST} = \frac{A_s\left(\frac{d}{2}\right) - \frac{A_{deck}}{n}\left(\frac{t_{deck}}{2}\right)}{A_s + \frac{A_{deck}}{n}} = \frac{(47.0\ in^2)\left(\frac{36.0\ in}{2}\right) - \frac{(595\ in^2)}{9.3}\left(\frac{6.5\ in}{2}\right)}{(47.0\ in) + \frac{(595\ in^2)}{9.3}}$$
$$= 5.75\ in$$

$$I_{tr\ ST} = I_s + A_s\left(\frac{d}{2} - y_{NA}\right)^2 + \frac{I_{deck}}{n} + \frac{A_{deck}}{n}\left(\frac{t_{deck}}{2} + y_{NA}\right)^2$$
$$= 9760\ in^4 + (47.0\ in^2)\left(\frac{36.0\ in}{2} - 5.75\ in\right)^2 + \frac{(2090\ in^4)}{9.3}$$
$$+ \frac{(595\ in^2)}{9.3}\left(\frac{6.5\ in}{2} + 5.75\ in\right)^2 = 22200\ in^4$$

$$S_{tr\ ST} = \frac{I_{tr\ ST}}{d - y_{NA}} = \frac{22200\ in^4}{(36.0\ in) - (5.75\ in)} = 734\ in^3$$

Long-term section:

$$3n = 3(9.3) = 27.9$$

$$y_{NA\ LT} = \frac{A_s\left(\frac{d}{2}\right) - \frac{A_{deck}}{3n}\left(\frac{t_{deck}}{2}\right)}{A_s + \frac{A_{deck}}{3n}} = \frac{(47.0\ in^2)\left(\frac{36.0\ in}{2}\right) - \frac{(595\ in^2)}{27.9}\left(\frac{6.5\ in}{2}\right)}{(47.0\ in) + \frac{(595\ in^2)}{27.9}}$$
$$= 11.4\ in$$

$$I_{tr\ LT} = I_s + A_s\left(\frac{d}{2} - y_{NA}\right)^2 + \frac{I_{deck}}{3n} + \frac{A_{deck}}{3n}\left(\frac{t_{deck}}{2} + y_{NA}\right)^2$$
$$= 9760\ in^4 + (47.0\ in^2)\left(\frac{36.0\ in}{2} - 11.4\ in\right)^2 + \frac{(2090\ in^4)}{27.9}$$
$$+ \frac{(595\ in^2)}{27.9}\left(\frac{6.5\ in}{2} + 11.4\ in\right)^2 = 16500\ in^4$$

$$S_{tr\ LT} = \frac{I_{tr\ LT}}{d - y_{NA}} = \frac{16500\ in^4}{(36.0\ in) - (11.4\ in)} = 671\ in^3$$

Now that the analysis of the fully composite section is complete, the iterative process of designing the partially composite section can be done. Since the plastic strength of the fully

composite section (2740 k-ft) is greater than the factored moments at the Maximum Load limit state (2130 k-ft), the girder can be strengthened using partial-composite design. To begin, choose an approximate composite ratio, and calculate the number of connectors required and the strength of the partially composite section, indicated by a subscript "PC". Recall that because the connectors are installed in pairs, the number of connectors should be rounded up to the nearest even number. The strength calculations are conducted in the exact same manner as for the fully composite section, except the interface shear (C_f) will now be controlled by the strength of the partially composite shear connection. This means that the plastic neutral axis will always be located in the steel beam.

A composite ratio (η) of approximately 30% will be chosen to start. This value represents the minimum recommended for design. The stress distribution for this partially composite case is shown in Figure A.5. Because the plastic neutral axis is now located in the web, a different equivalent stress distribution is used to simplify the calculations. In this case, the top half of the steel is shown under the yield stress in compression, while the bottom half of the steel is subjected to the yield stress in tension. This stress distribution creates two equal force resultants that form a force couple with the same magnitude as the plastic moment of the steel section ($M_{p\ steel}$). The portion of the steel above mid-depth of the beam and below the plastic neutral axis is also under a tensile stress of twice the yield stress. The unknown distance z represents the height of the web above mid-depth of the steel section but below the plastic neutral axis. Since the interface shear ($C_{f\ PC}$) is no longer controlled by the plastic force in the deck, only the top portion of the deck is assumed to be under compressive stress. The depth of the concrete compression block is denoted as a.

$$N = \eta\, N_{FC} = (0.3)(50.5) = 15.15 \;\rightarrow\; N = 16 = 8\ pairs$$

$$\eta_{actual} = \frac{N}{N_{FC}} = \frac{16}{50.5} = 0.317$$

$$C_{f\ PC} = min\begin{Bmatrix} 0.85 f_c' A_{deck} \\ A_s F_y \\ N\ Q_n \end{Bmatrix} = min\begin{Bmatrix} 0.85(3\ ksi)(595\ in^2) \\ (47.0\ in^2)(33\ ksi) \\ (16)(30.1\ k) \end{Bmatrix} = min\begin{Bmatrix} 1520\ k \\ 1550\ k \\ 482\ k \end{Bmatrix}$$
$$= 482\ k$$

$$743\ k > 482\ k \;\rightarrow\; P_{y\ web} > C_f \;\rightarrow\; Plastic\ neutral\ axis\ is\ in\ the\ web$$

$$a = \frac{C_{f\ PC}}{0.85 f_c' b_{eff}} = \frac{482\ k}{0.85(3\ ksi)(91.5\ in)} = 2.07\ in$$

$$T_s = z t_w \left(2F_y\right) = (z)(0.650\ in)\left(2(33\ ksi)\right) = \left(42.9 \frac{k}{in}\right)(z)$$

$$M_{p\ steel} = Z_x F_y = (624\ in^3)(33\ ksi) = 20600\ k.in$$

$$\Sigma F = 0 \;\rightarrow\; T_s - C_{f\,PC} = 0 \;\rightarrow\; \left(42.9\frac{k}{in}\right)(z) - 482\,k = 0 \;\rightarrow\; z = 11.2\,in$$

$$M_{p\,PC} = \Sigma M_{interface} = T_s\left(\frac{d}{2} - \frac{z}{2}\right) + C_{f\,PC}\left(t_{deck} - \frac{a}{2}\right) + M_{p\,steel}$$
$$= \left(\left(42.9\frac{k}{in}\right)(11.2\,in)\right)\left(\frac{(36.0\,in)}{2} - \frac{(11.2\,in)}{2}\right)$$
$$+ (482\,k)\left(6.5\,in - \frac{2.07\,in}{2}\right) + 20600\,k.in$$
$$= (29200\,k.in)\left(\frac{1\,ft}{12\,in}\right) = 2430\,k.ft$$

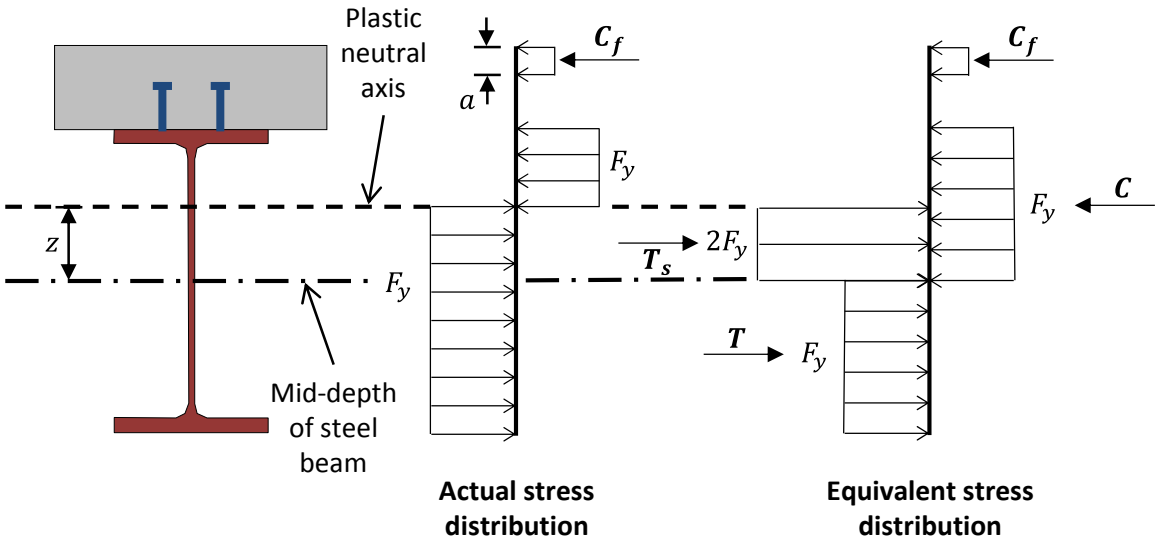

Figure A.5: Stress Distribution at Plastic Moment of Partially Composite Section – Exterior Span of Girder B

The plastic moment capacity of the approximately 30% partially composite section (2430 k-ft) exceeds the maximum factored moment at the Maximum Load limit state in the exterior spans (2100 k-ft). Because 30% is the minimum recommended composite ratio, choose $N = 16$ for the exterior spans to satisfy the requirements of the Maximum Load limit state.

Check the Design at the Overload Limit State – Exterior Spans

Next, check the Overload limit state with $N = 16$ in the exterior spans. This requires the computation of steel stresses due to bending moments and requires the use of different values of the section modulus for the different load types. For bridges strengthened with post-installed shear connectors, all dead load present prior to the installation of the connectors is applied to the non-composite section. Any dead load applied after the connectors are installed, such as an overlay of the driving surface, is applied to the long-term composite section, along with any redistribution moments at the Overload limit state, of which there are none in this case. The live load is applied

to the short-term composite section. The short- and long-term effective elastic moduli of the partially composite section (S_{eff}) are calculated by interpolation between the properties of the noncomposite steel beam and the properties of the transformed fully composite section (AISC 2010). Note that because there are no redistribution moments at the Overload limit state, the long-term effective elastic section modulus will not be used in any calculations, but is shown here as an example:

$$S_{eff\ ST} = S_x + \sqrt{\eta_{actual}}(S_{tr\ ST} - S_x)$$
$$= (542\ in^3) + \sqrt{0.317}\big((734\ in^3) - (542\ in^3)\big) = 650\ in^3$$

$$S_{eff\ LT} = S_x + \sqrt{\eta_{actual}}(S_{tr\ LT} - S_x)$$
$$= (542\ in^3) + \sqrt{0.317}\big((671\ in^3) - (542\ in^3)\big) = 615\ in^3$$

The following factored stress is calculated at the Overload limit state in positive bending at the critical section at 28':

$$\sigma_{u\ OL} = 1.0\left(\frac{442\ k.ft}{542\ in^3}\right)\left(\frac{12\ in}{1\ ft}\right) + (1.67)\left(\frac{679\ k.ft}{650\ in^3}\right)\left(\frac{12\ in}{1\ ft}\right) = 30.7\ ksi$$

For a composite section, the extreme stress in the steel beam is limited to 95% of the yield stress at the Overload limit state. Note that this requirement applies to only fully composite sections in the LRFD specifications, which do not currently allow for partial-composite design. The difference in stress limits between noncomposite (80%) and fully composite (95%) sections is primarily due to the vast difference in the ratio of maximum moment capacity (M_n) to yield moment (M_y) for the two types of sections. Because even with low composite ratios, partially composite sections have maximum moment-to-yield moment ratios much closer to fully composite sections than to non-composite sections, the 95% stress limit is recommended for use with partially composite strengthened girders. Thus, the capacity, or maximum allowed stress ($\sigma_{mx\ OL}$), at the Overload limit state is calculated as:

$$\sigma_{max\ OL} = 0.95F_y = 0.95(33\ ksi) = 31.4\ ksi$$

This maximum allowed stress (31.4 ksi) exceeds the stress from the factored loads, indicating that the requirements of the Overload limit state are satisfied by $N = 16$.

Thus, to satisfy the requirements of both the Overload and Maximum Load limit states, ***use $N = 16$ in the exterior spans on Girder B***. Note that *N* is the number of shear connectors required between points of zero and maximum moment. Thus, each of the exterior spans spans will contain two sets of 16 connectors.

Design for the Maximum Load and Overload Limit States – Interior Span

The same procedure is followed for the design of the connectors in the interior span. Table A.5 summarizes the results of the calculations for the critical section in the interior span (115') and for the location of cover plate termination in the interior span (106.5') at the Maximum Load limit state. Again, the minimum recommended composite ratio of 0.3 is used for the partially composite calculations.

Table A.5: Results from Partially Composite Design Calculations for the Interior Span of Girder B

	115'	**106.5'**
Section number	3	1
Factored Maximum Load moment ($M_{u\,ML}$, k-ft)	2310	2180
Deck force, fully composite ($C_{f\,FC}$, k)	1520	1520
Number of connectors, fully composite (N_{FC})	50.5	50.5
Plastic web force ($P_{y\,web}$, k)	743	743
Plastic neutral axis location, fully composite	Flange	Flange
Plastic moment, fully composite ($M_{p\,FC}$, k-ft)	3120	2740
Short term moment of inertia, fully composite ($I_{tr\,ST}$, in^4)	25400	22200
Short term section modulus, fully composite ($S_{tr\,ST}$, in^3)	839	734
Long term moment of inertia, fully composite ($I_{tr\,ST}$, in^4)	19000	16500
Long term section modulus, fully composite ($S_{tr\,ST}$, in^3)	765	671
Number of connectors, partially composite (N_{PC})	16	16
Actual composite ratio	0.317	0.317
Deck force, partially composite ($C_{f\,PC}$, k)	482	482
Plastic neutral axis location, partially composite	Web	Web
Plastic moment, partially composite ($M_{p\,PC}$, k-ft)	2780	2430
Short term section modulus, partially composite ($S_{eff\,ST}$, in^3)	1060	650
Long term section modulus, partially composite ($S_{eff\,LT}$, in^3)	866	615
Factored Overload stress ($\sigma_{u\,OL}$, ksi)	22.0	30.1
Maximum allowed Overload stress ($\sigma_{max\,OL}$, ksi)	31.4	31.4

The plastic moment capacity exceeds the factored moment at the Maximum Load limit state at both locations. The maximum allowed stress also exceeds the factored stress at the Overload limit state at both locations. Thus, the requirements for both limit states are satisfied with this design, so ***use $N = 16$ in the interior spans on Girder B***.

Locate Connectors and Check Fatigue

Before checking the fatigue behavior of the post-installed shear connectors, a connector layout must be chosen. Based on the recommendations made in Section 3.1.6, the layout in Figure A.6 is proposed. Because the girder is symmetric, only the left half is shown in the figure. Within a group, the connectors are spaced at 12 inches, which is equal to the transverse rebar spacing in the deck. The connector nearest to the end of the girder is located 6 inches away from the centerline of the support, while the connectors nearest to the interior support are located a distance equal to 15% of the span length from that support.

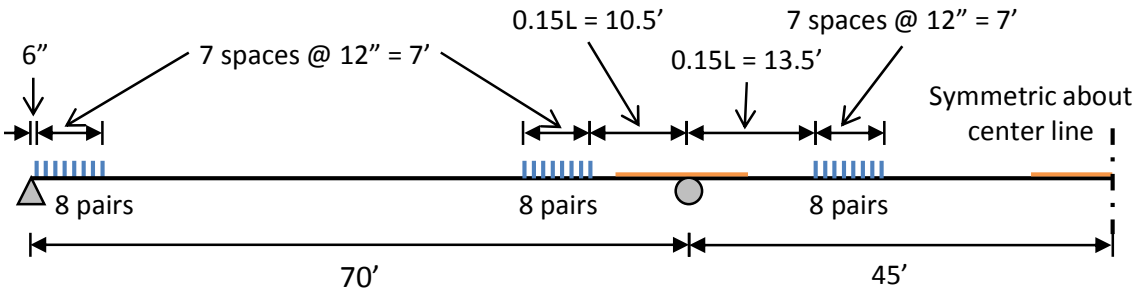

Figure A.6: Connector Layout for Girder B

In addition to the recommendations provided for locating the connectors, it is important to consider constructability and field conditions when choosing a connector layout, paying particular attention to the accessibility of the locations along the girder in which the connectors are to be installed. Because small changes in the connector layout will likely not significantly affect the behavior, some adjustments can be made in the field when necessary. It is highly recommended to use a rebar locator to find the transverse deck reinforcement in the locations where the connectors will be installed. Once the bars are located, modify the connector layout so that the connectors are installed approximately halfway between reinforcing bars and use a connector spacing equal to a multiple of the bar spacing. This should prevent conflicts with reinforcing bars when drilling into the deck to install the connectors.

The first step in checking the connectors for fatigue is to determine which load combination from the AASHTO LRFD specifications is to be used, by comparing the projected daily truck traffic in a single lane to the limiting value calculated from the provisions:

$$(ADTT)_{SL} = p\,(ADTT) = (0.8)\left(1160\frac{trucks}{day}\right) = 928\frac{trucks}{day} \qquad \textit{LRFD Equation 3.6.1.4.2-1}$$

$$(ADTT)_{SL\ limit} = \frac{8{,}700{,}000}{Y} = \frac{8{,}700{,}000}{25} = 348{,}000\frac{trucks}{day}$$

Because the projected truck traffic is below the limiting value, the Fatigue II load combination is used to design for finite life. The nominal fatigue resistance is calculated as follows:

$$\begin{aligned} N &= (365)(Y)(n)(ADTT)_{SL} \\ &= \left(365\frac{days}{year}\right)(25\ years)\left(1.0\frac{cycles}{truck}\right)\left(928\frac{trucks}{day}\right) \\ &= 8{,}470{,}000\ cycles \end{aligned}$$

$$(\Delta F)_n = \left(\frac{A}{N}\right)^{1/m} = \left(\frac{4.24\ x\ 10^{15}\ ksi^7}{8{,}470{,}000\ cycles}\right)^{1/7} = 17.5\ ksi$$

Figure A.7 shows the results from the fatigue analysis, conducted in a manner that explicitly considers the interface slip. This analysis was carried out using an Excel-based program

called UT-Slip, which was developed during the course of this research and models the connectors as linear springs (Ghiami Azad 2016). The recommended stiffness of 900 kips per inch was used for the spring representing each individual connector. The figure plots the stress range in each connector induced by the fatigue loading defined in the Fatigue II load combination in the LRFD specifications. Because of symmetry, only one-half of the girder is shown.

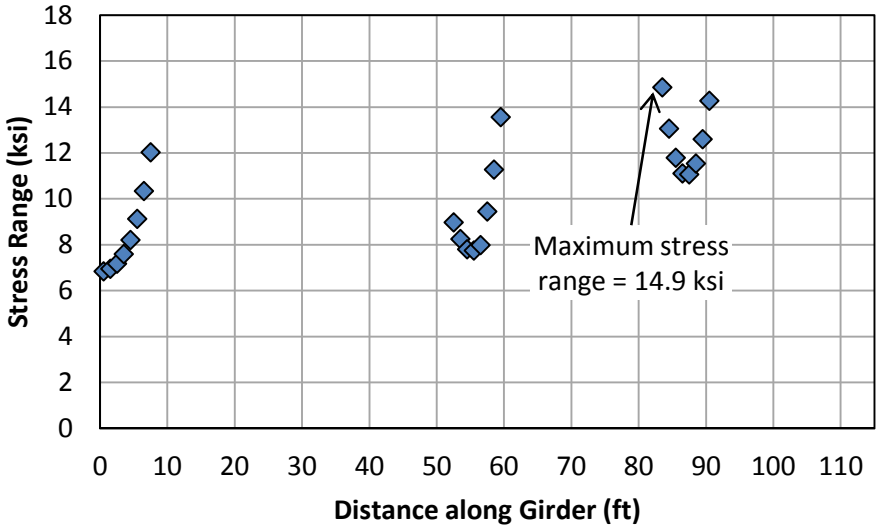

Figure A.7: Results from Fatigue Analysis for Girder B

The maximum stress range (ΔF) that a connector undergoes during fatigue loading is 14.9 ksi. As shown in the figure, this critical connector is the closest connector to the interior support in the interior span. This maximum stress range is less than the nominal fatigue resistance (17.5 ksi), indicating that ***the connectors have adequate fatigue life to satisfy the design requirement of a 25-year remaining life***.

The actual remaining life can be estimated by reversing the design equations to solve for the number of cycles and corresponding number of years that can be resisted at a given stress range. These calculations indicate that ***the connectors in Girder B are estimated to have a remaining fatigue life of 77 years***:

$$N_{actual} = \frac{A}{(\Delta F)^m} = \frac{4.24\ x\ 10^{15}\ ksi^7}{(14.9\ ksi)^7} = 26{,}000{,}000\ cycles$$

$$Y_{actual} = \frac{N_{actual}}{(365)(n)(ADTT)_{SL}} = \frac{26{,}000{,}000\ cycles}{\left(365\frac{days}{year}\right)\left(1.0\frac{cycles}{truck}\right)\left(928\frac{trucks}{day}\right)}$$

$$= 77\ years$$

Conduct Load Rating of Strengthened Girder

Following the strengthening a load rating of each of the critical sections can be done in the same manner as the initial evaluation of the existing non-composite structure. A slight

modification should be made to the equation to calculate the rating factor to include the redistribution moment at a section (RD):

$$RF = \frac{C - A_1\, DL - (1.0)RD}{A_2(LL + I)}$$

Modified MBE Equation 6B.4.1-1

Critical Location at 28' (Section #1, N = 16):

The Overload limit state must be addressed in terms of stresses now, because different types of loads are resisted by different sections. The capacity, or limiting stress, for the Overload limit state of a composite section was calculated previously as:

$$C_{OL\ 28'} = 31.4\ ksi$$

The dead load is resisted by the non-composite section, while the live load is resisted by the short-term partially composite section. If there were any redistribution moments at the Overload limit state, these would be resisted by the long-term partially composite section. Thus, the unfactored stresses for each of these load types are:

$$\sigma_{DL\ 28'} = \frac{M_{DL\ 28'}}{S_x} = \frac{442\ k.ft}{542\ in^3}\left(\frac{12\ in}{1\ ft}\right) = 9.79\ ksi$$

$$\sigma_{LL\ 28'} = \frac{M_{LL\ 28'}}{S_{eff\ ST}} = \frac{679\ k.ft}{650\ in^3}\left(\frac{12\ in}{1\ ft}\right) = 12.5\ ksi$$

The Maximum Load limit state is always evaluated in terms of moment. The unfactored moments are given in Table A.4, and the capacity is the plastic moment capacity of the partially composite section:

$$C_{ML\ 28'} = M_{p\ PC} = 2430\ k.ft$$

The rating factor and load rating for the Overload and Maximum Load limit states for this critical location are:

$$RF_{OL\ 28'} = \frac{31.4\ ksi - (1.0)(9.79\ ksi)}{(1.67)(12.5\ ksi)} = 1.03$$

$$RT_{OL\ 28'} = (1.03)(20) = 20.7 \quad \rightarrow \quad HS\ 20.7$$

$$RF_{ML\ 28'} = \frac{2430\ k.ft - (1.3)(442\ k.ft) - (1.0)(52\ k.ft)}{(2.17)(679\ k.ft)} = 1.22$$

$$RT_{ML\ 28'} = (1.22)(20) = 24.5 \quad \rightarrow \quad HS\ 24.5$$

Critical Location at 62' (Section #1):

Because moments are redistributed from the adjacent interior pier section, the Overload capacity is not subjected to the stress limits and is simply the nominal moment capacity of the section. Thus, the capacity for both the Overload and Maximum Load limit states are the same. This capacity was calculated in Section 0 after the addition of the new cross frames around the interior pier:

$$C_{OL\,62'} = C_{ML\,62'} = -1720\ k.ft$$

The unfactored moments are given in Table A.4. The rating factor and load rating for the Overload and Maximum Load limit states for this critical location are:

$$RF_{OL\,62'} = \frac{-1720\ k.ft - (1.0)(-503\ k.ft)}{(1.67)(-432\ k.ft)} = 1.69$$

$$RT_{OL\,62'} = (1.69)(20) = 33.7 \quad \rightarrow \quad HS\ 33.7$$

$$RF_{ML\,62'} = \frac{-1720\ k.ft - (1.3)(-503\ k.ft) - (1.0)(111\ k.ft)}{(2.17)(-432\ k.ft)} = 1.26$$

$$RT_{ML\,62'} = (1.26)(20) = 25.1 \quad \rightarrow \quad HS\ 25.1$$

Critical Location at 70' (Section #2):

Because moments are redistributed from this interior pier section, the Overload and Maximum Load capacities are the effective plastic moments calculated in Section 0:

$$C_{OL\,70'} = M_{pe\,OL} = -2550\ k.ft$$

$$C_{ML\,70'} = M_{pe\,ML} = -2550\ k.ft$$

The unfactored moments are given in Table A.4. The rating factor and load rating for the Overload and Maximum Load limit states for this critical location are:

$$RF_{OL\,70'} = \frac{-2550\ k.ft - (1.0)(-967\ k.ft)}{(1.67)(-657\ k.ft)} = 1.44$$

$$RT_{OL\,70'} = (1.44)(20) = 28.9 \quad \rightarrow \quad HS\ 28.9$$

$$RF_{ML\,70'} = \frac{-2550\ k.ft - (1.3)(-967\ k.ft) - (1.0)(130\ k.ft)}{(2.17)(-657\ k.ft)} = 1.00$$

$$RT_{ML\,70'} = (1.00)(20) = 20.0 \quad \rightarrow \quad HS\ 20.0$$

Critical Location at 76' (Section #1):

Because moments are redistributed from the adjacent interior pier section, the Overload capacity is not subjected to the stress limits and is simply the nominal moment capacity of the section. Thus, the capacity for both the Overload and Maximum Load limit states are the same. This capacity was calculated in Section 0 after the addition of the new cross frames around the interior pier:

$$C_{OL\,76'} = C_{ML\,76'} = -1720\ k.ft$$

The unfactored moments are given in Table A.4. The rating factor and load rating for the Overload and Maximum Load limit states for this critical location are:

$$RF_{OL\,76'} = \frac{-1720\ k.ft - (1.0)(-606\ k.ft)}{(1.67)(-452\ k.ft)} = 1.48$$

$$RT_{OL\,76'} = (1.48)(20) = 29.5 \quad \rightarrow \quad HS\ 29.5$$

$$RF_{ML\,76'} = \frac{-1720\ k.ft - (1.3)(-606\ k.ft) - (1.0)(130\ k.ft)}{(2.17)(-452\ k.ft)} = 1.08$$

$$RT_{ML\,76'} = (1.08)(20) = 21.7 \quad \rightarrow \quad HS\ 21.7$$

Critical Location at 106.5' (Section #1, N = 16):

The Overload limit state must be addressed in terms of stresses again, because different types of loads are resisted by different sections. The capacity, or limiting stress, for the Overload limit state of a composite section was calculated previously as:

$$C_{OL\,106.5'} = 31.4\ ksi$$

The unfactored dead and live load stresses are:

$$\sigma_{DL\,106.5'} = \frac{M_{DL\,106.5'}}{S_x} = \frac{434\ k.ft}{542\ in^3}\left(\frac{12\ in}{1\ ft}\right) = 9.61\ ksi$$

$$\sigma_{LL\,106.5'} = \frac{M_{LL\,106.5'}}{S_{eff\ ST}} = \frac{666\ k.ft}{650\ in^3}\left(\frac{12\ in}{1\ ft}\right) = 12.3\ ksi$$

The Maximum Load limit state is always evaluated in terms of moment. The unfactored moments are given in Table A.4, and the capacity is the plastic moment capacity of the partially composite section:

$$C_{ML\,106.5'} = M_{p\,PC} = 2430\ k.ft$$

The rating factor and load rating for the Overload and Maximum Load limit states for this critical location are:

$$RF_{OL\ 106.5'} = \frac{31.4\ ksi - (1.0)(9.61\ ksi)}{(1.67)(12.3\ ksi)} = 1.06$$

$$RT_{OL\ 106.5'} = (1.06)(20) = 21.2 \quad \rightarrow \quad HS\ 21.2$$

$$RF_{ML\ 106.5'} = \frac{2430\ k.ft - (1.3)(434\ k.ft) - (1.0)(130\ k.ft)}{(2.17)(666\ k.ft)} = 1.20$$

$$RT_{ML\ 106.5'} = (1.20)(20) = 24.0 \quad \rightarrow \quad HS\ 24.0$$

Critical Location at 115' (Section #3, N = 16):

The Overload limit state must be addressed in terms of stresses again, because different types of loads are resisted by different sections. The capacity, or limiting stress, for the Overload limit state of a composite section was calculated previously as:

$$C_{OL\ 115'} = 31.4\ ksi$$

The unfactored dead and live load stresses are:

$$\sigma_{DL\ 115'} = \frac{M_{DL\ 115'}}{S_x} = \frac{486\ k.ft}{653\ in^3}\left(\frac{12\ in}{1\ ft}\right) = 8.93\ ksi$$

$$\sigma_{LL\ 115'} = \frac{M_{LL\ 115'}}{S_{eff\ ST}} = \frac{694\ k.ft}{757\ in^3}\left(\frac{12\ in}{1\ ft}\right) = 11.0\ ksi$$

The Maximum Load limit state is always evaluated in terms of moment. The unfactored moments are given in Table A.4, and the capacity is the plastic moment capacity of the partially composite section:

$$C_{ML\ 115'} = M_{p\ PC} = 2780\ k.ft$$

The rating factor and load rating for the Overload and Maximum Load limit states for this critical location are:

$$RF_{OL\ 115'} = \frac{31.4\ ksi - (1.0)(8.93\ ksi)}{(1.67)(11.0\ ksi)} = 1.22$$

$$RT_{OL\ 115'} = (1.22)(20) = 24.5 \quad \rightarrow \quad HS\ 24.5$$

$$RF_{ML\ 115'} = \frac{2780\ k.ft - (1.3)(486\ k.ft) - (1.0)(130\ k.ft)}{(2.17)(694\ k.ft)} = 1.34$$

$$RT_{ML\ 115'} = (1.34)(20) = 26.8 \quad \rightarrow \quad HS\ 26.8$$

The results of this load rating for the strengthened girder are summarized in Table A.6. After post-installing the shear connectors and considering moment redistribution, the ***inventory load factor rating of Girder B is increased from HS 13.3 to HS 20.0***. This load rating is controlled by the section at the interior piers at the Maximum Load limit state.

Table A.6: Load Rating Results of Strengthened Girder B

Location (ft)	Section Type	Inventory Load Factor Rating	
		Overload	Maximum Load
28	Critical, Span	HS 20.7	HS 24.5
62	Critical, Transition	HS 33.7	HS 25.1
70	Critical, Pier	HS 28.9	HS 20.0
76	Critical, Transition	HS 29.5	HS 21.7
106.5	Critical, Transition	HS 21.2	HS 24.0
115	Critical, Span	HS 24.5	HS 26.8

Summary of Strengthening Design for Girder B

To strengthen Girder B to a minimum inventory load factor rating of HS 20, a total of 96 adhesive anchor shear connectors should be post-installed and approximately 5% of the factored moment at the interior piers must be redistributed at the Maximum Load limit state. In order to allow for moment redistribution, double-sided 5-inch by 3/8-inch bearing stiffeners need to be installed at the interior piers. Additionally, new cross frames must be installed to reduce the unbraced length at the interior piers to satisfy the requirements of Appendix B6 of the LRFD specifications. These cross frames should be placed 10 feet into the exterior span and 10.5 feet into the interior span, measured from the interior pier.

The connectors are installed in pairs on opposite sides of the web of the steel beam in a cross section, as illustrated in Figure A.8. The transverse spacing of 6 inches was determined by approximately centering the connectors on the protruding portion of the flange. The connectors are grouped in six locations, with one group located near each end of the positive moment regions in all three spans. The specific connector layout is shown in Figure . This layout can be modified slightly due to constraints in the field during installation, such as transverse deck reinforcing bars or other obstacles.

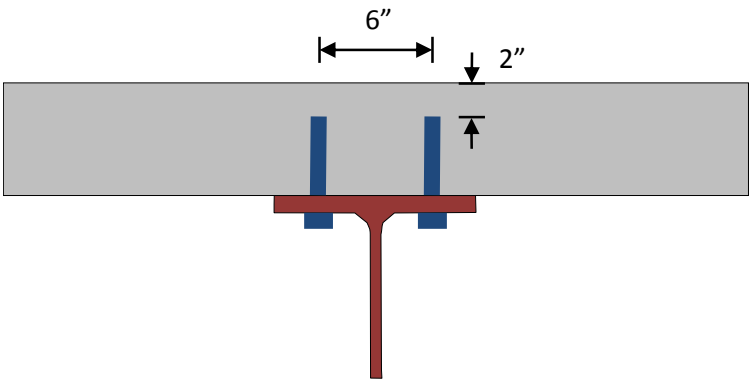

Figure A.8: Cross Sectional Connector Layout

Summary of Design Process and Results for Girder A

Girder A is identical to Girder B, so refer to the half-elevation view shown in Figure A.1 and the section properties in Table A.1.

Conduct Structural Analysis

The distribution factor for Girder A is calculated using the lever rule, assuming that the deck acts as a simple span between the girders (Section 3.23.2.3.1.2). This calculation is illustrated in Figure A.9. The wheels of the design truck are spaced 6 feet apart in the transverse direction, and the centerline of the wheel cannot be closer than 2 feet from the curb. The distribution factor for Girder A is thus calculated to be 0.607. Figure A.10 and Table A.7 summarize the results of the structural analysis for Girder A.

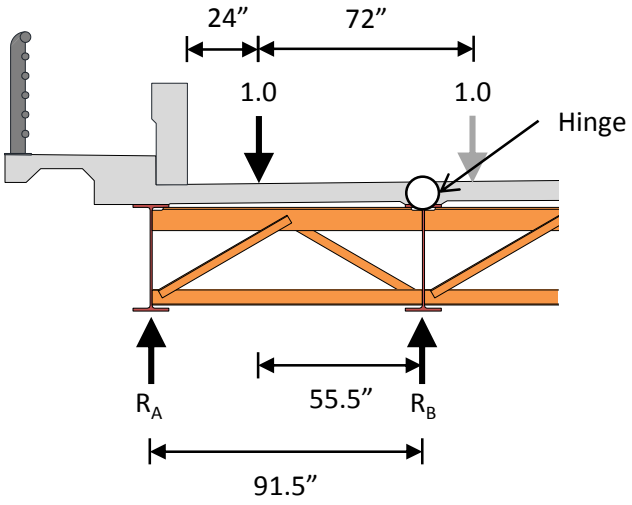

$$\Sigma M_{hinge} = 0 = R_A(91.5\ in) - (1.0)(55.5\ in)$$

$$\rightarrow \quad R_A = DF = 0.607$$

Figure A.9: Lever Rule for Distribution Factor Calculation for Girder A

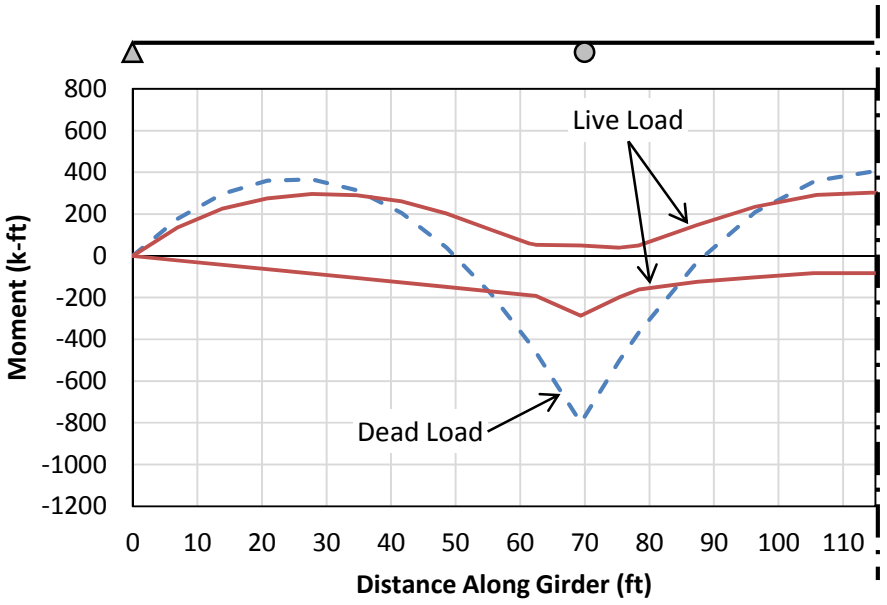

Figure A.10: Plot of Unfactored Moments for Girder A

Table A.7: Unfactored Moments at Critical Sections and at Lateral Brace Locations around the Interior Pier Section in Girder B

Location (ft)	Section Type	Section Number	Unfactored Moment (k-ft)		
			Dead Load	Live Load	
				Pos.	Neg.
28	Critical, Span	1	366	297	-85.4
46.7	Lateral Brace	1	100	225	-142
62	Critical, Transition	1	-416	59.3	-189
70	Critical, Pier and Lateral Brace	2	-800	50.8	-287
76	Critical, Transition	1	-501	29	-198
92.5	Lateral Brace	1	89.5	192	-114
106.5	Critical, Transition	1	359	291	-83.4
115	Critical, Span	3	402	303	-83.4

Evaluate Existing Non-composite Girder

All of the capacity calculations are for Girder A are identical to those for Girder B. The results of the load rating for Girder A are summarized in Table A.8. The controlling load rating is HS 33.2, which occurs at the Overload limit state at the critical section at the maximum positive moment in the exterior span (28'). All of the load ratings are greater than the target value of HS 20, so no strengthening is necessary for this girder. This is because it is subjected to very little

traffic load in comparison to the other girders. Although the check is not shown here, the girder is also adequate for the combination of sidewalk and traffic loading in the Standard specifications.

Table A.8: Load Rating Results of Existing Non-Composite Girder A

Location (ft)	Section Type	Capacity (k-ft)		Inventory Load Rating	
		Overload	Maximum Load	Overload	Maximum Load
28	Critical, Span	1190	1720	HS 33.2	HS 38.1
62	Critical, Transition	-1190	-1490	HS 49.0	HS 45.7
70	Critical, Pier	-1800	-2250	HS 41.7	HS 38.3
76	Critical, Transition	-1190	-1490	HS 41.7	HS 38.5
106.5	Critical, Transition	1190	1720	HS 34.2	HS 39.2
115	Critical, Span	1440	2050	HS 41.0	HS 45.8

Summary of Strengthening Design for Girder A

The existing non-composite Girder A has an inventory load factor rating of HS 33.2. Thus, no strengthening is necessary for this girder.

Summary of Design Process and Results for Girder C

A half-elevation view of Girder C is shown in Figure A.11. This girder was built as part of the original bridge in 1943. It is constructed of a 36WF150 rolled steel shape, with riveted splices and cover plates riveted to the top and bottom flange at the interior pier and in the middle of the interior span. Table A.9 summarizes the section properties for design for the steel beam (Section 1), as well as for the steel beam with cover plates at the interior pier (Sections 2 and 3) and in the interior span (Section 3). Note that because this girder sits on the boundary between the original and widened portions of the bridge, the deck thickness and girder spacing are different on either side of the girder. Thus, average values of the deck properties are used here. Additionally, the lateral bracing is more closely spaced than in the other girders because the cross frame locations are different on either side of Girder C.

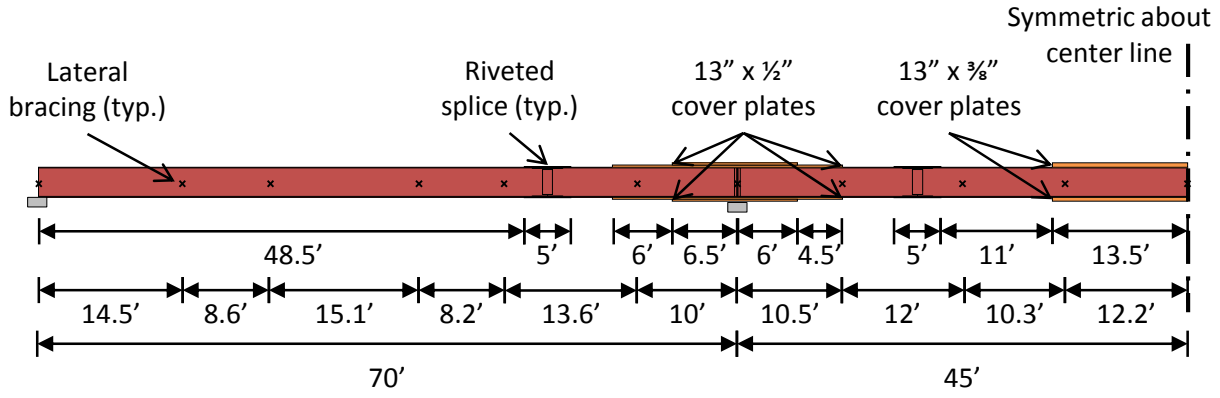

Figure A.11: Half-Elevation View of Girder C

Table A.9: Section Properties for Girder C

	Section 1	Section 2	Section 3	Section 4
Cover plate width (b_{pl}, in)	0	13.0	13.0	13.0
Cover plate thickness (t_{pl}, in)	0	0.500	1.00	0.375
Flange width (b_f, in)	12.0	12.0	12.0	12.0
Flange thickness (t_f, in)	0.940	0.940	0.940	0.940
Flange area (A_f, in^2)	11.3	17.8	24.3	16.2
Flange moment of inertia (I_{yc}, in^4)	135	227	318	204
Total depth (d, in)	35.9	36.9	37.9	36.7
Web thickness (t_w, in)	0.625	0.625	0.625	0.625
Area (A_s, in^2)	44.3	57.3	70.3	54.1
Moment of inertia (I_x, in^4)	9040	13300	17900	12200
Elastic section modulus (S_x, in^3)	504	723	944	668
Plastic section modulus (Z_x, in^3)	581	818	1060	758
Radius of gyration (r_y, in)	2.47	2.81	3.01	2.75
Polar moment of inertia (J, in^4)	10.1	11.2	18.8	10.6
Web depth (D, in)	34.0	34.0	34.0	34.0
Depth of web in compression, elastic (D_c, in)	17.0	17.0	17.0	17.0
Depth of web in compression, plastic (D_{cp}, in)	17.0	17.0	17.0	17.0
Effective deck width (b_{deck}, in) and girder spacing (S, in)	92.8	92.8	92.8	92.8
Deck thickness (t_{deck}, in)	7.25	7.25	7.25	7.25
Deck area (A_{deck}, in^2)	673	673	673	673
Deck moment of inertia (I_{deck}, in^4)	2950	2950	2950	2950

Conduct Structural Analysis

The distribution factor for interior Girder C is calculated to be 1.41. Figure A.12 and Table A.10 summarize the results of the structural analysis for Girder C.

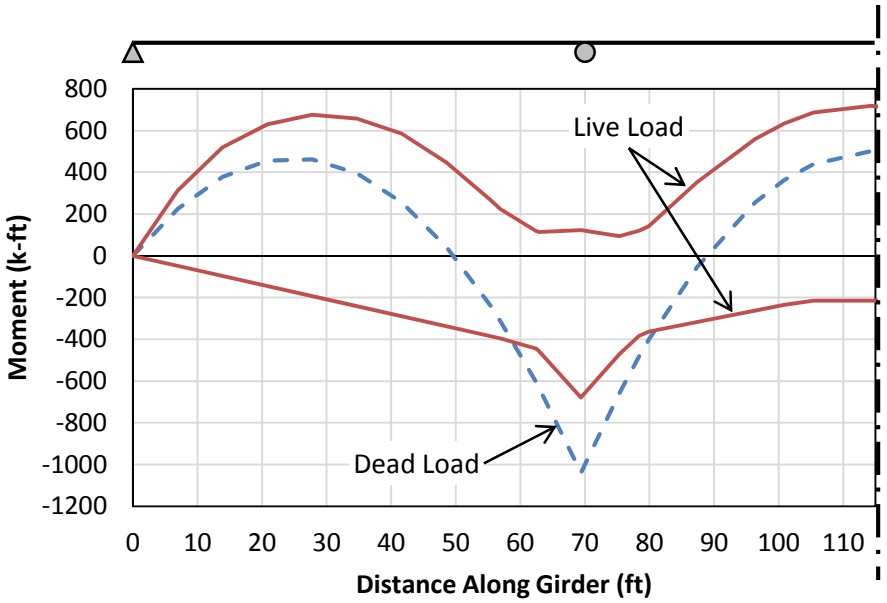

Figure A.12: Plot of Unfactored Moments for Girder C

Table A.10: Unfactored Moments at Critical Sections and at Lateral Brace Locations around the Interior Pier Section in Girder C

Location (ft)	Section Type	Section Number	Unfactored Moment (k-ft)		
			Dead Load	Live Load	
				Pos.	Neg.
28	Critical, Span	1	463	676	-193
38.2	Lateral Brace	1	338	628	-261
57.5	Critical, Transition	1	-311	225	-395
60	Lateral Brace	2	-438	179	-417
63.5	Critical, Transition	2	-630	114	-457
70	Critical, Pier	3	-1038	123	-679
76	Critical, Transition	2	-655	94.7	-470
80.5	Critical, Transition and Lateral Brace	1	-404	142	-363
101.5	Critical, Transition	1	363	635	-234
102.8	Lateral Brace	4	384	649	-229
115	Critical, Span	4	502	720	-215

Evaluate Existing Non-Composite Girder

All of the capacity calculations for Girder C are done in the same manner to those for Girder B. The results of these and of the load rating calculations for Girder C are summarized in Table A.11. The controlling load rating is HS 11.5, which occurs at the Overload limit state at the

critical section at the maximum positive moment in the exterior span (28'). In fact, this is the controlling load rating for all of the steel girders.

Table A.11: Load Rating Results of Existing Non-Composite Girder C

Location (ft)	Section Type	Capacity (k-ft)		Inventory Load Rating	
		Overload	Maximum Load	Overload	Maximum Load
28	Critical, Span	1110	1600	HS 11.5	HS 13.4
57.5	Critical, Transition	-1110	-1600	HS 24.2	HS 27.9
63.5	Critical, Transition	-1590	-2250	HS 25.2	HS 28.9
70	Critical, Pier	-2080	-2920	HS 18.4	HS 21.3
76	Critical, Transition	-1590	-2250	HS 23.8	HS 27.4
80.5	Critical, Transition	-1110	-1600	HS 23.3	HS 27.3
101.5	Critical, Transition	1110	1600	HS 14.1	HS 16.2
115	Critical, Span	1470	2080	HS 16.1	HS 18.0

Set Strengthening Targets

The same strengthening targets are used for Girder C as for Girder B. Thus, the goals of the strengthening design are to increase the inventory load factor rating to HS 20, and to provide a minimum remaining life of 25 years for the purposes of fatigue design of the post-installed shear connectors. The same average annual daily truck traffic ($(ADTT)_{SL}$) of 1160 trucks per day will be used.

Check Negative Moment Regions and Redistribute Moments

In a similar manner to Girder B, the capacity of the negative moment regions at the interior piers (70') of Girder C is evaluated and compared to the factored moments at the Overload and Maximum Load limit states to determine whether or not inelastic moment redistribution is needed. The factored moments are calculated from those given in Table A.10. Because these regions will remain non-composite, the capacities are the same as those in Table A.11. A summary of these values is given in Table A.12.

Table A.12: Necessity of Moment Redistribution for Girder C

Factored Overload moment ($M_{u\,OL}$, k-ft)	-2170
Factored Maximum Load moment ($M_{u\,ML}$, k-ft)	-2840
Overload capacity (C_{OL}, k-ft)	-2080
Maximum Load capacity (C_{ML}, k-ft)	-2920

The factored moment at the interior pier section exceeds the capacity only at the Overload limit state. This means that ***moment redistribution should be considered at the Overload limit***

state. As with the design of Girder B, the requirements from Appendix B6 of the LRFD specifications must be satisfied to allow for moment redistribution:

1. The bridge must be straight with supports not skewed more than 10° $\rightarrow$ OK
2. The specified minimum yield stress does not exceed 70 ksi $\rightarrow$ OK
3. Holes in the tension flange may not be present within a distance of twice the web depth from each interior pier section from which moments are redistributed $\rightarrow$ $NOT\ OK$

   Because this girder has riveted cover plates on the top and bottom flanges at the interior pier section, this requirement is not satisfied, although the holes are filled completely with rivets. Although there is little to no literature available about the inelastic moment-rotation behavior of wide flange steel beams with riveted cover plates, tests on riveted plate connections have not indicated any significant lack of ductility or otherwise poor behavior that would adversely impact the moment-rotation behavior. In this case, engineering judgement is used to eliminate this requirement, and allow for moment redistribution. Additionally, essentially no redistribution is actually necessary (as is calculated later), and the extent of inelastic behavior in this region is expected to be minimal.
4. Web proportion requirements $\rightarrow$ OK
5. Compression flange proportion requirements $\rightarrow$ OK
6. Compression flange bracing requirements

   As with Girder B, because one the cover plates terminates within the unbraced length, the properties of the smallest section (Section 2) are used to be conservative. The calculations result in:

   $L_{b\ ext} = 10.0\ ft < 15.3\ ft = L_{b\ limiting}$ $\rightarrow$ OK

   $L_{b\ int} = 10.5\ ft < 16.1\ ft = L_{b\ limiting}$ $\rightarrow$ OK

   Thus, the existing cross frames provide adequate lateral bracing to allow for moment redistribution.
7. There shall be no section transitions within the unbraced length of the interior pier section $\rightarrow$ $NOT\ OK$

   Because the cover plates at the interior pier terminate within the adjacent unbraced lengths from the pier, this requirement is actually not satisfied. However, for the same reasons discussed in the design for Girder B, namely that the section properties used in calculating the lateral-torsional buckling requirements and that the controlling section in negative flexure is the centerline of the interior pier, not the section transitions at the ends of the cover plates, this requirement is ignored. The reduced flexural capacity at each transition need to be checked against the factored moments after redistribution to ensure that the section has adequate strength.

Note that alternatively, this requirement could be directly satisfied by adding two cross frames and placing each at or closer to the interior pier than the ends of the cover plate.

8. The shear limit state must not be exceeded within the unbraced lengths adjacent to the interior pier regions. → OK

   Although a check for shear is not shown here, the shear strength requirements are satisfied for this girder.

9. Bearing stiffeners must be present at the interior pier locations → OK

   Riveted bearing stiffeners constructed of L-shapes are present at the interior support on this girder

By adding an additional cross frame at the interior pier to satisfy number 6 in the preceding list, moment redistribution can be allowed for this girder. Table A.13 summarizes the results of calculations for the redistribution moment, following the provisions in Section B6.5 of the LRFD specifications in a similar manner to the design of Girder B.

Table A.13: Results from Moment Redistribution Calculations for Girder C

Ultracompact web?	Yes
Effective plastic moment at Overload ($M_{pe\ OL}$, k-ft)	2920
Overload redistribution moment ($M_{rd\ OL}$, k-ft)	-750 → 0

Although it was determined previously that moment redistribution is necessary at the Overload limit state, in fact no moment redistribution is actually needed at either limit state. This is again because of the significant increase in the strength that is attributed to the section when considering moment redistribution from the strength defined by the stress limit of 80% of the yield stress. Thus, while moment redistribution needs to be considered and the aforementioned requirements of Section B6.2 of the LRFD specifications should be followed, ***no redistribution moments are necessary for the design of Girder C***.

Design Connectors for Positive Moment Regions

In a similar manner to Girder B, the partially composite positive moment regions are now designed and checked at both the Overload and Maximum Load limit states. For this girder, a different design needs to be conducted for the exterior span, which has a critical section at 28', and for the middle span, which has a critical section at 115'. The design is also checked at the transition location at the termination of the cover plate in the interior span at 101.5'.

Table A.14 summarizes the results from these calculations. As with Girder B, the partially composite design was begun with the minimum recommended composite ratio of 0.3, which ended up controlling the design in the interior span. However, in the exterior spans, a composite ratio of 0.66 is necessary to satisfy the requirements of the Overload limit state.

Table A.14: Results from Partially Composite Design Calculations for Girder C

	28'	**115'**	**101.5'**
Section number	1	4	1
Factored Maximum Load moment ($M_{u\,ML}$, k-ft)	2090	2340	1870
Deck force, fully composite ($C_{f\,FC}$, k)	1710	1710	1710
Number of connectors, fully composite (N_{FC})	48.6	57.0	48.6
Plastic web force ($P_{y\,web}$, k)	717	717	717
Plastic neutral axis location, fully composite	Deck	Flange	Deck
Plastic moment, fully composite ($M_{p\,FC}$, k-ft)	2690	3240	2690
Short term moment of inertia, fully composite ($I_{tr\,ST}$, in^4)	22200	27000	22200
Short term section modulus, fully composite ($S_{tr\,ST}$, in^3)	707	869	707
Long term moment of inertia, fully composite ($I_{tr\,ST}$, in^4)	16400	20100	16400
Long term section modulus, fully composite ($S_{tr\,ST}$, in^3)	642	793	642
Number of connectors, partially composite (N_{PC})	32	18	18
Actual composite ratio	0.658	0.316	0.370
Deck force, partially composite ($C_{f\,PC}$, k)	962	541	541
Plastic neutral axis location, partially composite	Flange	Web	Web
Plastic moment, partially composite ($M_{p\,PC}$, k-ft)	2590	2890	2390
Short term section modulus, partially composite ($S_{eff\,ST}$, in^3)	669	781	627
Long term section modulus, partially composite ($S_{eff\,LT}$, in^3)	616	739	588
Factored Overload stress ($\sigma_{u\,OL}$, ksi)	31.3	21.9	22.0
Maximum allowed Overload stress (σ_{max}, ksi)	31.4	31.4	31.4

The plastic moment capacity exceeds the factored moment at the Maximum Load limit state at all three locations. The maximum allowed stress also exceeds the factored stress at the Overload limit state at all three locations. Thus, the requirements for both limit states are satisfied with this design, so ***use $N = 32$ in the exterior spans and $N = 18$ in the interior span on Girder C.***

Locate Connectors and Check Fatigue

The connector layout in Figure A.13 is proposed, based on the same recommendations as were used in the design of Girder B. However, the layout has been modified to avoid the splice

plates, shown as green lines in the figure, and cover plates, shown as orange lines in the figure. It is not practical to post-install adhesive anchor shear connectors through these riveted plates. Thus, the connector groups nearest to the interior support in the exterior span have to be located farther than the recommended 15% of the span length. The connector groups in the interior span have been shifted closer than the recommended 15% of the span length to the interior support to compensate. Additionally, there is a 6-ft gap within each connector group to avoid the splice plates. The final positioning of the connector groups was determined by trial and error to determine the minimum overall fatigue demand on the connectors while keeping all connectors outside of the splice and cover plate regions. Because the girder is symmetric, only the left half is shown in the figure. Within a group, the connectors are spaced at 12 inches, which is equal to the transverse rebar spacing in the deck. The connector nearest to the end of the girder is located 6 inches away from the centerline of the support, and no connector is closer than 6 inches to a cover plate.

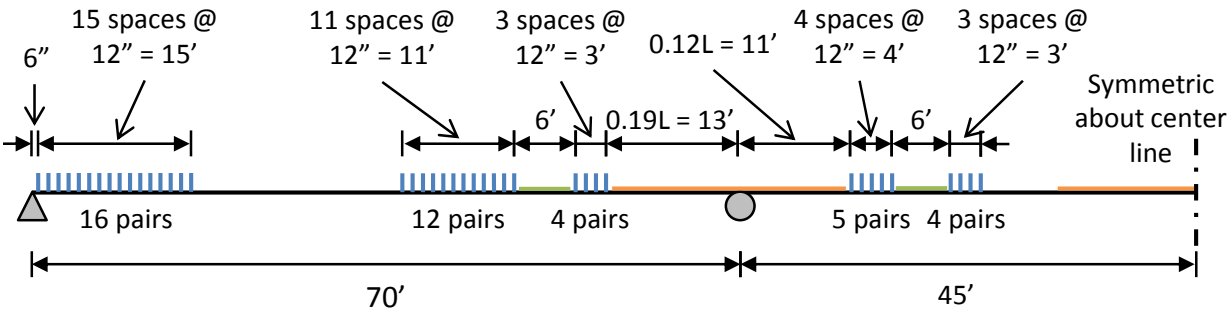

Figure A.13: Connector Layout for Girder C

The fatigue check is conducted in the same manner as for Girder B. Because the predicted truck traffic and required remaining life are the same as for Girder B, the nominal fatigue resistance of a single connector is also the same ($(\Delta F)_n = 17.5\ ksi$).

Figure A.14 shows the results from the fatigue analysis, conducted in the same way as for Girder B, which explicitly considers the interface slip and uses a stiffness of 900 kips per inch for the linear springs that represent each shear connector. The figure plots the stress range in each connector induced by the fatigue loading defined in the Fatigue II load combination in the LRFD specifications. Because of symmetry, only one-half of the girder is shown.

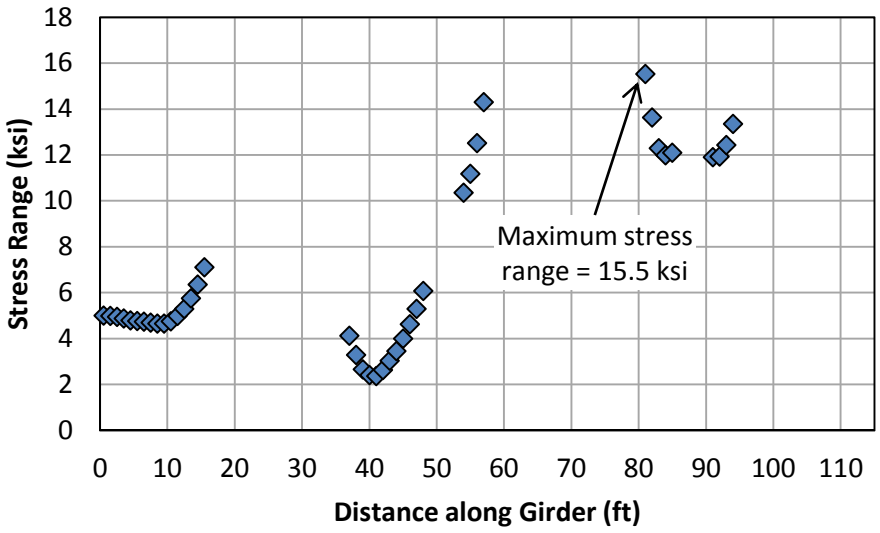

Figure A.14: Results from Fatigue Analysis for Girder C

The maximum stress range (ΔF) that a connector undergoes during fatigue loading is 15.5 ksi. As shown in the figure, this critical connector is the closest connector to the interior support in the interior span. This maximum stress range is less than the nominal fatigue resistance (17.5 ksi), indicating that ***the connectors have adequate fatigue life to satisfy the design requirement of a 25-year remaining life***. By reversing the design equations, ***the connectors in Girder C are estimated to have a remaining fatigue life of 58 years***.

Conduct Load Rating of Strengthened Girder

A load rating of the strengthened girder is carried out in the same manner as for Girder B. The results of this load rating are summarized in Table A.15. After post-installing the shear connectors and considering moment redistribution, the ***inventory load factor rating of Girder C is increased from HS 11.5 to HS 20.1***. This load rating is controlled by the section near the middle of the exterior spans at the Overload limit state.

Table A.15: Load Rating Results of Strengthened Girder C

Location (ft)	Section Type	Inventory Load Factor Rating	
		Overload	Maximum Load
28	Critical, Span	HS 20.1	HS 27.1
57.5	Critical, Transition	HS 24.2	HS 27.8
63.5	Critical, Transition	HS 42.5	HS 28.8
70	Critical, Pier	HS 33.2	HS 21.3
76	Critical, Transition	HS 40.7	HS 27.4
80.5	Critical, Transition	HS 23.3	HS 27.3
101.5	Critical, Transition	HS 22.3	HS 27.8
115	Critical, Span	HS 24.2	HS 28.7

Summary of Design for Girder C

To strengthen Girder C to a minimum inventory load factor rating of HS 20, ***a total of 164 adhesive anchor shear connectors should be post-installed.*** While moment redistribution does need to be considered, ***no actual moments need to be redistributed at either the Overload or Maximum Load limit state***. However, ***additional lateral bracing must be provided to the girder at the interior piers*** to reduce the unbraced length to satisfy the requirements of Appendix B6 of the LRFD specifications.

The connectors are installed in pairs on opposite sides of the web of the steel beam through a cross section, as illustrated in Figure A.8. They are grouped in six locations, with one group located near each end of the positive moment regions in all three spans. The specific connector layout is shown in Figure A.13. This layout can be modified slightly due to constraints in the field during installation, such as transverse deck reinforcing bars or other obstacles.

After post-installing the shear connectors and considering moment redistribution, the ***inventory load factor rating of Girder C is increased from HS 11.5 to HS 20.1***. This load rating is controlled in the strengthened bridge by the section near the middle of the exterior spans at the Overload limit state.

Summary of Design Process and Results for Girder D

A half-elevation view of Girder D is shown in Figure A.15. This girder was built as part of the original bridge in 1943. It is constructed of a 36WF150 rolled steel shape, with cover plates riveted to the top and bottom flange at the interior pier and in the middle of all three spans. Table A.16 summarizes the section properties for design for the steel beam (Section 1), as well as for the steel beam with cover plates in the exterior spans (Section 2), at the interior pier (Sections 3 and 4) and in the interior span (Section 3).

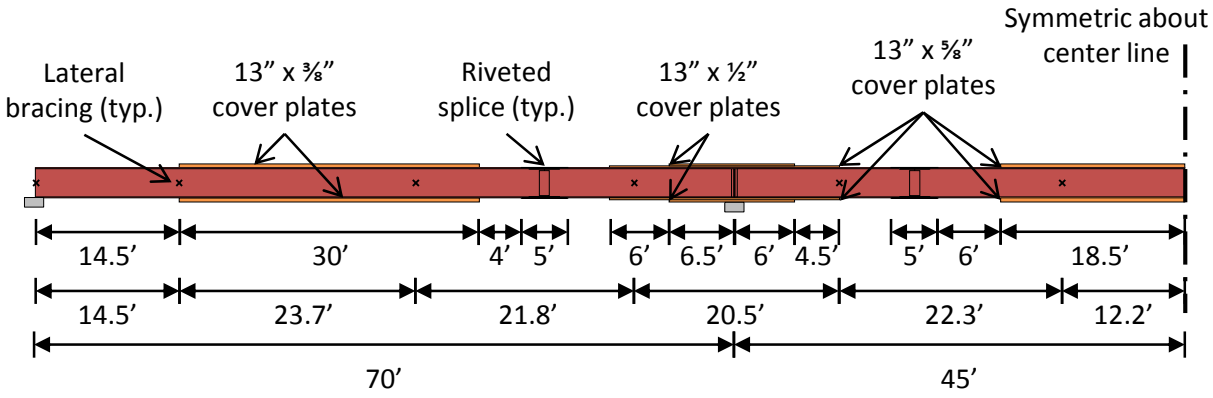

Figure A.15: Half-Elevation View of Girder D

Table A.16: Section Properties for Girder D

	Section 1	Section 2	Section 3	Section 4
Cover plate width (b_{pl}, in)	0	13.0	13.0	13.0
Cover plate thickness (t_{pl}, in)	0	0.375	0.625	1.125
Flange width (b_f, in)	12.0	12.0	12.0	12.0
Flange thickness (t_f, in)	0.940	0.940	0.940	0.940
Flange area (A_f, in^2)	11.3	16.2	19.4	25.9
Flange moment of inertia (I_{yc}, in^4)	135	204	250	341
Total depth (d, in)	35.9	36.7	37.2	38.2
Web thickness (t_w, in)	0.625	0.625	0.625	0.625
Area (A_s, in^2)	44.3	54.1	60.6	73.6
Moment of inertia (I_x, in^4)	9040	12200	14500	19100
Elastic section modulus (S_x, in^3)	504	668	778	999
Plastic section modulus (Z_x, in^3)	581	758	878	1120
Radius of gyration (r_y, in)	2.47	2.75	2.87	3.04
Polar moment of inertia (J, in^4)	10.1	10.6	12.2	22.4
Web depth (D, in)	34.0	34.0	34.0	34.0
Depth of web in compression, elastic (D_c, in)	17.0	17.0	17.0	17.0
Depth of web in compression, plastic (D_{cp}, in)	17.0	17.0	17.0	17.0
Effective deck width (b_{deck}, in) and girder spacing (S, in)	94.5	94.5	94.5	94.5
Deck thickness (t_{deck}, in)	8	8	8	8
Deck area (A_{deck}, in^2)	756	756	756	756
Deck moment of inertia (I_{deck}, in^4)	4030	4030	4030	4030

Conduct Structural Analysis

The distribution factor for interior Girder D is calculated to be 1.43. Figure A.16 and Table A.17 summarize the results of the structural analysis for Girder D.

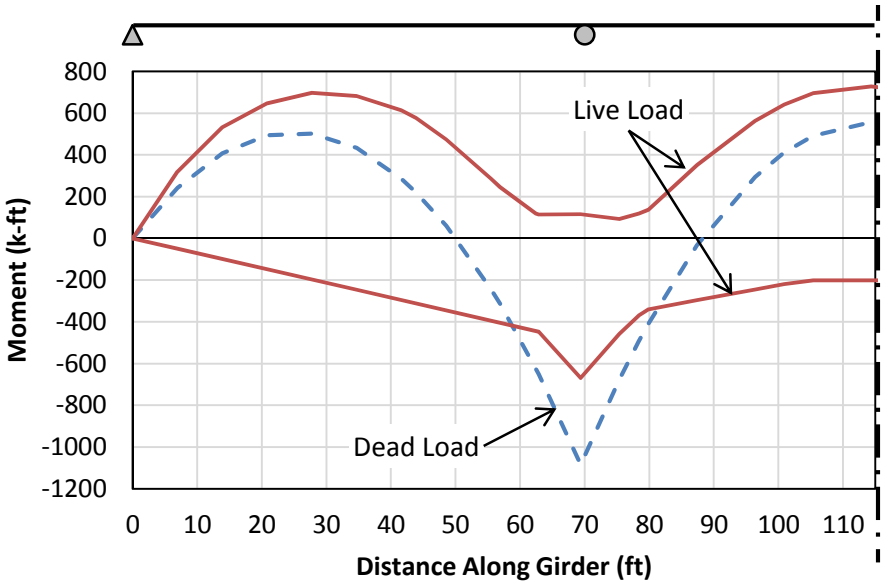

Figure A.16: Plot of Unfactored Moments for Girder D

Table A.17: Unfactored Moments at Critical Sections and at Lateral Bracing in Girder D

Location (ft)	Section Type	Section Number	Unfactored Moment (k-ft)		
			Dead Load	Live Load	
				Pos.	Neg.
14.5	Critical, Transition	1	408	533	-98.6
28	Critical, Span	2	503	698	-197
38.2	Lateral Brace	2	372	654	-267
44.5	Critical, Transition	1	221	577	-312
57.5	Critical, Transition	1	-313	246	-394
60	Lateral Brace	3	-454	189	-422
63.5	Critical, Transition	3	-652	114	-447
70	Critical, Pier	4	-1090	117	-670
76	Critical, Transition	3	-677	92.4	-458
80.5	Critical, Transition and Lateral Brace	1	-408	137	-340
96.5	Critical, Transition	1	295	563	-245
102.8	Lateral Brace	3	433	657	-214
115	Critical, Span	3	558	729	-202

Evaluate Existing Non-composite Girder

All of the capacity calculations for Girder D are done in the same manner to those for Girder B. The results of these and of the load rating calculations for Girder D are summarized in

Table A.18. The ***controlling load rating is HS 15.8***, which occurs at the Overload limit state at the end of the cover plate in the exterior span nearest the exterior support (14.5').

Table A.18: Load Rating Results of Existing Non-composite Girder D

Location (ft)	Section Type	Capacity (k-ft)		Inventory Load Rating	
		Overload	Maximum Load	Overload	Maximum Load
14.5	Critical, Transition	1110	1600	HS 15.8	HS 18.2
28	Critical, Span	1470	2080	HS 16.6	HS 18.6
44.5	Critical, Transition	1110	1600	HS 18.5	HS 20.7
57.5	Critical, Transition	-1110	-1600	HS 24.2	HS 27.5
63.5	Critical, Transition	-1710	-2140	HS 28.3	HS 26.3
70	Critical, Pier	-2200	-2750	HS 19.8	HS 18.1
76	Critical, Transition	-1710	-2140	HS 27.0	HS 25.0
80.5	Critical, Transition	-1110	-1390	HS 24.7	HS 23.0
96.5	Critical, Transition	1110	1600	HS 17.3	HS 19.6
115	Critical, Span	1710	2410	HS 18.9	HS 21.0

Set Strengthening Targets

The same strengthening targets are used for Girder D as for Girder B. Thus, the goals of the strengthening design are to increase the inventory load factor rating to HS 20, and to provide a minimum remaining life of 25 years for the purposes of fatigue design of the post-installed shear connectors. The same average annual daily truck traffic ($(ADTT)_{SL}$) of 1160 trucks per day will be used.

Check Negative Moment Regions and Redistribute Moments

In a similar manner to Girder B, the capacity of the negative moment regions at the interior piers (70') of Girder D is evaluated and compared to the factored moments at the Overload and Maximum Load limit states to determine whether or not inelastic moment redistribution is needed. The factored moments are calculated from those given in Table A.18. Because these regions will remain non-composite, the capacities are the same as those in Table A.17. A summary of these values is given in Table A.19.

Table A.19: Necessity of Moment Redistribution for Girder D

Factored Overload moment ($M_{u\,OL}$, k-ft)	-2210
Factored Maximum Load moment ($M_{u\,ML}$, k-ft)	-2890
Overload capacity (C_{OL}, k-ft)	-2200
Maximum Load capacity (C_{ML}, k-ft)	-2750

The factored moment at the interior pier section exceeds the capacity at both the Overload and Maximum Load limit states. This means that ***moment redistribution should be considered at both limit states***. As with the design of Girder B, the requirements from Appendix B6 of the LRFD specifications must be satisfied to allow for moment redistribution:

1. The bridge must be straight with supports not skewed more than 10° $\rightarrow$ OK
2. The specified minimum yield stress does not exceed 70 ksi $\rightarrow$ OK
3. Holes in the tension flange may not be present within a distance of twice the web depth from each interior pier section from which moments are redistributed $\rightarrow$ $NOT\ OK$

   As with Girder C, because this girder has riveted cover plates on the top and bottom flanges at the interior pier section, this requirement is not satisfied. However, in a similar manner as with Girder C, engineering judgement is used to eliminate this requirement in this case. This is partially because limited experimental testing of riveted connections has not indicated a lack of ductility, and very little redistribution is actually necessary in this case so the extent of inelastic behavior is expected to be minimal.
4. Web proportion requirements $\rightarrow$ OK
5. Compression flange proportion requirements $\rightarrow$ OK
6. Compression flange bracing requirements

   As with Girder B, because one the cover plates terminates within the unbraced length, the properties of the smallest section (Section 2) are used to be conservative. The calculations result in:

   $L_b = 20.5\ ft > 10.9\ ft = L_{b\ limiting}$ $\rightarrow$ $NOT\ OK$

   Thus, the existing cross frames do not provide adequate lateral bracing to allow for moment redistribution. To redistribute moments in this girder, ***at least one additional cross frame must be added at or near the interior pier to reduce the unbraced length***.

   Recall that there is not a cross frame located at the centerline of this interior support, although there are cross frames at this location on Girders A and B which were constructed at a later date. Thus, ***add a cross frame at the centerline of the interior pier*** for this girder. This reduces the unbraced length to 10 feet in the exterior span and to 10.5 feet in the interior span. Repeating the calculations for the limiting unbraced lengths with an additional cross frame located at the interior pier shows that the new unbraced lengths satisfy the lateral bracing requirements:

   $L_{b\ ext} = 10.0\ ft < 15.2\ ft$ $\rightarrow$ OK

   $L_{b\ int} = 10.5\ ft < 16.3\ ft$ $\rightarrow$ OK
7. There shall be no section transitions within the unbraced length of the interior pier section $\rightarrow$ $NOT\ OK$

Because the cover plates at the interior pier terminate within the adjacent unbraced lengths from the pier, this requirement is actually not satisfied. However, for the same reasons discussed in the design for Girder B, namely that the section properties used in calculating the lateral-torsional buckling requirements and that the controlling section in negative flexure is the centerline of the interior pier, not the section transitions at the ends of the cover plates, this requirement is ignored. The reduced flexural capacity at each transition need to be checked against the factored moments after redistribution to ensure that the section has adequate strength.

Note that this requirement could be directly satisfied by adding two cross frames and placing each at or closer to the interior pier than the ends of the cover plate.

8. The shear limit state must not be exceeded within the unbraced lengths adjacent to the interior pier regions. → OK

   Although a check for shear is not shown here, the shear strength requirements are satisfied for this girder.

9. Bearing stiffeners must be present at the interior pier locations → OK

   Riveted bearing stiffeners constructed of L-shapes are present at the interior support on this girder

By adding an additional cross frame at the interior pier to satisfy number 6 in the preceding list, moment redistribution can be allowed for this girder. Table A.20 summarizes the results of calculations for the redistribution moment, following the provisions in Section B6.5 of the LRFD specifications in a similar manner to the design of Girder B.

Table A.20: Results from Moment Redistribution Calculations for Girder D

Ultracompact web?	Yes
Effective plastic moment at Overload ($M_{pe\ OL}$, k-ft)	3080
Effective plastic moment at Maximum Load ($M_{pe\ ML}$, k-ft)	3080
Overload redistribution moment ($M_{rd\ OL}$, k-ft)	-870 → 0
Maximum Load redistribution moment (M_{rd_ML}, k-ft)	-190 → 0

Although it was determined previously that moment redistribution is necessary at both the Overload and the Maximum Load limit states, in fact no moment redistribution is actually needed at either limit state. For the Overload limit state, this is again because of the significant increase in the strength that is attributed to the section when considering moment redistribution from the strength defined by the stress limit of 80% of the yield stress. For the Maximum Load limit state, this is a result of the addition of at least one cross frame that allows the section to reach the full plastic moment capacity without lateral-torsional buckling occurring. Thus, while moment redistribution needs to be considered and the aforementioned requirements of Section B6.2 of the LRFD specifications should be followed including the addition of one or more cross frames, ***no redistribution moments are necessary for the design of Girder D***.

Design Connectors for Positive Moment Regions

In a similar manner to Girder B, the partially composite positive moment regions are now designed and checked at both the Overload and Maximum Load limit states. For this girder, a different design needs to be conducted for the exterior span, which has a critical section at 28', and for the middle span, which has a critical section at 115'. The design is also checked at the transition locations at the termination of the cover plate in the exterior span at 14.5' and 44.5', as well as in the interior span at 96.5'.

Table A.21 summarizes the results from these calculations. As with Girder B, the partially composite design was begun with the minimum recommended composite ratio of 0.3, which ended up controlling the design.

Table A.21: Results from Partially Composite Design Calculations for Girder D

	28'	**14.5'**	**44.5'**	**115'**	**96.5'**
Section number	2	1	1	3	1
Factored moment ($M_{u\,ML}$, k-ft)	2190	1700	1560	2330	1620
Deck force, fully composite ($C_{f\,FC}$, k)	1780	1460	1460	1920	1460
Number of connectors, fully composite (N_{FC})	59.3	48.6	48.6	63.8	48.6
Plastic web force ($P_{y\,web}$, k)	717	717	717	717	717
Plastic neutral axis location, fully composite	Deck	Deck	Deck	Flange	Deck
Plastic moment, fully composite ($M_{p\,FC}$, k-ft)	3360	2790	2790	3730	2790
Short term moment of inertia, fully composite ($I_{tr\,ST}$, in^4)	28300	23300	23300	31600	23300
Short term section modulus, fully composite ($S_{tr\,ST}$, in^3)	1540	1300	1300	1700	1300
Long term moment of inertia, fully composite ($I_{tr\,ST}$, in^4)	2110	17300	17300	23600	17300
Long term section modulus, fully composite ($S_{tr\,ST}$, in^3)	1150	962	962	1270	962
Number of connectors, partially composite (N_{PC})	18	18	18	20	20
Actual composite ratio	0.303	0.370	0.370	0.314	0.411
Deck force, partially composite ($C_{f\,PC}$, k)	541	541	541	601	601
Plastic neutral axis location, partially composite	Web	Web	Web	Web	Web
Plastic moment, partially composite ($M_{p\,PC}$, k-ft)	2920	2420	2420	3320	2470
Short term section modulus, partially composite ($S_{eff\,ST}$, in^3)	1080	986	986	1290	1010
Long term section modulus, partially composite ($S_{eff\,LT}$, in^3)	859	782	782	1050	797
Factored Overload stress ($\sigma_{u\,OL}$, ksi)	16.8	16.2	12.3	15.4	13.7
Maximum allowed Overload stress (σ_{max}, ksi)	31.4	31.4	31.4	31.4	31.4

The plastic moment capacity exceeds the factored moment at the Maximum Load limit state at all five locations. The maximum allowed stress also exceeds the factored stress at the Overload limit state all five locations. Thus, the requirements for both limit states are satisfied with this design, so ***use $N = 18$ in the exterior spans and $N = 20$ in the interior span on Girder D***.

Locate Connectors and Check Fatigue

The connector layout in Figure A.17 is proposed, based on the same recommendations as were used in the design of Girder B. However, in a similar manner as with Girder C, the layout has been modified to avoid the splice plates, shown as green lines in the figure, and cover plates,

shown as orange lines in the figure. It is not practical to post-install adhesive anchor shear connectors through these riveted plates. Thus, the connector groups nearest to the interior support in the exterior span have to be located farther than the recommended 15% of the span length. The connector groups in the interior span have been shifted closer than the recommended 15% of the span length to the interior support to compensate. Additionally, there is a 5-ft 8-in gap within the connector group nearest the interior support in the exterior span and a 6-ft gap within the connector group nearest the interior support in the interior span to avoid the splice plates. Due to the limited available space between plates in the exterior span, the connectors nearest the interior support in this span are spaced at 10 inches, which is not a multiple of the transverse rebar spacing in the deck. During installation, minor adjustments can be made to this spacing to avoid the reinforcement. All other connectors are spaced at 12 inches, which is equal to the transverse rebar spacing. The final positioning of the connector groups was determined by trial and error to determine the minimum overall fatigue demand on the connectors while keeping all connectors outside of the splice and cover plate regions. Because the girder is symmetric, only the left half is shown in the figure. The connector nearest to the end of the girder is located 6 inches away from the centerline of the support, and no connector is closer than 6 inches to a cover plate.

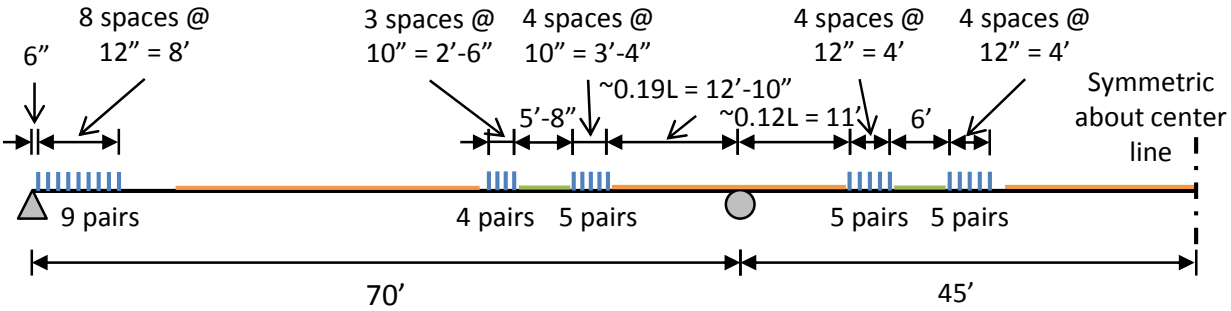

Figure A.17: Connector Layout for Girder D

The fatigue check is conducted in the same manner as for Girder B. Because the predicted truck traffic and required remaining life are the same as for Girder B, the nominal fatigue resistance of a single connector is also the same ($(\Delta F)_n = 17.5\ ksi$).

Figure A.18 shows the results from the fatigue analysis, conducted in the same way as for Girder B, which explicitly considers the interface slip and uses a stiffness of 900 kips per inch for the linear springs that represent each shear connector. The figure plots the stress range in each connector induced by the fatigue loading defined in the Fatigue II load combination in the LRFD specifications. Because of symmetry, only one-half of the girder is shown.

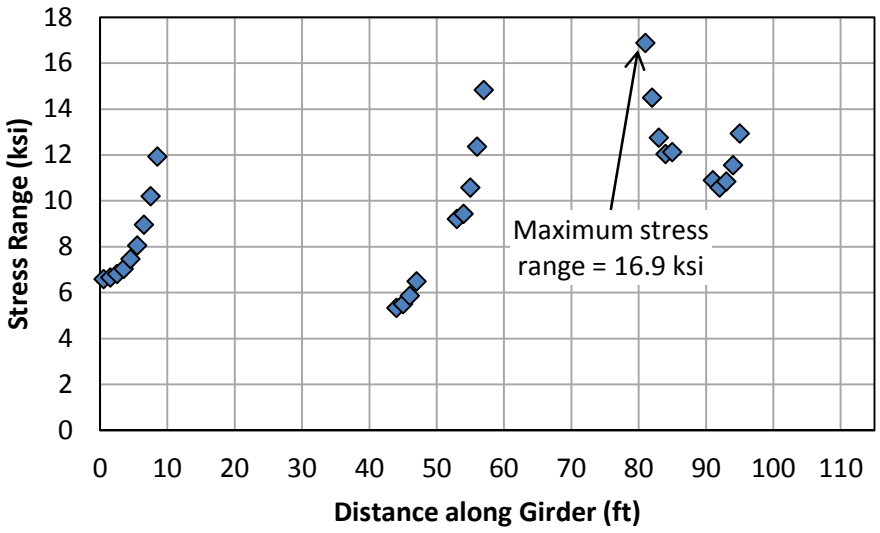

Figure A.18: Results from Fatigue Analysis for Girder D

The maximum stress range (ΔF) that a connector undergoes during fatigue loading is 16.9 ksi. As shown in the figure, this critical connector is the closest connector to the interior support in the interior span. This maximum stress range is less than the nominal fatigue resistance (17.5 ksi), indicating that ***the connectors have adequate fatigue life to satisfy the design requirement of a 25-year remaining life***. By reversing the design equations, ***the connectors in Girder D are estimated to have a remaining fatigue life of 32 years***.

Conduct Load Rating of Strengthened Girder

A load rating of the strengthened girder is carried out in the same manner as for Girder B. The results of this load rating are summarized in Table A.22. After post-installing the shear connectors and considering moment redistribution, the ***inventory load factor rating of Girder C is increased from HS 15.8 to HS 22.9***. This load rating is controlled by the section near the middle of the exterior spans at the Overload limit state.

Table A.22: Load Rating Results of Strengthened Girder D

Location (ft)	Section Type	Inventory Load Factor Rating	
		Overload	Maximum Load
14.5	Critical, Transition	HS 26.0	HS 32.7
28	Critical, Span	HS 22.9	HS 30.0
44.5	Critical, Transition	HS 28.7	HS 34.1
57.5	Critical, Transition	HS 23.6	HS 27.1
63.5	Critical, Transition	HS 47.3	HS 32.3
70	Critical, Pier	HS 35.9	HS 23.1
76	Critical, Transition	HS 45.5	HS 30.9
80.5	Critical, Transition	HS 24.7	HS 29.0
96.5	Critical, Transition	HS 27.8	HS 34.2
115	Critical, Span	HS 28.1	HS 32.8

Summary of Design for Girder D

To strengthen Girder D to a minimum inventory load factor rating of HS 20, ***a total of 112 adhesive anchor shear connectors should be post-installed***. While moment redistribution does need to be considered, ***no actual moments need to be redistributed at either the Overload or Maximum Load limit state***. However, ***additional lateral bracing must be provided to the girder at or near the interior piers*** to reduce the unbraced length to satisfy the requirements of Appendix B6 of the LRFD specifications.

The connectors are installed in pairs on opposite sides of the web of the steel beam through a cross section, as illustrated in Figure A.8. They are grouped in six locations, with one group located near each end of the positive moment regions in all three spans. The specific connector layout is shown in Figure A.17. This layout can be modified slightly due to constraints in the field during installation, such as transverse deck reinforcing bars or other obstacles.

After post-installing the shear connectors and considering moment redistribution, the ***inventory load factor rating of Girder D is increased from HS 15.8 to HS 22.9***. This load rating is controlled in the strengthened bridge by the section near the middle of the exterior spans at the Overload limit state.